THE REPRESENTATION OF RESPIRATORY MOVEMENTS IN THE INFERIOR OLIVE

BY

DR. MOHAMMED SALAH ELDIN MOHAMMED ALI MAGZOUB
M.B., B.Ch.

Thesis submitted for the degree of Doctor of Philosophy
to the University of London

(1995)

Sobell Department of Neurophysiology,
Institute of Neurology,
National Hospital for Neurology and Neurosurgery,
Queen Square,
London WC1N 3BG.

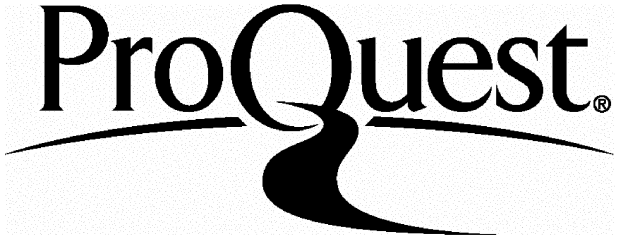

This work is dedicated to my family

ABSTRACT

It has been previously proposed that the inferior olive (IO) acts as a 'comparator' signalling to the cerebellum differences (errors) between signals conveying the command for movement from 'higher motor centres' and the activity these signals evoke at spinal 'centres' which also are in reciept of peripheral inputs (Oscarsson, 1973). Validation of this hypothesis has been hindered by the lack of direct access to the command signals. A review of the literature revealed that the respiratory system, as a source of centrally initiated automatic movements, offers a unique opportunity for studying both the command and outcome for a naturally occurring movement. The experiments in the first section of the thesis reinvestigate the interactions between the central respiratory drive and segmental (chest wall) reflexes. Muscle afferent activity was also monitored in intercostal nerve filaments to define proprioceptive inputs to the spinal cord and brainstem during artificial ventilation. Against this background the IO was explored by extracellular recording to seek evidence of central and peripheral-related respiratory activities. Three principal types of respiratory related activities were encountered in the dorsal accessory olive (DAO); 1), respiratory phased, mass activity; 2), respiratory phased, low frequency activity; 3), respiratory pump locked activity. The spatial location of these activities was found to correspond to a narrow, longitudinal strip in the DAO representing the

segmental projection of the spino-olivary neurones located in the thoracic spinal cord, as identified anatomically by Matsushita et al. (1992). The source of these activities was investigated by cold block of the cervical spinal cord at C3. Whereas the central respiratory activity was abolished in spinal motoneurones, it persisted in the DAO indicating that the DAO receives a phasic respiratory input of supraspinal origin. Lowering the CO_2 while holding the mechanical conditions in the thorax constant, resulted in changes in the olivary discharge, further indicating that the central command is fed to the olive, thus supporting the view that the olivary neurones act as a comparator signalling differences between the command for movement and the outcome.

ACKNOWLEDGEMENT

I am indebted to my supervisor, Professor T. A. Sears, without whom this work would never have been done, for his patient guidance, generosity with his time and kind encouragement throughout the course of this work. I am grateful to Mr. C. P. Seers for his technical expertise, advice and assistance. I would like to express my thanks to Mrs. K. Sunner for her assistance in the histological part of this work, Miss. J. Savvides for secretarial work, and the entire staff of the Sobell Department of Neurophysiology for many help and technical support. I would like to thank also Professor T. Taylor and his colleagues for accommodating me in the Division of Physiology, Sherrington School of Physiology at St Thomas' Hospital for the last 2 years. I gratefully acknowledge the financial support of the Sudanese Government, the Medical Research Council and Africa Educational Trust.

LIST OF CONTENTS

CHAPTER II METHODS

LIST OF FIGURES

LIST OF TABLES

CHAPTER I INTRODUCTION

1. General

The inferior olive (IO) of the ventrolateral tegmentum of the medulla oblongata is believed to (be) of (central) importance for the proper functioning of the cerebellum as a co-ordinating centre for movements. The belief can be traced to the year 1902 when Babinski and Nageote (in Dietrichs and Walberg's review, 1989) examined a terminal, long standing neurosyphylitic patient who presented with motor disturbance, vertigo, inability to walk unless supported and a tendency to fall towards the left side, beside a severe headache. The patient died a few days after admission. At autopsy his brain was removed and histologically examined to reveal lesions affecting the dorsal lamella of the principal olive (PO), the dorsal accessory olive (DAO) and the crossing olivocerebellar fibres. The degenerating fibre terminals were traced to the dentate and emboliform nuclei. Later lesioning experiments, partly or completely destroying the olive, were found to produce motor deficits similar in nature to injury of the cerebellum itself (Ito, Orlov and Shimoyama, 1978, Haddad, Demer and Robinson, 1980; Demer and Robinson, 1982). This strong influence of the IO on the cerebellum stems from the fact that it is the entire source of climbing fibres to the cerebellar cortex and nuclei (Armstrong, 1974; Armstrong, Campbell, Edgley and Schild, 1982). The climbing fibre (CF)

projection to the cerebellum is extremely precise and oriented topographically such that groups or bands of olivary neurones project to the contralateral cerebellar cortex dividing it into eight sagittally orientated zones (Voogd, 1969; Oscarsson, 1969; 1980; Brodal and Walberg, 1977a,b; Groenewegen and Voogd 1977; Groenewegen, Voogd and Freedman, 1979), each of which in turn projects ipsilaterally to a separate part of a cerebellar nucleus (Dietrichs and Walberg, 1989; Trott and Armstrong 1987a,b) or the lateral vestibular nucleus (Andersson and Oscarsson 1978a,b; Billard et al., 1989). Most of these nuclear areas were found to be bi-directionally connected to the contralateral olivary bands of neurones that determine the cortical sagittal zone (Dietrichs and Walberg, 1989) and the majority represent sites of convergence of afferents from several sources, e.g. from the cerebral cortex and mid brain structures as well as the spinal cord. The latter, namely the spino-olivary inputs, which originate from spinal interneurones associated with spinal reflex arcs, are subjected to control by descending pathways (Miller and Oscarsson, 1970). In 1973, Oscarsson postulated that such convergence in the olive might permit 'command' signals from higher motor centres to be correlated with the activity these signals evoke at lower motor levels which are also affected by activity from the periphery, so that the olive might be used as a 'comparator' in the cerebellar integration of higher motor and reflex activities. He further developed

this hypothesis to state that each cerebellar sagittally oriented zone in the anterior lobe, with its corresponding olivary and nuclear connections represents a functional unit controlling a particular motor mechanism (Oscarsson, 1980). In the same vein, and based on recordings in awake animals of olivary or Purkinje cell complex spike activity elicited in response to unexpected foot displacement during locomotion, or during exploratory voluntary movements, Armstrong (1974) suggested that the olivary neurones may act as 'event detectors' signalling to the cerebellum the timing of the movement perturbation. Similarly, whereas cutaneous stimuli applied to the paws in the awake but passive animal evoked responses in the inferior olive, comparable stimuli resulting from the animal's own active movements were without effect, leading Gellman, Gibson and Houk (1985) also to conclude that olivary neurones signal unexpected events to the cerebellum. Subsequently, Andersson and Armstrong (1987) recorded from Purkinje cells during locomotion in the awake animal but CF responses were only secure when the ongoing movement was suddenly perturbed by unexpected peripheral events. Further investigation of these findings led Apps, Lidierth and Armstrong (1990) to conclude that cutaneous reflexes are gated during locomotion in such a manner that unexpected peripheral inputs are transmitted to the cerebellum, whilst predictable inputs resulting from the animal's own motor activities are not transmitted. By recording the field potentials in the C1 zone of the cerebellar cortex in

response to stimulation of the superficial radial nerve in cats walking on a moving belt, Lidierth and Apps (1990) found that the amplitude and timing of evoked potentials were step related and were invariably larger in mid to late swing of the ipsilateral forelimb. They related this variability to a central effect modulating transmission in the spino-olivo cerebellar pathways (SOCPs) (cf. Baker, Seers and Sears, 1989 for transmission of chest wall afferents). Monitoring the action potential in the stimulated nerve, they showed that the modulation was not due to a peripheral effect. This modulation was suggested to occur at a precerebellar level, as it was established not to occur at the Purkinje cell level. Thus the strongest candidate for modulating transmission over the SOCPs, was postulated to be the IO as it receives other inputs which could interact with the information ascending in these paths (see later). Furthermore, it had previously been found that the movement-related discharges of the IO occur in clusters of neighbouring neurones (Gellman et al. 1985), which exhibit multiple spikes on stimulation (Armstrong and Harvey, 1966; Crill, 1970) due to the electronic coupling between these neurones (Llinas and Yarom 1981). Such neurones were known to have a continuous, fluctuating spontaneous activity which sometimes may carry the excitability of the SOCPs sufficiently far from threshold to induce firing of the Purkinje cells. In addition to that process, Lidierth and Apps (1990) did not exclude an 'on-off' switch mechanism acting in parallel,

which produces inhibitory actions during the stance phase of the cycle, thus preventing transmission of the stimulus-evoked activity, when self generated stimuli are induced by the animal's own movements.

Collectively, the above results led to the view that by detecting inputs generated by unexpected loads the olivocerebellar system signal errors of performance in learnt motor acts. Similar insights regarding the role of the IO in motor control, had previously been developed from studies of the adaptive properties of the optokinetic response (OKR) and the vestibulo-ocular reflex (VOR) by Ito (1972; 1982; 1984). These reflexes control eye position on the basis of information carried by visual, vestibular and neck proprioceptive afferents. Adaptive changes in gain of the vestibulo-ocular reflex (VOR) depend on the integrity of the dorsal cap of the IO and the flocculus of the cerebellum and these structures mediate information about slip of the retinal image which serves as the error signal previously mentioned for the case of locomotion. Microstimulation of the dorsal cap in unanaesthetized rabbits evoked low-velocity, conjugate eye movements towards the side of stimulation (Barmack and Simpson, 1980). They suggested that the visual CFs act in a feedback loop that functions to correct retinal slip of low velocity. Essentially similar results were obtained by Barmack and Hess (1980a,b), however during trains of microstimulation (10-60 impulses/s for a duration of 2-8s)

the velocity of the eye movements was actually increased and decreased gradually after the stimulation was terminated. Destruction of the dorsal cap neurones by electrolytic lesions (Haddad et al. 1980) or by chemical inactivation (Demner and Robinson 1982) prevented adaptation of the VOR. Also transection of the olivocerebellar pathways or destruction of the contralateral cerebellar flocculus, resulted in failure of microstimulation of the dorsal cap to evoke ipsilaterally directed eye movements (Barmack and Hess 1980).

2. The inferior olive; Morphology and fine structure

In order to understand the role played by the IO in motor control, a knowledge of its cytoarchitecture as well as the topographic organization of its afferent and efferent connections is essential. Except where stated the following description refers to the cat. The inferior olive is one of the largest defined structures within the brain stem, located in the caudal medulla immediately dorsal to the pyramids. It is formed by small clumps of small, round to oval cells of mean diameter of 25um, arranged in layers dorso-ventrally and comprising three subnuclei, namely the dorsal accessory olive (DAO); the principal olive (PO); and the medial accessory olive (MAO). Knowledge of its fine structure goes back to 1886-1887 when Vincenzi (cited in Scheibel and Scheibel, 1955) described the olivary neurone and its typical features. The study of the IO was extended

and further developed by Cajal (1909) who described the dendritic tree and arbor complexity of its afferent fibres in impregnated human material. Later, using the Golgi method Scheibel and Scheibel (1955) described 3 types of neurone in the olive; small cells with widespread ramifying dendrites in the rostral part of the complex and particularly in the PO; large, non-ramifying cells in the caudal olive; and a third less ramified cell named transitional. Similar findings were obtained in guinea pig by Foster and Peterson (1986), who used intracellular labelling techniques and also gave a different nomenclature; type I, corresponding to the non-ramifying cells of the Scheibels'; and type IIa and b corresponding to the well, and less, ramified cells respectively.

The dendrites of olivary neurones branch extensively giving rise to primary, secondary and tertiary branches which curl back towards the cell occupying an area of 125-300um in diameter. Adjacent dendritic trees heavily overlap due to the high packing density of cells within the olive in cats (Scheibel and Scheibel, 1955) and in the guinea pig (Foster and Peterson 1986). However, more phylogenetically developed species such as man show less overlapping of their dendrites because the olivary cells are more widely spaced. This led Scheibel and Scheibel (1955) to suggest that such an organization may reduce the degree of convergence within the nucleus allowing a more individual behaviour of olivary neurones than would be possible in an

olive with a greater packing density of dendritic arbors.

Ultrastructural studies show that neighbouring cells, through one or more of their dendrites, together with a number of specific axonal terminals, form a structural arrangement separated from the environment by a capsule of glial processes, the whole defined by Szentagothai (1970) as a 'glomerulus' or, to allow for less compact organizations, a 'synaptic cluster' according to King (1976). These appear to correspond to the orange bodies in Golgi stained material previously described by the Scheibels (1955) who assumed that they may represent interneurones important for the function of the olive. The glomerulus was found to be composed of a central core made up of small diameter dendrites which exhibit attachment plaques and gap junctions, spines and spiny appendages arising from dendrites of typical cells. The central core forms the post synaptic element of the glomerulus and its presynaptic element is formed by vesicle-containing axonal terminals arranged around the core (Sotelo, Llinas and Baker 1974; James King 1976; King et al. 1976).

Utilising degeneration techniques Brodal (1940, cited in Scheibel and Scheibel, 1955) and Brodal, Walberg and Blackstad (1950) provided a concise summary of olivary connections. According to Berkley and Worden (1978) and Ito (1984) the inferior olive receives afferent inputs from at least 24 structures, which terminate in the olive with

different morphologies, e.g., descending, heavily staining afferents bearing bouton clusters crossing a wide olivary field to contact cell bodies in selected areas; fine afferents from regions of white matter near the midline; and, of special relevance to the present work, afferents from the spinal cord with ascending afferent collaterals ending in bushy terminals covering many olivary neurones and distributed to a wide area covering the caudal parts of both the MAO and DAO and the rostral part of the DAO (Scheibel and Scheibel, 1955; Foster and Peterson, 1986; Molinari, 1988). The fibres and their collaterals were found to be intermingled with the olivary dendritic trees to form a mesh network. However, aggregates of 2-3 type I and 5-6 type II cells were found to be yoked together through gap junctions, as shown by the intracellular injection of lucifer yellow in individual olivary neurones, whose electrical properties had previously been determined (Foster and Peterson 1986). These cellular aggregates were suggested to be distributed throughout the olivary nucleus and to behave as an electrical syncytium.

3. Spinal inputs to the Inferior Olive

The IO receives both direct and indirect pathways from the spinal cord. The direct paths ascend in the ventral and adjoining lateral funiculi while the indirect pathways ascend in the dorsal and dorsolateral funiculi. They were named according to their termination in the cerebellum as

the ventral funiculus spino-olivocerebellar pathway (VF-SOCP); the lateral funiculus (LF-SOCP), the dorsal funiculus (DF-SOCP) and the dorsolateral funiculus (DLF-SOCP), respectively.

3:1. The VF-SOCP

This direct pathway was first studied by Brodal et al (1950) by transection of the spinal cord at different segmental levels in cat. The degenerating fibres were identified as ascending in the ventral funiculus ipsilateral to the olive and terminating in the caudal parts of the DAO and the MAO, hence known as the 'spinal' olive. Using Marchi and Nauta methods, Mizuno (1966) confirmed the results of Brodal in cat and rabbit and additionally, found that spino-olivary fibres take origin in the posterior horn and the intermediate grey virtually at all levels of the spinal cord to terminate bilaterally in the olive, but mainly contralateral to the cells of origin. This termination was found to involve the caudal portion of the MAO and the whole extent of the DAO except its rostromedial portion, but it lacked a somatotopic organization. Subsequent studies with the retrograde transport of HRP succeeded in identifying the cells of origin of the ventral funiculus fibres in three different locations; 1), the dorsal horn of the lumbosacral region; 2), the intermediate grey of the cervico-thoracic and lumbosacral regions; 3) the ventromedial lumbosacral grey matter (Armstrong and Schild 1979, 1980). Whereas the vast

majority (95%) of lumbosacral cells are contralateral to the tract and olive, the number of ipsilateral cells reaches 24% in the cervicothoracic segments. Later investigations utilising orthograde transmission of label by the injection of tritiated leucine into different segmental levels of the spinal cord (Armstrong et al. 1982) emphasized a somatotopic projection in the caudal parts of the MAO and DAO and the rostral part of the DAO. This projection resulted in three rostrocaudally oriented columns in the caudal MAO, with the cervico-thoracic segments located medially and the lumbosacral segments laterally and the column in between occupied by the overlapping terminals of both the cervico-thoracic and lumbosacral fibres. With regard to the projection to the DAO, which is of special relevance for the current work, Armstrong et al. (1982) demonstrated that successively more rostral lumbosacral segments projected precisely to successive more rostral and medial strips or columns of olivary neurones located in its rostrolateral portion. The rostromedial portion of DAO was found to receive a cervico-thoracic projection, not reported previously, while the caudal part of the DAO received partially overlapping projections from both the cervico-thoracic and lumbosacral segments, with the latter located more laterally. Subsequently Matsushita, Yaginuma and Tanami (1992) studied the sites of termination in the olive following the injection of WGA-HRP at each segmental level of the spinal cord, from the first cervical to the last sacral. The

results confirmed and further extended those of Armstrong et al (1982). They showed that the C1-T1 segments project to the medial part of the caudal MAO, while the L6-S1 segments project to its lateral part, but with no overlap; also, they emphasized that the caudal MAO does not receive terminations from the T2-L5 segments. They also showed that each spinal segment from C1-S1 is represented throughout the rostrocaudal length of the DAO in a somatotopical arrangement with a medio-lateral distribution. This projection is again in agreement with Armstrong et al. (1982), that successively more rostral spinal segments project to successively more medial strips or columns of olivary cells. However, no new conclusions were reached concerning the laterality of the projections as many of the injections were made bilaterally in the spinal cord.

The axon terminals of the spino-olivary neurones contact small diameter dendritic shafts or occasionally spiny appendages, of olivary neurones in the caudal DAO and MAO where gap junctions are more numerous (Gwyn, Rutherford and Nicholson, 1985). Molinari (1988) further investigated these terminals in the DAO, to demonstrate that they are rostro-caudally oriented and end in dendritic thickets in its rostral part while more often ending on isolated dendrites in its caudal part.

As these anatomical studies were being carried out, the VF-SOCP was also studied functionally (Armstrong, Eccles,

Harvey and Matthews, 1968; Oscarsson 1968; Oscarsson and Sjolund 1977a,b.c.) These studies were based on transecting the spinal cord at C3, but sparing the ventral funiculus, and subsequently recording the distribution of climbing fibre evoked responses in the anterior lobe of the cerebellum following limb nerve stimulation. Five paths were identified based on their response latency, receptive fields and projection areas A, B, C1 and C3 sagittal zones of the cerebellum as described by Voogd (1969). Thus these paths carried the names of their termination zones; e.g. The lower case letter 'a' signifies that the VF-SOCP terminates in the A zone. The A zone was found to receive bilateral hind limb inputs located medially, and bilateral forelimb inputs laterally, through the aVF-SOCP, with the cells of origin corresponding to the ventromedial neurones of the spinal cord identified by Armstrong et al. (1982). The b1VF-SOCP terminates in the forelimb area of the B zone and its cells of origin are located in the intermediate gray of the cervico-thoracic segments; the b2VF-SOCP terminates in the hindlimb area of the B zone with its cells of origin located in the intermediate grey of the lumbosacral segments. The c1- and c3VF-SOCP terminate in the hindlimb areas of C1 and C3 respectively with their cells of origin in the dorsal horn of the lumbosacral segments.

The VF-SOCP is activated bilaterally, both through interneurones, and by flexor reflex afferents (FRA) i.e.,

cutaneous and high threshold group II and III muscle afferents (Armstrong et al. 1968). Weak excitation was also reported from group I muscle afferents and tendon organs confined to the ipsilateral hind limb. The fibres of this pathway have a conduction velocity of 24-30m/s.

3:2. The DF-SOCP

The DF-SOCP is a physiologically identified indirect pathway which ascends in the dorsal funiculus and relays in the dorsal part of the dorsal column nuclei. From there it projects to the contralateral inferior olive and eventually to the cerebellar cortex in eight sagittal zones ipsilateral to the side of stimulation (Oscarsson 1969a, Armstrong et al. 1973a,b. Ekerot and Larson 1979a,b).

The A, X, B, C1, C3 and D2 zones receive direct paths activated ipsilaterally by cutaneous and high threshold muscle afferents belonging to the FRA. Under Chloralose anaesthesia Ekerot and Larson (1979) found that the X, C1, C3 and D2 zones also receive indirect pathways with long latency from distal cutaneous afferents, suggesting a convergence at the inferior olive level. The C2 was found to receive long latency evoked climbing fibre responses over a path activated bilaterally by distal cutaneous afferents, while the D1 receives this input through the same path as a result only of ipsilateral stimulation. The C1 and C3, and probably the D2 zones, showed a detailed somatotopical organization of the ipsilateral body half.

Accordingly, Ekerot et al. (1979) have demonstrated the presence of some olivary neurones projecting to the X and C1 and another group projecting to the C3 and D2 zones, the same results having been obtained previously by Armstrong, Harvey and Schild (1973) when they showed climbing fibres originating in the rostral DAO branching to the cerebellar C1 and C3 zones.

3:3. The DLF-SOCP

The cells of origin of this path are activated monosynaptically from primary afferent fibres mainly from distal cutaneous afferents and their fibres ascend in the dorsal portion of the lateral funiculus (Oscarsson, 1969a, Larson, Miller and Oscarsson, 1969a). The DLF-SOCP occupies a lateral position in the lumbar cord and dorsolateral position in the cervical cord and after an olivary relay in the rostral DAO it terminates in the anterior lobe and paramedian lobule. However, in addition to the forelimb C1, C3 and the ipsilateral D1 terminations, Andersson and Erikson (1981) showed other terminations in the vermal X and B zones and in D2. Evoked responses mediated by this path to the B zone are activated from ipsilateral limb nerves with long latencies; namely 20-25ms for forelimb nerves and 22-30ms for hindlimb nerves, with a somatotopic organization similar to that of the VF-SOCP, although the synaptic linkage is weaker. The conduction velocity of the fibres in the spinal cord was found to be around 70m/s, but when this pathway was activated by direct stimulation in

the spinal cord, the presence of 3-4 synapses in the brainstem was indicated.

3:4. The LF-SOCP

The LF-SOCP path is activated polysynaptically from FRA equally effectively from all limbs (bilateral inputs). The fibres of this pathway ascend in the ventral part of the lateral funiculus to relay presumably through a chain of interneurones before their termination in the inferior olive and eventual projection to C2 in lobule V and paramedian lobule, lacking however, a somatotopic organization (Larson, Miller and Oscarsson, 1969b; Armstrong et al. 1973b).

4. Olivocerebellar projection

Early experiments of Jansen and Brodal (1940) showed that the climbing fibres from particular subdivisions of the inferior olivary complex terminate in longitudinally oriented strips or bands in the cerebellum. Moreover, they showed that the cerebellar cortical outflow to the deep cerebellar nuclei is also organized longitudinally, such that the vermal cortex projects to the fastigial nucleus, the paravermal cortex to the interposed nucleus, while the hemispheral part ends in the lateral nucleus. Subsequent investigations, based on examination of the cerebellar white matter, carried out by Voogd (1969), showed a strict arrangement into longitudinal compartments that connect the

cortical Purkinje cells to the deep cerebellar nuclei. They were designated A, B and D according to their fibre calibre and mediolateral arrangement which was determined by raphe, i.e., concentrations of thin fibres. Later these compartments were found to convey the olivocerebellar fibres. The A and B compartments are confined to the vermis and receive CFs from the caudal parts of the MAO and DAO respectively. Later anatomical studies (Courville, 1975; Brodal and Walberg, 1977a,b; Groenewegen and Voogd 1976, 1977; Groenewegan, Voogd and Freedman, 1979) extended and developed the finding of Voogd (1969) to provide a principle for the olivocerebellar projection such that; a small circumscribed area of the IO projects through one or two compartments to one or two narrow cerebellar longitudinally orientated strips or zones of the cerebellar cortex, that same portion of the olive issuing collaterals to a central cerebellar nucleus which in turn receives its Purkinje cell axons from that particular strip or zone.

Electrophysiological studies of the termination of the spino-olivocerebellar pathways (see below) showed that they terminate in one or more longitudinally orientated cortical zones that appeared each to correspond with one of the olivocerebellar projection strips or zones identified anatomically (Oscarsson 1969; Oscarsson and Sjolund, 1977a,b,c; Larsson et al. 1969; Armstrong, Harvey and Schild, 1973; Ekerot and Larsson, 1979a).

According to the above studies and following the nomenclature introduced by Voogd (1969), the cerebellar cortex of the cat is now divided into eight sagittally orientated zones of width varying from 0.5-1.5mm. Each zone receives a contralateral projection from a specific portion of the IO and projects to a particular location in the cerebellar deep nuclei. Starting from the midline these are the A, X and B zones confined to the vermis, the C1, C2 and C3 located in the paravermal cortex while the hemispheral part contains the D1 and D2 zones. The longitudinal organization of these zones is also created as a result of the repeated branching of the parent olivocerebellar fibres which fan towards the cortical surface to supply Purkinje cells in many folia across different lobules. This branching was revealed from the physiological studies of Armstrong (1968, 1974). Later anatomical studies, first provided by Brodal et al. (1980) using a retrograde double labelling technique, confirmed the physiological results of Armstrong by demonstrating the branching of an individual olivary axon to two separate target areas as confirmed later by Voogd et al. (1982). Further evidence for longitudinal branching was provided by fluorescent double labelling technique (Rosina and Provini, 1987; Hrycyshyn, Ghazi and Flumerfelt, 1989) on cells in the middle one third of the contralateral MAO and DAO which send axons that divide contralaterally to terminate in both the caudal part of the anterior lobe and the rostral part of the paramedian lobule. Climbing fibres also branch in a

transverse plane to link different zones, as demonstrated in the C1 and C3 zones (Armstrong et al. 1973; Ekerot and Larson, 1982) C3 and D2 (Ekerot and Larson, 1982) and the X and C1 zones (Campbell and Armstrong, 1985).

In the following section each zone will be described under a separate heading, together with its related olivo- and nuclear connections, to emphasize that they form a functional unit controlling a particular motor mechanism as suggested by Oscarsson (1973). Particular emphasis is directed towards those zones which are of special interest in relation to the present work.

5. Sagittal zones of the cerebellum

5:1. The A zone

Starting from the midline, the A zone is the most medial longitudinal zone of the cerebellar cortex. It extends through the anterior and posterior lobe both in the cat (Groenewegen and Voogd 1977) and in the rat (Azizi, 1989; Azizi and Woodward, 1987). Its medial part designated A1 (hind limb area) receives input from the lateral part of the caudal MAO which represents the spinal inputs from the lumbosacral region. More laterally, A2 (forelimb area) receives input from the medial portion of the contralateral caudal MAO, the projection area of the spinal cervico-thoracic segments as shown by Armstrong et al. (1982) and Matsushita et al. (1992). The A zone projects to the

fastigial nucleus which exhibits reciprocal connection with the caudal MAO (Groenewegen and Voogd, 1977; Dietrich and Walberg, 1989). In the anterior lobe the A zone was found to project also to the lateral and inferior vestibular nuclei (Voogd et al. 1991). The fastigial nucleus projects to the medial reticular formation and the lateral vestibular nucleus bilaterally (Walberg et al. 1962a,b). Hence, the A zone is connected to the spinal cord through the reticulospinal and the lateral vestibulospinal paths which terminate in the medial and ventromedial regions of the spinal cord gray matter; such regions were shown by Armstrong and Schild (1980) to contain aggregates of neurones that give rise to the fibres of the ventral funiculus spino-olivary pathway. The A zone was thus suggested to be involved in the motor control of axial and proximal musculature with regard to stance and equilibrium.

5:2. The B zone

The B zone occupies the lateral portion of the vermis and extends through lobules I-VI with a width of one mm, tapering laterally in lobule VI (Groenewegen and Voogd, 1977). By recording CF evoked responses in the B zone following stimulation of the peripheral nerves or their corresponding areas of representation, Andersson and Eriksson (1981) demonstrated a somatotopic representation of the whole body, with successively more rostral segments projecting to successively more medial narrow columns or microzones. The spinal input was found to ascend through

the DF-SOCP, DLF-SOCP, and the VF-SOCP, with a relay at the olivary level. Also, these authors showed a remarkable, matched overlapping of the cortical and spinal inputs over the VF-SOCP with respect to somatotopy, as well as in the amplitude and latency differences between ipsilateral and contralateral projections. The olivocerebellar fibres to the B zone originate in the caudal portion of the DAO, which itself was shown to receive a mediolaterally arranged somatotopic input from the rostrocaudal extent of the spinal cord (Matsushita et al 1992). Visceral afferents were found to project also to the B zone following stimulation of the splanchnic nerve (Langhof, Hoppener and Rubia, 1973) and somatic afferents were thought to be activated for the thoracic nerve evoked responses (Andersson and Eriksson, 1981). The B zone projects to the lateral vestibular nucleus (LVN) in five small and distinct areas corresponding to the overlying cortical strips which were revealed already by Andersson and Oscarsson (1978b). A corresponding reciprocal innervation was also revealed between the LVN and the caudal DAO (Billard et al. 1989). The LVN, which also receives inputs from the fastigial nucleus (see above), gives rise to the lateral vestibulospinal pathway which influences axial motoneurones at different levels of the spinal cord (Wilson and Yoshida, 1969b; Wilson, Yoshida and Schor, 1970; Peterson and Coulter, 1977).

5:3. The X zone

The X zone is a wedge like strip located between the A and B zones of lobule V and VI with a maximum width of 0.5mm. It was first recognized electrophysiologically by Ekerot and Larsson (1979) in their study of the projection of the DF-SOCP. It was originally thought that the X zone receives its CFs input from the rostral part of the DAO in common with that supplying the forelimb area of the C1. However, subsequent investigations of Campbell and Armstrong (1985) identified a row of olivary neurones in the middle part of the MAO projecting to both the X and the lateral part of C1 (see below). The X zone receives a matched overlapping input from the contralateral forelimb through the DF-SOCP and its corresponding input in the cerebral cortex (Andersson and Eriksson 1981). The X zone was found to project to the adjacent portions of the fastigial nucleus and the nucleus interpositus posterior (Armstrong, 1990). Through their nuclear projections to the red nucleus the X and CX zones are thought to be involved in the control of oculomotor mechanisms (see later).

5:4. The C zones

The C zones are located in the paravermal cortex with the C1 medially and the C3 laterally enclosing C2 between. Anteriorly C1 and C3 join in lobule I-III of the anterior lobe and extend to lobule VIII, while C2 extends over lobule III-IX (Groenewegen and Voogd, 1979); C1 and C3 receive inputs from the rostral part of the DAO while the C2 receives from the rostral MAO. Electrophysiological

studies of Ekerot and Larsson (1979) showed that C1 and X, and, C3 and D2, through branching of individual climbing fibres, share the same inputs. Subsequent investigations by Campbell and Armstrong (1985) demonstrated that the C1 can be further divided into a medial C1 and a lateral C1 or CX zone. They showed that the CX and X zones are innervated by partially overlapping olivary neurones originating from the middle portion of the MAO, with those projecting to the X zone extending caudally while the neurones supplying the CX are centred further rostrally. With regard to C3 and D2, it was shown that the C3 is also divided into two subzones, medial C3 and lateral C3 according to their olivary inputs. The lateral C3 receives its olivary fibres from a rostrocaudally oriented band of olivary neurones located in the medial portion of the rostral DAO which innervates some Purkinje cells in the D2 zone; however, the majority of CF to this zone arise from the ventral lamella of the PO. Hence it was suggested by Armstrong (1990) that the common input to both zones may arise from olivary neurones at the junction of the rostral DAO and the ventral lamella of the PO. Campbell and Armstrong showed also that the medial C1 and the medial C3 subzones are innervated from a rostrocaudally oriented column, 2.5mm long, in the lateral portion of the rostral DAO (Armstrong, 1990). Olivocerebellar fibres to the C2 arise from a row of olivary neurones in the rostral MAO.

The C1, C3 and probably the D2 were found to receive a

somatotopic representation of the ipsilateral body half, with the medial C3 receiving a mirror image of the lateral C3 (Ekerot and Larsson, 1979). Recent investigations carried out by Ekerot et al. (1991) showed a detailed, topographically organized nociceptive CF input to the forelimb area of the C3 zone, such that specific receptive fields project to specific groups of CFs organized in a narrow rostrocaudal microzone, 100-300um wide and less than 1mm long. In addition it was found that there is an abrupt change between receptive fields to these microzones. This organization within the C3 reflects the somatotopical organization of the spinal input to the DAO demonstrated previously by Armstrong et al. (1982) and confirmed later by Matsushita et al. (1992). The former proposed "....that each cortical microzone receives CFs from narrow longitudinally orientated column of olive cells within the larger population supplying the whole Voogd zone".

According to Trott and Armstrong (1989) the C1 projects to the medial nucleus interpositus anterior (NIA) and the C3 projects to the lateral NIA, with partial overlapping. Recent investigations carried out by Garwicz and Ekerot (1994) demonstrated that the cerebellar cortical projection from the C3 to the NIA has a detailed topographical organization, such that microzones with specific CF receptive fields terminate within restricted areas in the nucleus. The NIA projects to the red nucleus and hence, through the rubrospinal tract, connects the C zones to the

spinal cord. It has been shown that microstimulation of the NIA and red nucleus elicits discrete movements in single muscle or group of synergistic muscles in the ipsilateral forelimb (Asanuma and Hunsperger, 1975). They predict that CF projecting to each microzone convey information from spinal multireceptive reflex arcs acting on a single muscle or group of synergistic muscles, and in turn each microzone controls the activity of the corresponding motoneurone pool/s (Garwicz and Ekerot, 1994). The C2 was shown to project to the NIP (Trott and Armstrong, 1987). Both the NIA and NIP send inputs to the cerebello-thalamocortical system (Angaut et al. (1985b) which influences the pyramidal pathways projecting to the head, trunk and forelimb (Buisseret-Delmas and Angaut, 1992).

5:5. The D zones

The DI and D2 occupy the lateral hemisphere of the cerebellar cortex and extend over lobules IV-IX (Voogd 1969). The D1 which is more medial receives its olivocerebellar fibres from the dorsal lamella of the PO, while the D2 receives inputs mainly from the ventral lamella of the PO (Brodal and Kawamura 1980) and shares some common CFs with the lateral C3 (Armstrong 1990), see above. The D1 projects to the caudoventral parts of the dentate nucleus while the D2 projects to its rostrodorsal part. Reciprocal connections between these portions of the dentate nucleus and the olivary regions that issue CFs to their respective and corresponding cortical zones, were

identified by Dietrichs and Walberg (1989).

The D1 and D2 outputs are fed via the dentate nucleus into the ventrolateral nucleus of the thalamus and the parvocellular red nucleus. Such connections are thought on the one hand to influence large regions of the cerebral motor cortex which command movements of the limbs and to provide fine cortical control of discrete movements and on the other to influence the medullary areas concerned with buccopharyngeal mechanisms e.g. feeding (Angaut et al 1985b, Cicirata et al. 1986, 1992; Buisseret-Delmas and Angaut 1992)

6. The Inferior Olive; Oscillatory behaviour

Olivary neurones were observed to exhibit non-sinusoidal, continuous regular oscillation of 3-10Hz as studied intracellularly both in vitro and in vivo with, or without, the injection of harmaline (Armstrong et al., 1968; Crill, 1970; Llinas and Volkind, 1973; Benardo and Foster 1986; Yarom, 1989). The oscillations are attributed both to electrical coupling between the cells and on the other, to the unique intrinsic properties of the olivary neurones which promote continuous rhythmic fluctuation of membrane potentials due to the concerted action of five different voltage and time-dependent conductances.

In addition to the normal Na+ and K+ conductances there are

1), a high threshold Ca^{++} conductance restricted to the dendritic membrane: 2) a Ca^{++} dependent K^{+} conductance giving a long duration after-hyperpolarization which is responsible for the low frequency of firing; 3) and a low threshold Ca conductance in the somatic membrane which, when de-inactivated by the hyperpolarization, results in a rebound excitation (Llinas and Yarom, 1981; Bernardo and Foster, 1986). Hence, the somatic, low threshold Ca^{++} conductance leads to an initial spike generated by an Na+ conductance. This is followed by a prolonged after depolarisation which may carry a series of high frequency wavelets, generated by the dendritic high threshold Ca conductance. Subsequently it ends in the afterhyperpolarization stage generated by the Ca dependent K conductance. Olivary oscillations were maximal when the neurone was at its resting membrane potential or hyperpolarized relative to it, indicating that the oscillations are regenerative. Nevertheless, spike responses evoked in olivary neurones were found always to occur near the peak of an individual oscillation, the cell appearing less excitable or even refractory to spiking between oscillatory peaks (Bernardo and Foster, 1986).

7. Representation of the thorax in the olivocerebellar system

From the above studies the thorax was found to project both to the caudal parts of the MAO and DAO (the classical

spinal olive) as well as to the rostral part of the latter, as revealed by direct anatomical studies (Armstrong and Schild 1980; 1982; Matsushita et al. 1992) and as inferred from electrophysiological studies of the termination sites of the SOCPs (Ekerot and Larsson 1979a,b; Andersson and Eriksson 1981).

The T1 segment projects directly to the medial part of the caudal MAO, together with the cervical segments, occupying a medial strip projecting to the cerebellar parasagittal A zone. The rest of the thorax projects directly to the DAO as a long central strip extending from its caudal pole nearly to its rostral end, with T2-T7 represented medially and T10-T12 laterally. This thoracic region occupies the central position in a entire rostro-caudal sequence of segments in the spinal cord (Matsushita et al. 1992). Projection of the cervicothoracic fibres to the rostral part of the DAO was found to be entirely crossed while that to its caudal part appeared to be bilateral, although predominantly crossed (Armstrong et al 1982).

Using natural and electrical stimulation of various parts of the body, Gellman et al. (1983) defined a cutaneous map of the entire body in the DAO, with the trunk occupying its rostral pole. The thorax also was found to project over the DF-SOCP to the C1, C3 and probably the D2 zones (Andersson and Erikson, 1981). The C1 and C3 representations presumably corresponding to those in the intermediate

cortex previously described by Coffey, Godwin-Austin, MacGillivray and Sears, (1971).

The above account has dealt with the anatomical and physiological organization of the olivocerebellar system, and how, as a comparator, the IO might monitor the performance of self generated movements and detect the occurrence of unexpected perturbations of ongoing movements. Thus the IO signals errors in motor performance, alerting the system for the need for corrective action which is achieved, according to the hypothesis by the responsible functional unit of the olivocerebellar system (Oscarsson, 1980) and, in the particular case of the adaptive properties of the vestibulo-ocular reflex shown to involve specific zones within the flocculus (Ito, 1989; see also Ito, 1984).

Several studies have been performed to test the role of the IO in motor performance. However all such studies lack one essential component of this operation, assumed to be fed to the IO, namely information about the actual 'command' for the movement in question. Hence, the purpose of this work, is to utilize the unique properties of the respiratory system to study the principles of motor control undertaken by the olivocerebellar system. Not only do breathing movements continue automatically in the experimental animal, but the 'command' for these movements can be altered by manipulating the chemical drive (see below).

Furthermore, the effects of the command at lower motor centres and the resultant movement are under experimental control and much is known about the integrative functions performed at the level of the motoneurone itself.

8. Respiration as a motor act

Respiration is a complex motor act. It is not only responsible for gas exchange and thus contributing to haemostasis, but the respiratory muscles are also involved in many sophisticated motor behaviours. For example, in the control of posture, and in the expulsive motor acts such as coughing, sneezing, micturition and defecation which all are dependent on the synergistic action of many if not all of the respiratory muscles. The rib cage is an integral component of the axial skeleton, and is therefore directly involved in the structural integration and stability of the body. This apparatus is so articulated as to allow for the flexion and rotation of the trunk and to permit the different breathing manouvers which depend on the changes in configuration of the chest wall (Da Silva Sayers, Sears and Stagg, 1977). Underlying these are the specific breath by breath changes in the configuration of the chest wall (rib cage, diaphragm and hydraulically linked abdominal wall) resulting from the tension developed by the respiratory muscles (Sears, 1964b; Da Silva et al., 1977; for review, see Campbell, Agostini and Newsom Davis, 1970). In man, one of the most important functions of the

respiratory system is during phonation and speech, when it provides the source of power executing these acts by generating a subglottal pressure matching the demanded sound intensity and pitch of the tone. Of course, this regulation is shared with other organs (larynx, pharynx, palate etc..) in the upper part of the system (Sears, 1971). Hence respiratory movements may be considered as a motor behaviour rather than simply as a mechanism for gas exchange, and can best be understood from the conclusion of Fenn (1963) "Breathing should be considered as a behaviour governed by a set of control systems hierachially arranged to regulate ventilation and the breathing pattern in accordance with the ever occurring variations in metabolic needs and the many non homeostatic demands on them". So that the respiratory muscles are controlled by many descending functional systems, e.g., from the cerebral cortex (Aminoff and Sears, 1971), from the cerebellum (Decima and von Euler, 1969) from the bulbospinal respiratory groups of neurones (Bianchi, 1971; Merrill, 1970, 1972, 1974), from the reticular formation (Pitts, Magoun and Ranson, 1939a; Andersen and Sears, 1970). As well as through collaterals in the mid and hindbrain, all of these control systems converge on the spinal respiratory motoneuronal pools where further integration takes place with proprioceptive afferents (Sears, 1964d; Critchlow and von Euler, 1963) and hence, to provide reflex adjustment of the movements of the chest and abdomen and postural activities so as to compensate immediately for any changes

in muscle length or direction of forces produced by the muscles (von Euler, 1983). Thus, for better understanding of the above account concerning the motor control of respiration, in the following sections more details will concentrate on the discussion of the genesis of respiratory rhythm, and the homeostatic control of breathing.

9. Genesis of respiratory rhythm

9:1. Ramp of central inspiratory activity

According to von Euler (1983, 1986) generation of the respiratory rhythm is achieved in the medulla through a neuronal network with three functionally distinct groups of neurones connected serially and referred to as the A-,B- and C-pools. These pools are subjected to substantial influences from different sources, namely the central and peripheral chemosensors, pulmonary stretch receptors (PSRs), chest wall proprioceptors, the nucleus parabrachialis, and temperature sensors. The respiratory cycle is first initiated in the A-pool which generates a ramp of inspiratory augmenting activity referred to as the central inspiratory activity (CIA). The CIA is a conceptual input that is fed in parallel to the B-pool and to the spinal respiratory motoneurones, which accounts for the pattern of augmenting activity (ramp) with abrupt onset and rapid decline as recorded from the phrenic and external intercostal nerves. In addition to the CIA, the B-pool receives an input from the PSRs that mediate the Hering-

Breuer reflex which inhibits inspiration and excites expiration. The outcome of this interaction between the CIA and the PSRs in the B-pool is fed as an input to the C-pool, known as the 'off-switch' mechanism. The excitability of the C-pool, which determines the abrupt termination of the CIA, is dependent on the state of the preparation i.e., depth of anaesthesia, whether the vagi are intact, or not (through pneumothoracic mechanisms), and to the chemical drive produced by the chemosensors, as in anaesthetized or decerebrated preparations the rate of rise and peak amplitude of the CIA (as phrenic discharge) is found to be almost proportional to the CO_2. Hence the off-switch mechanism has a variable threshold with respect to drive (CO_2). This threshold was found to be lowered by inputs from the PSRs, and elevated in vagotomized preparations or when lung inflation is withheld during artificial ventilation in paralysed preparations (von Euler and Trippenbach, 1976). Hence in the latter case, the CIA alone determines the threshold of the off-switch, leading to longer inspiratory periods, low respiratory rate and larger tidal volumes. A similar effect can result from bilateral lesions in the region of the medial parabrachial nucleus of the pons (von Euler and Trippenbach, 1976).

From the above it can be seen that this model for respiratory rhythm generation is essentially based on the inspiratory phase of the cycle and effectively ignores the neurogenesis of the expiratory phase essentially on the

basis that in eupnoea, expiration is seen as a passive mechanical act. However, Feldman and Cohen (1978) demonstrated a central inspiratory inhibition (CII) that declines during expiration and determines the period of expiration by acting both on the CIA and the inspiratory promoting reflexes. Furthermore, Merrill (1970) clearly demonstrated a phasic excitation of expiratory bulbospinal neurones in the ventral respiratory group which persists in deep anaesthesia, emphasising that from a neural point of view, expiration is not a passive event.

9:2. Intrinsic organization of rhythm generation

Whereas von Euler's model provides a global description of three interacting systems that allow control aspects of breathing to be better understood and quantitatively analyzed (see Sears, 1990), the three phase model introduced by Richter and colleagues is based on the cellular mechanisms underlying rhythm generation. According to them (Richter, 1982; Richter et al. 1986) generation of the respiratory rhythm is the result of an interaction between six different categories of medullary respiratory neurones based on their firing pattern within the cycle, with a particular and important role for the early inspiratory (e-I) and post inspiratory (PI) interneurones to create a three phase respiratory cycle. This consists of an inspiratory phase and stage 1 and stage II expiration. Stage I corresponds to von Euler's CIA and following its abrupt termination there is a brief pause followed by a

post inspiratory discharge, as recorded from the phrenic nerve of spontaneously or fictively breathing animal, which period corresponds to stage I expiration; stage II expiration corresponds to the silent period in the phrenic nerve and the active phase of expiration during which 'low threshold' intercostal and abdominal motoneurones may be active (e.g. see Sears, 1964; Aminoff and Sears, 1971).

The central idea in this model stems from a reciprocal phasic inhibition of the eI and pI interneurones, which are characterized by their specific membrane properties and their balanced synaptic input as indicated by their abrupt onset of firing with rapid augmentation followed by a decline. To explain how the model works, two other components of the network are required, namely ramp inspiratory neurones (Ir) and the late inspiratory interneurones (L-I). The inspiratory bulbospinal (IBS) and expiratory bulbospinal (EBS) neurones feed the output of the medullary network to the spinal and cranial respiratory motoneurones.

A tonic drive attributed to the reticular activating system and pons is fed to the Ir and e-I neurones and the system generates the CIA which is fed into the IBS neurones and eventually to the phrenic and the inspiratory motoneurones. The late inspiratory neurones L-I also receive a parallel input from the Ir neurones, but do not fire early as they are concurrently subjected to an inhibition from the e-I

interneurones. Following the deep inhibition induced by the e-I interneurones on the p-I ones and through the phenomenon of 'rebound' excitation, the latter discharge abruptly. The discharge of the post inspiratory neurones causes widespread inhibition throughout the network directly inhibiting e-I, Ir, IBS and EBS neurones. Through parallel inhibition of the reticular formation, disfacilitation of Ir, e-I and EBS neurones, thus terminating inspiration and leading to stage I expiration. This is followed by stage II expiration, in which the bulbospinal expiratory neurones become active due to the declining activity of p-I neurones induced by disinhibition of the reticular activating system. Expiratory duration seems to be very much affected by the inhibitory gating effects of the p-I interneurones which delays the early onset of stage II expiration, as well as the state of the preparation itself that strongly influences the intensity of expiratory activation. The cycle repeats itself as the inhibitory effect on the e-I neurones declines steadily under the effect of the tonic activity induced by the reticular activating system.

9:3. Central respiratory drive potentials (CRDPs)

Ideas regarding respiratory rhythm generation in the mammal have inevitably concentrated mainly on supraspinal neuronal networks with relatively little attention being given to the spinal output stage, the respiratory motoneurones and associated segmental interneurones, but in recent years,

these have proved to have an important integrative role in the on-going phasic respiratory activity. Intracellular recordings from thoracic respiratory motoneurones in spontaneously breathing, anaesthetized and decerebrate cats, demonstrated the presence of slow rhythmic changes in the membrane potentials, with the periodicity of the respiratory cycle (Eccles, Sears and Shealy, 1962; Sears, 1964d). They were named 'central respiratory drive potentials' (CRDPs) to link them with the central command for respiratory movements (Sears, 1964) as they persisted in paralysed preparations and were absent in high spinal preparations. Each cycle of the CRDP is composed of alternating phases of depolarization and hyperpolarization due to a waxing and waning excitatory synaptic drive followed by a phase of active inhibition, such hyperpolarization being 'reversed' by injection of chloride ions into the motoneurones (Sears, 1964). With reference to the phrenic neurogram, these sequences of CRDPs occur in a reciprocal manner in the external intercostal (inspiratory) and internal intercostal (expiratory) motoneurones (Sears, 1964d) with some overlap of the excitatory and inhibitory synaptic drives, the breath by breath shape of the CRDP determining consequently the discharge pattern of the motoneurones (Sears, 1964b).

The reciprocal inhibition of the thoracic inspiratory and expiratory motoneurones is believed to be subserved by a spinal network of interneurones as the synaptic drives of

supraspinal origin show an interdependence in which if the excitation of one group of motoneurones is increased there is simultaneously a greater inhibition of the other. So the amplitude of the CRDP plays an essential role in the firing pattern of the respiratory alpha motoneuron, such that an added chemical drive can bring their membrane potentials to the firing level leading to phasic activity recorded as single unit discharges from their respective intercostal nerve filaments. Similarly, segmental inputs from muscle spindles can summate with the prevailing level of the CRDP to cause an otherwise subliminal CRDP to reach firing threshold (Sears, 1965).

9:4. Effects of CO_2 on rhythm generation

Carbon dioxide, via central and peripheral chemoreceptors, exerts the most important chemical stimulus for breathing, as its level in the circulating blood determines the pulmonary ventilation and thus provides homeostasis of gas exchange requirements. The central effects of CO_2 are eventually transmitted via the system of bulbospinal neurones to the respiratory motoneurones and their respective muscles (Merrill, 1974; Bianchi, 1970).

It has long been known that hyperventilation causes an apnoea (hypocapnic apnoea) and traditional concepts would have predicted that at low levels of CO_2 both inspiratory and expiratory motoneurones would be silenced. However, by recording the efferent discharges from 'low threshold'

expiratory motoneurones (those active at eupnoeic levels of CO_2), Sears (1963) and Aminoff and Sears (1970) demonstrated that in hypocapnic apnoea although the inspiratory motoneurones are silenced, the alpha and gamma expiratory motoneurones could show a tonic discharge with a respiratory pump modulation in phase with inflation of the lungs and chest wall. This phenomenon was examined in more detail by Bainton, Kirkwood and Sears (1978) who confirmed the findings electrophysiologically in non-paralysed decerebrate cats ventilated artificially at low tidal volume and high rate such that without added CO_2 the preparation developed hypocapnic apnoea. The majority of such preparations were expiratory biassed. The tonic CO_2 dependent drive to the motoneurones facilitated the segmental stretch reflex induced by chest wall inflation, this reflex being abolished by sectioning the dorsal roots in the same and adjacent segments (Sears, 1958, 1963). It was known already that respiratory movements cease with mid-sagittal lesions in the vicinity of the obex (Salmoraghi and Burns, 1960; Sears, 1966), while the work of Bianchi (1970) and Merrill (1974), had demonstrated the almost complete decussation of inspiratory and expiratory bulbospinal axons rostral and caudal to the obex. Drawing on this, Bainton et al (1978) demonstrated the selective loss of periodic inspiratory or expiratory motoneuronal activity with small incisions (2-3mm) above and below the obex, respectively, the CO_2 level being maintained constant throughout by artificial ventilation. In particular,

selective loss of the inspiratory drive caused the expiratory activity to persist for a longer period within the cycle, while remaining periodic, this being consistent with the loss of inspiratory-linked inhibition (see above). Such disinhibition also allowed the chest wall inflation reflex of the expiratory motoneurone to be exhibited during the inspiratory phase of the cycle (Bainton et al. 1978. Fig. 10). While performing such lesions they found that rostral extensions of the mid-sagittal lesions (rostral to the obex) elevated the CO_2 threshold for rhythm generation. This allowed them to demonstrate that the CO_2 responsiveness of the brain-stem-mediated tonic activity exists over the entire physiologically relevant range of CO_2 levels (1.5 - 6.0%). When CO_2 was progressively elevated it was demonstrated that the onset and rhythm of breathing was exhibited as a progressively deepening periodic inhibition of the tonic activity of the expiratory motoneurones and also of the inflation reflex, if the artificial ventilation was still present. On the basis of this and the earlier work of Cohen (1964), Bainton et al. (1978) postulated that the immediate source of the tonic drive in the brainstem was the system of expiratory bulbospinal neurones which were known to be at least monosynaptically coupled to expiratory motoneurones (Kirkwood and Sears, 1974) finding that a significant number of expiratory neurones in the medulla discharge tonically during hypocapnic apnoea. Subsequently this hypothesis was confirmed by Bainton and Kirkwood (1979) in extracelluar recordings from

antidromically identified expiratory bulbospinal neurones. Later, Sears, Berger and Phillipson (1982) showed in anaesthetized cats that when a preparation in hypocapnic apnoea was exposed to hypoxia a tonic inspiratory discharge of motoneurones occurred with reciprocal inhibition of the tonic expiratory discharge. Further lowering of 0_2, coupled with a gradual increase in the $C0_2$, induced by stopping artificial ventilation, resulted in a progressive increase in the discharge of the inspiratory motoneurones coupled with a progressive inhibition of the expiratory motoneurone discharge, until eventually, rhythm generation occurred as an alternating periodic inhibition of the tonic discharge of the two groups of motoneurones. The effects of hypoxia were shown to be mediated by the peripheral chemoreceptors as after section of the aortic and carotid sinus nerves, only the central effects of $C0_2$ persisted.

From the above account it seems clear that both the inspiratory and expiratory motoneurones are potentially in receipt of tonic, brainstem mediated chemical drives and that their rhythmic discharge is only induced by periodic inhibition of this tonic activity, depending on the particular state of the preparation at any time and the current balance of the chemical (and other drives) to which they are subjected. These interactions are represented schematically in Fig. 1. (taken from Sears, 1990). Panel 1, represents the state of hyperoxic hypocapnic apnoea, in which the expiratory motoneurones are tonically active,

Fig. 1.

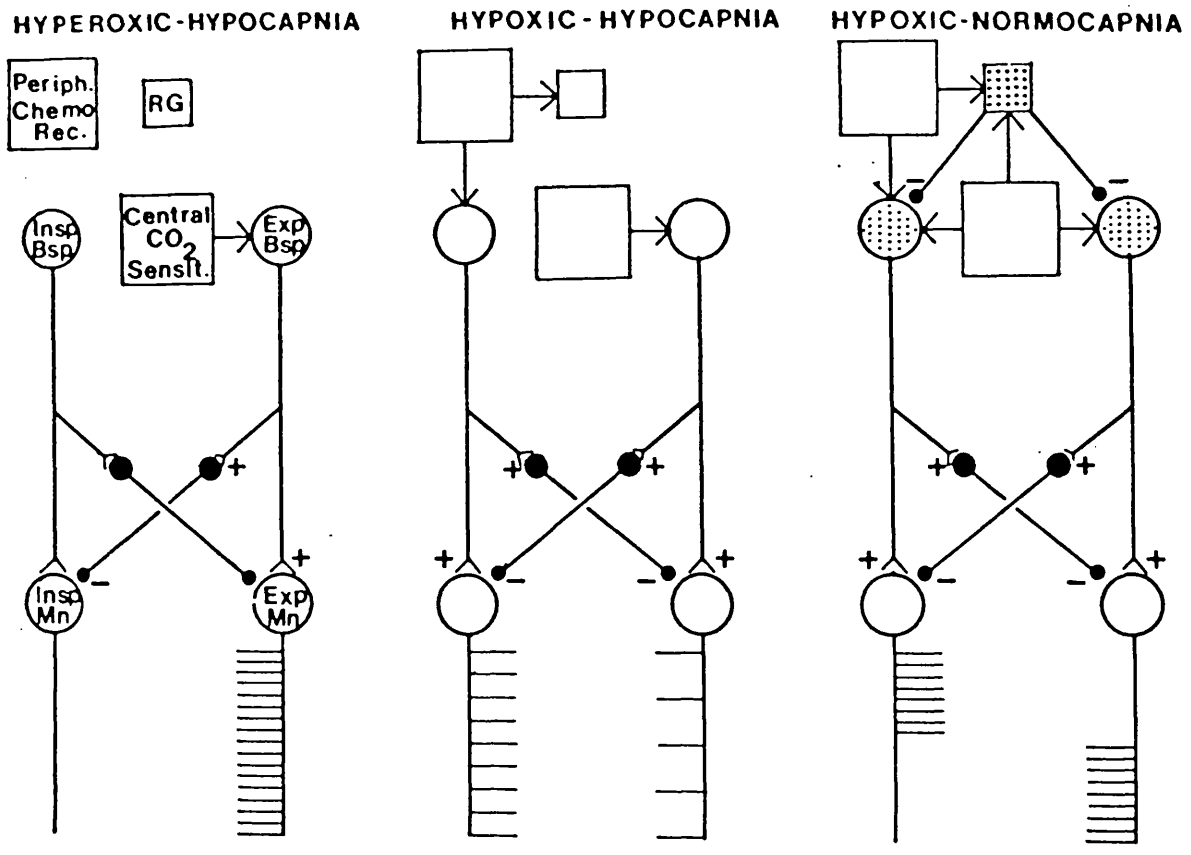

Fig.1. Schematic representation of brainstem-mediated central and peripheral chemoreceptors drives to inspiratory (Insp Mn) and expiratory (Exp Mn) motoneurones. Arrows indicates inputs currently effective in evoking discharges. Peripheral chemoreceptors inputs to rhythm generator (RG) is also indicated by arrow to represent the effect it has on lowering CO_2 threshold for rhythm generation. Note that rhythm generator is operative only when CO_2 is elevated (right hatched panel) leading to alternating inhibition of inspiratory (Insp Bsp) and expiratory (Exp Bsp) bulbospinal neurones (From Sears, 1990).

while the inspiratory motoneurones show no activity. The activity of peripheral chemoreceptors is eliminated due to the hyperoxia, so the prevailing CO_2 level determines the balance of the tonic expiratory and inspiratory activities. Panel 2 shows the state of hypoxic hypocapnia, and manipulation of the drive (see above) by gradually increasing C02, resulted in an inspiratory shift in the pattern of discharge coupled with inhibition of the expiratory discharge. Panel 3 shows a state of normocapnia where CO_2 was increased to generate rhythmic activity. Hence in this scheme, rhythm generation is not represented as a phasic excitation of the motoneurones mediated by inspiratory and expiratory bulbospinal neurones, but rather, as the phasic inhibition of their tonic excitation by the chemical drive. Accordingly Sears (1990) concluded that, with balanced central and peripheral drives there can be a co-activation of inspiratory and expiratory motoneurones (Sears, Berger and Phillipson, 1982) which can also be seen after peripheral chemoreceptor deinnervation at slowly increasing levels of CO_2 penultimate to the onset of rhythm generation.

10. Chest wall reflexes

Studies on the afferent and efferent innervation of the intercostal muscle spindles have revealed an important role of this receptor and its reflexes in breathing. Intercostal motoneurones receive both monosynaptic and polysynaptic

connections from primary and secondary muscle spindles in homonymous nerves of the same and adjacent segments (Sears, 1964; Kirkwood & Sears, 1974; Kirkwood & Sears, 1981). Stimulation of higher threshold afferents, (2x threshold or above), gives rise to a later reflex discharge in expiratory nerves to several adjacent segments, the polysynaptic intercostal-to-intercostal reflex (Downman 1955). The reflex was evoked by stimulation of the internal intercostal and lateral intercostal branch but only with much higher stimulus intensity from the primary muscle nerve to the external intercostal and reflects activation of cutaneous or high threshold muscle afferents. (Aminoff & Sears, 1971). Using intracellular recording Eccles, Sears and Shealy (1962) found that EPSPs are evoked monosynaptically in the thoracic motoneurons by the excitation of low threshold afferents that give rise to group 'Ia' component of the afferent volley recorded at the root entry zone and presumed to arise from muscle spindle primary endings (Sears, 1964b). Also, it was found that unlike the limbs, no 'direct' reciprocal inhibition occurs between inspiratory and expiratory motoneurones with regard to the Ia afferent fibres from their respective muscles.
By recording efferent discharge in the intercostal nerve filaments Sears (1962) found that the fusimotor neurones innervating external intercostal muscle spindles fire maximally during inspiration, while those innervating internal intercostal muscle spindles fire maximally during expiration. This reciprocal activation during breathing is

supraspinal in origin and is altered in a similar way to the response of alpha respiratory motoneurons by such factors as hypoxia, hypercapnia, hypocapnia and the Hering Breuer reflexes (Sears, 1963, 1964c). Independently Critchlow and von Euler (1962, 1963) showed that the inspiratory muscle spindles primary endings discharge maximally during inspiration which indicated that a rhythmic fusimotor activation must exist to offset the unloading of the spindle that would otherwise occur during shorting of the extrafusal muscle fibres. This activation was partly due to spinal reflex drive of the fusimotor neurons from the rhythmic movement of the chest wall. Subsequently by recording efferent activity in the internal intercostal filament, Eklund, von Euler and Rukowski (1963, 1964) showed a close temporal relation between the increased afferent discharge and the volume (chest) record, as obtained by changes in the chemical drive which exerted reciprocal effects on the expiratory and inspiratory fusimotor and alpha motoneuron excitability. The effects of changes in the chemical drive persisted after complete curarization, and were abolished following high spinalization, indicating a close linkage between the fusimotor and alpha motoneuron systems, most probably at a supraspinal level.

The automatic rhythmic activation of alpha and fusimotor neurons during spontaneous breathing represents the demand for a certain change in the length of the respiratory

muscles i.e., to demand for a tidal volume appropriate for the prevailing chemical drive and hence, to match the particular metabolic state. However, during voluntarily breathing as in the awake state i.e., during phonation and expulsive acts, the regulation of respiratory movements is characterized by complex interactions between various control mechanisms subserving various forebrain activities, emotional states, general somatosensory inputs, and peripheral and central chemoreceptors as well as the pulmonary afferent feedbacks, to increase a state of tonic activity for the performance of the specific act.

Following this, Andersen and Sears, (1970) reexamined the work of Pitts, Magoun and Ranson (1939a) using tetanic stimulation of a localized area of the nucleus reticularis giganto-cellularis and ventralis, to demonstrate an inspiratory apneusis with coactivation of the intercostal alpha and gamma motoneurones, accompanied by reciprocal inhibition of the antagonistic motoneurones. Stimulation of surrounding areas evoked an expiratory apneusis with inhibition of the antagonistic (inspiratory) motoneurones. These areas were known to give rise to the long predominately ipsilateral reticulospinal tracts (Pitts, 1946; Pitts, Magoun and Ranson, 1939a) where cells of origin are not located in sites known to fire rhythmically with respiration (see Andersen and Sears, 1970). Thus the authors suggested that these areas mediate the action of systems concerned with the adjustment of a tonic excitatory

bias on the intercostal alpha and fusimotor neurones with reciprocal inhibition of their respective antagonistic motoneurones, to provide a 'bias' controlling the 'operating point' of the motoneurones and hence to regulate the pattern of breathing movements, (Sears, 1965).

As stated above, an intact olivocerebellar system is essential for the coordination integration and smoothing of movements. According to Oscarsson (1980), this role depends on the discharge of the olivary neurones signalling errors to the cerebellum where, according to Ito (1984), plastic changes in synaptic transmission provide the basis of motor learning. Furthermore, it requires the IO to distinguish between self-generated movements during learnt motor behaviours and afferent inputs in response to unexpected perturbations. As a comparator the IO receives inputs regarding both the central command for movement and the effects that command exerted on lower motor centres and the actual movement achieved.

As reviewed above, several studies have been carried out involving limb and eye movement to test the role of the olivocerebellar system in motor control, however, in no case has there been direct access to the central motor command so that its nature and properties could only be surmised via hypothesis.

In the present work the respiratory system is used to study

principles of motor control undertaken by the olivocerebellar system, as the respiratory movements occur naturally, they remain subject to normal control and persist during anaesthesia so they can be studied in spontaneously breathing or artificially ventilated animals, with or without paralysis. Furthermore this system allows control over the endogenous command for respiratory movements by manipulation of the chemical drive, thus providing an ideal opportunity for studying the interactions between the different inputs to the olive (see above).

11. Aims of the study

The aims of this work are: firstly, systematically to probe the IO of paralysed, anaesthetized, artificially ventilated animals for 'central' and proprioceptive respiratory activities; secondly, to determine the origin of these activities by using reversible cold block of the spinal cord; thirdly, to manipulate the chemical drive and hence modify the central command for respiratory movement to study the behaviour of olivary activity as a result of these perturbations.

CHAPTER II METHODS

1. Animals

The experiments were performed, on 8 rabbits and 37 cats with body weights ranging from 1.9 -3.8kg for rabbits and 1.85 - 4.3kg for the cats.

2. Anaesthesia

2:1. Rabbits

Anaesthesia was induced by a mixture of xylazine 'Rompun' (Bayer Ltd., Germany) 3mg/kg body weight and ketamine (Parke Davis Ltd., U.K) 10mg/kg, followed by urethane 500mg/kg and chloralose 70mg/kg in 2 animals, urethane 1.2gm/kg alone in 3 animals and sodium pentobarbitone, Sagatal, (May and Baker Ltd., Dagenham, England.) 40mg/kg in 3 animals through a cannulated ear vein or intraperitoneally. Experience showed that for these long duration experiments on rabbits, urethane alone gave the best overall result in maintaining anaesthesia without the hazards associated with the other two anaesthetics, such as cardio-respiratory depression which was observed in three animals after using pentobarbitone and urethane chloralose mixture, despite artificial ventilation, atropine, noradrenaline and cardiac massage. Supplements of one tenth of the dose of urethane-chloralose mixture or urethane alone were used, while for pentobarbitone an increment of

one fifth the initial dose was used approximately hourly.

2:2 Cats

Sodium pentobarbitone in a dose of 40mg/kg body weight I.P. was used to induce anaesthesia. Increments of 4mg/kg were injected i.v when needed through the cannulated right jugular vein or forearm veins. Anaesthesia was maintained at a level that just abolished the flexor withdrawal reflex of the forelimb (observed at the shoulder) to strong pinch at which level the hindlimb flexor reflex is deeply depressed (Sears, 1964) In paralysed animals anaesthesia was judged by the pattern and stability of breathing and its response to noxious stimuli. Incremental anaesthesia was administered at the same rate as in non paralysed animals and anaesthesia was also checked regularly as the effects of Flaxedil wore off between doses.

3. Surgical procedures

3:1 General

Animals were placed supine with the neck over a cotton roll. A midline incision was made on the ventral surface of the neck, the sternohyoid muscles were separated to expose the trachea for insertion of a Y-shaped canula bearing a polythene tube for the measurement of end tidal F_ACO_2. In cats both the forelimb veins (radial) or the right jugular vein were cannulated. The right femoral artery was dissected, ligated distally and cannulated for blood

pressure recording. In rabbits the ear veins were exposed and identified and then cannulated. These routes were used for supplementary doses of anaesthetics, fluid replacements and the administration of drugs (flaxedil, atropine, noradrenaline) as needed. The animals were then placed prone and the longissimus dorsi, dorsal extensor muscles, and the thoracic multifidus were dissected at T2 and T3 to expose the thoracic spinous processes and at T10 or T11 to expose the mamilliary processes. Then animals were placed prone in a rigid stereotaxic Horsley-Clarke frame with the head rigidly fixed by bars in each external auditory meatus and clamps over the inferior orbital ridge and under the upper jaw on each side. The body was held rigid between clamps gripping the thoracic spinous processes and the mamilliary processes. These procedures resulted in a pendant thorax and partial or slight support of the abdomen. For exposure of the ventral surface of the medulla, the head was supported between ear bars and orbital and mouth clamps while the legs were tied to the frame.

3:2. Dissection of the medulla

Dissection of the medulla was performed from the ventral approach in five rabbits and one cat and from the dorsal side in the remaining animals.

3:2:1. Ventral approach

A midline incision was made on the ventral side of the neck

by extending the tracheostomy incision to the floor of the mouth anteriorly and the skin was reflected back. The omohyoid and sternohyoid muscles were cut proximally near their insertion and reflected. The hyoid bones were dissected free and removed; anastomosing blood vessels traversing the field were divided between ligatures. The larynx and oesophagus were either cut or pulled aside to expose the floor of the atlanto-occipital joint caudally and the pharyngeal tubercle proximally. The anterior longitudinal ligament was cut to expose the anterior atlanto-occipital membrane and working rostrally the occipital bone was freed from the attached fascia by scraping and reflecting the periosteum, thence to expose a large area of the occipital bone The anterior arch of the atlas was removed using dental drill and rongeur, and bone wax used to prevent bleeding from the bone and to prevent air embolism. Minor bleeding from small blood vessels and capillaries was dealt with by cauterization. These procedures exposed the caudal end of the medulla, the spino-medullary junction and the rostral end of the spinal cord which was identified by the convergence of the vertebral arteries to form the basilar artery and by the emergence of the roots of the hypoglossal nerve on each side.

3:2:2. Dorsal approach

Animals were supported in the animal frame as described above. A vertical incision of the skin over the occipital

bone and the rostral half of the neck was made, and the skin reflected. The trapezoid, sternomastoid (medial part) and the posterior group of the capitis muscles were cut proximally at their insertion. The periosteum over the occipital bone was incised and reflected back together with the occipital belly of the occipital frontalis and the superficial blood vessel to avoid any bleeding. A large area of occipital bone and the atlanto occipital joint was removed using a dental drill and rongeur and the diploe packed with bone wax. The overlying dura was incised and reflected to expose most of the posterior lobe of the cerebellum. After dividing the overlying pia-arachnoid membrane the vermis was either displaced rostrally by a plastic retractor cemented to the occiput or was removed by suction to expose the obex and the floor of the medulla.

3:3. Laminectomy

The muscles overlying the second, third and fourth cervical vertebrae were dissected by continuing the dissection of the head more caudally. The spinous processes and the arch of the second and third vertebrae were removed by using a dental drill and rongeur and the dissection was carried laterally as far as possible to expose a wide surface of the dorsal and dorsolateral parts of the cord. The dura was incised and reflected laterally to expose the spinal cord at C2 and C3 segments for application of a cold thermode (see below).

3:4 Dissection of the intercostal nerves

3:4:1 General

A parasaggital incision was performed from T3-T10 on the left side and the underlying latissimus dorsi sectioned and sewn back to the skin edges. The longissimus dorsi was cut between two ligatures at T6 and removed rostrally and caudally over the length of the incision by cutting the attachments to the ribs thus exposing intercostal and levator costi muscles medial to the longitudinally orientated iliocostalis muscle.

3:4:2 Cat

3:4:2:1 Dissection of the internal intercostal nerve

All of these dissections were done using a Leitz dissecting microscope. The iliocostalis muscle was removed at T7, T8 or T9 intercostal spaces. The levator costae was removed by piecemeal stripping, starting at its insertion in the caudal rib. This exposed the medial border of the external intercostal muscle and the underlying internal intercostal muscle with its fibres running ventrolateral at a right angle to those of the external intercostal muscles. The intercostal nerve could usually be seen through the most proximal sector of the internal intercostal muscle lying just caudal to the rib. The dissection of the internal intercostal nerve and its filaments was undertaken with great care as the nerve lies on the extremely thin intercostalis muscle (the inner layer of the intercostal muscle) which separates it from the pleura and ideally a

pneumothorax was to be avoided. Using fine forceps the internal intercostal muscle was removed starting the dissection over the nerve and stripping caudally which progressively exposed the filaments running obliquely. A thin black thread was looped around each filament and this loop tightened around the free distal end of the filament which was then cut distal to the knot. The main nerve was either cut or left in 'continuity' for stimulation (see below). Usually two filaments were dissected to secure against damage. If a pneumothorax was developed during the dissection, the animal was then artificially ventilated and the hole closed with small piece of muscle, covered by gauze or absorbable gelatin sponge and sealed with cyanoacrylic (superglue).

3:4:2:2 Dissection of the external intercostal nerve

The same procedures above were followed as for the dissection of the internal intercostal nerves but usually at the third and fourth intercostal spaces, where the muscles are thicker than those caudally and more 'low threshold' inspiratory motoneurones are encountered. The nerve and the first two filaments were freed by dissecting the external intercostal muscle proximally, where the external intercostal nerve perforates the internal intercostal muscle.

3:4:3 Rabbit

3:4:3:1 Dissection of the internal intercostal nerve

The internal intercostal nerve in the rabbit is thinner than its corresponding external intercostal. It originates from the main intercostal nerve trunk more proximally. Its origin is extremely proximal in the more caudal spaces such that below the T8 level its origin often can not be traced. As above for cat a window was made at the level of the spinal ramus where the internal intercostal nerve was found lying caudal in the segment between the main trunk and the intercostalis. The nerve was exposed and freed for stimulation.

3:4:3:2 The external intercostal nerve

In the upper thorax the external intercostal nerve has 3 main divisions which arise at different parts of the main trunk nerve, one proximal and two distal, the latter pass parallel to the main trunk to supply the distal segments. the distal branch was exposed free by fine dissection and prepared for stimulation 'see below'.

4. Artificial ventilation

Animals were left to breathe spontaneously during the surgical and initial setting up procedures, followed by artificial ventilation with gases under positive pressure using a Harvard Ventilator, Model 683 in closed or open circuit operation. The gas composition could be controlled by different mixtures of air, CO_2 and O_2 fed to the input of the ventilator through reducing valves and flowmeters. The

rate of the ventilator was usually set at 60/minute, and the ventilator stroke volume adjusted to cause hypocapnic apnoea in the absence of added CO2. Without added CO_2 the end tidal F_ACO_2 fell to 2-2.5%. In open circuit, the resistance of the side arm connected to the tracheal cannula was altered to determine the fraction of stroke volume entering the lungs to give apnoea. These procedures minimised both entrainment of the central respiratory rhythm generator through the Breuer-Hering reflexes and transferred movement due to the positive pressure artificial ventilation.

5. General Management

End tidal F_ACO_2 was measured by an infra red gas analyzer (P.K. Morgan Ltd., Chatham, Kent, U.K. Type 9012 MK2). The analyzer was calibrated so that 10% CO_2 gave a one volt output. Blood pressure was continuously monitored from the femoral cannula connected to a pressure transducer (Sanborn 267BC). Mean BP was displayed digitally and the waveform displayed on an oscilloscope. Rectal temperature was maintained at 37°C through a radiant heat and homeothermic blanket (CFP Homeothermic Blanket Control 8140) controlled thermostatically by a rectal probe.

6. Stimulating procedures

The internal intercostal T8 or T9 and the external

intercostal nerves T5 or T6 were the usual sites of stimulation. In three rabbits studied initially the nerves were freed for more than 2cm and ligated at their distal ends using black sutures and cut. The cut nerve was positioned within a narrow tube 5-6mm long and 2mm diameter containing a pair of silver stimulating electrodes 3-4mm apart. However, this led to ischaemia of the nerve detected by the rising threshold of the nerve during the long duration of the experiment. Therefore stimulation was made with the nerve in continuity. The nerve was carefully positioned on a pair of silver electrodes 4-5mm apart. A polythene sheet was placed underneath and above the stimulating electrodes and the sides covered by vaseline to insulate them from the volume conductor. In each preparation the cathode was situated proximally. Stimuli were delivered from a battery operated isolated stimulator (Digitimer Ltd. DS2, England) triggered by pulses from a Digitimer (Devices type D40 30, England). Stimuli were 0.05 - 0.1ms duration square wave pulses of 0.5 - 5 volts amplitude which range was adequate to excite most proprioceptive and cutaneous afferents contributing to mono and polysynaptic intercostal-to-intercostal reflexes (Sears, 1964; Aminoff and Sears, 1970). They were delivered either as single stimuli or as 2-3 successive stimuli 3ms apart and an overall repetition rate 2s.

7. Recording procedures

7:1 Intercostal nerve filaments

Recording was performed through bipolar platinum electrodes positioned ideally at least 5mm apart. In paralysed preparations one electrode was positioned at the base of the filament in the volume conductor and the other at its cut end proximal to the ligature and the filament lifted away from the volume conductor. This procedure maximised the amplitude of the monophasic action potentials and minimized contamination by the ECG.

The first filament of the external intercostal nerve in the proximal sector of the rostral intercostal spaces (usually T3) was found to be the most active at eupnoeic levels of CO_2. On the other hand the first filament of the internal intercostal nerve in the caudal intercostal spaces (T7, T8 or T9) was chosen for recording the central expiratory activity. Sometimes only a short length of the first filament was obtained or it might be thin. In this case the first and second filament or even the main external intercostal nerve were mounted together on the electrodes for recording as explained earlier in the dissection procedures. After the filaments were positioned on their electrodes soft vaseline wax was applied through a hypodermic needle so as to cover all exposed tissues.

7:2 Recording from the inferior olive

Recording was made through glass-coated, platinum-tipped tungsten microelectrodes of impedance 1-4Mohms. The electrodes were connected to a differential FET emitter

follower head-stage attached to a computer controlled motor stepper (significant, ScAT 01-Ultrastepper). The electrode was advanced either from the ventral (3 rabbits) or dorsal (32 cats) aspects of the medulla. Prior to recording, the exposed medulla was rinsed with 0.9% sodium chloride, and any accumulated CSF or other body fluids were aspirated through a thin polythene canula attached to a glass syringe.

7:2:1 Recording from the dorsal approach

The reference point for electrode placement was the obex identified at the apex of the walls of the IV ventricle (calamus scriptorious) under, or lying just caudal to the web of blood vessels, this position corresponds to 14.5-15P in the Horsley-Clarke stereotaxic plane. At this level the most caudal part of the olivary complex is just 0.5-1mm caudally as confirmed by my own histological measurements. Under microscopic control, the electrode tip was carefully positioned at the obex and the reference electrode was usually placed in the subcutaneous tissue, together with a local 'earth' when required. Recording was usually performed on the right side of the medulla, contralateral to the dissected nerves; systematic probing was first begun laterally at the level of the obex or just caudal to it. The electrode was inserted into the medulla and advanced in 50um steps in depth for 3mm then slowly in 10um or smaller steps until the inferior olive activity was heard as identified by its low frequency 'sputtering' sound, much

like 'popcorn popping' (Gellman et al. 1983). This protocol was continued by moving the electrode medio-laterally and caudo-rostrally in tracks 0.1 - 0.5mm apart as required by the specific aims of the experiment

7:2:2 Recording from the ventral surface of the medulla

The ventral reference point was the origin of the basilar artery where the vertebral arteries converge. The area investigated was contralateral to the side of the dissected nerves, lying medial to the hypoglossal rootlets and rostral to the vertebral arteries. A silver ball reference electrode was placed on the occiput close to the microelectrode. The procedures of probing were the same on both sides. From the ventral side, olivary activity was after encountered in less than one mm of electrode travel during penetration.

8. Signal processing

The animal was earthed through the animal frame which was connected to the common earth point. The recording electrodes from the intercostal filaments were connected via 'driven' shielded leads, to high-impedance differential FET input stage connected to a preamplifier (D160 Digitimer Ltd., England). For the filaments a low frequency cut of 3ms, a high frequency cut of 3KHz and a sensitivity of 50-100uV/V was used, while for EMG and ECG signals only a band width of 1.6-500Hz and a sensitivity of 500uv/V was used.

For olivary signals the microelectrode together with the reference and earth electrodes were connected to a differential FET emitter Follower head stage (NL 100, Digitimer Ltd. England) connected to a preamplifier with a band width usually of 1.6 - 3KHz and a gain typically of 50- 500uV/V, these parameters and those of the magnetic tape speed being adjusted as required.

Signals at the volt level were displayed on a dual beam, 2 channel 'persistence' storage oscilloscope (Tektronix 5113) and a 3 channel digitizing Oscilloscope (Tektronix 5223), and fed in parallel to a computer based interface (CED 1401 - Cambridge Electronic Design Ltd., Cambridge U.K.) for on line or off line later analysis by CED Sigavg or Spike2 programmes. Signals were also full wave rectified and low pass filtered through 'leaky' integrators with a time constant of 100-200ms to display the respiratory phasing of any of the recorded signals. Some signals were processed with a window discriminator (D130 Digitimer Ltd., U.K.). Whereas one was used to select olivary spikes from the baseline noise, the other was used to detect trigger pulses in the tape recording.

All signals were recorded on a half an inch 4-channel magnetic tape recorder (Store 4 Racal Instruments, England) at a tape speed of $1^{7}/_{8}$ - $3^{3}/_{4}$ inches/sec and a modulation of $\pm$1 volt. Typically 3 channels were used for nerve recordings and the fourth for the trigger pulse fed to the

interface or for recording end-tidal F_ACO_2, the phasing of the respiratory pump or the ECG.

9. Cold blocking procedures

The spinal cord was cooled at the level of the second or third cervical segments through a closed cooling system that circulates fluid at a controlled temperature through a thermode. This system as illustrated in Fig. 2 comprised a Circulator (C-400 Techne-Cambridge Ltd. U.K.), a Flow Cooler (FC 200 Techne-Cambridge Ltd. U.K.) and a thermode (kindly lent to us by Prof. F. Cervero). The thermode is a hollow copper block arched and faced with a thin silver plate at one side to fit on the curvature of the spinal cord. Its opposite side carries narrow-in and out- rigid pipes connected to rubber tubes connected to the circulator and the flow cooler (Fig. 2). The efficient operation of this system depended on an optimum flow rate of fluid through the circulator to maintain the rate of heat transfer from the system to the circulator via the exchanger. This was achieved by shunting the high flow-impedance of the probe with a low-resistance bypass. To avoid pressure block of transmission within the spinal cord, the thermode was placed gently on the dorsolateral surface of the cord. The second or third cervical segments were chosen as sites for thermode application so as to avoid direct cooling of the phrenic nucleus. Temperatures were monitored by a calibrated sensor placed on the flat

Fig. 2.

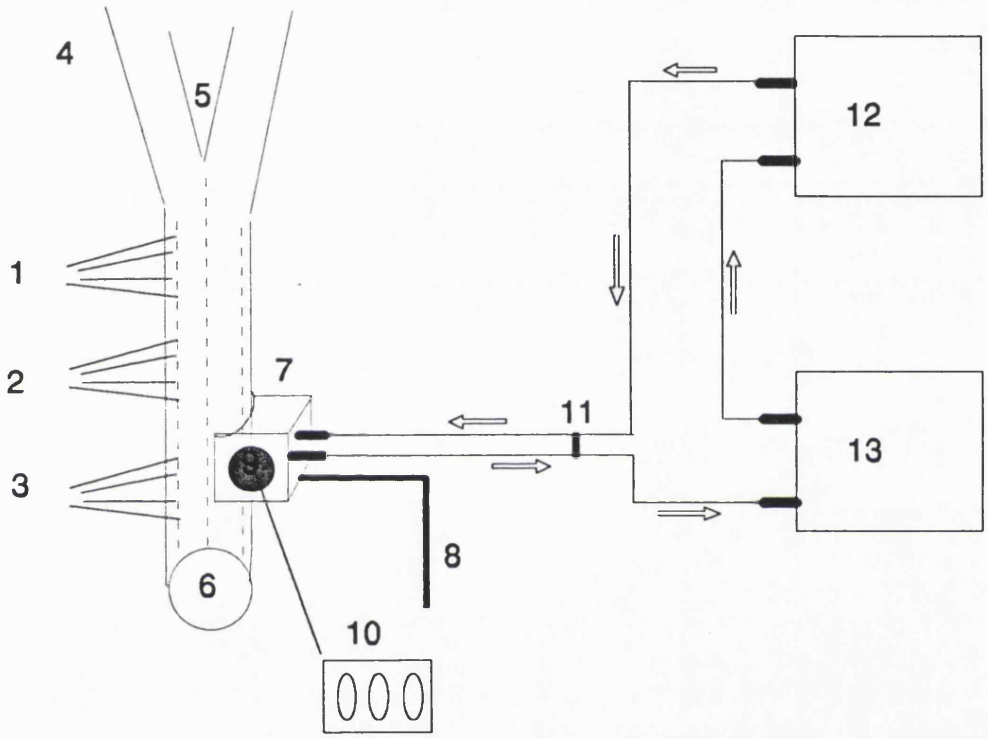

Fig. 2. Schematic drawing showing the cooling system of the spinal cord. 1, 2 and 3 represent the 1st, 2nd and 3rd cervical segments; 4, caudal medulla; 5, obex; 6, spinal cord; 7, thermode (hollow brass block with silver coating); 8, thermode holder; 9, thermocouple; 10, calibrated temperature sensor; 11, by-pass; 12, flow cooler; 13, circulator.

surface of the thermode.

10. Histology

At the end of each of 21 experiments two or more electrodes were left in the medulla as landmarks of recording sites. The animal was then killed by intravenous injections of large doses of anaesthetic. An additional electrode or a short length of wire was inserted immediately at the obex perpendicular to the medulla and left also as a marker. The brainstem was excised between the first cervical segment caudally and the pons rostrally and fixed in 10% formal saline for 3-5 days. Specimens were either cut in 70-100um thick sections by a vibratome, or embedded in paraffin and cut in 15-20um thin sections. The majority of sections were transverse (17 experiments), some were parasagittal (2 experiment) and horizontal (2 experiment). Every other, or every third paraffin section was stained with a combination of Cresyl Fast Violet and Luxol Fast Blue. Thick vibratome sections were stained with Cresyl Fast Violet alone. Stained sections were mounted in DPX and covered by slide covers. Slides were examined under the light microscope to identify the location of the tracts and to study the dimensions and morphology of the inferior olive.

Using the microelectrodes as landmarks, it was possible by interpolation to determine fairly precisely the location in the olive of any recording site and its relation to the

obex which was used as a reference point during recording from the inferior olive. Locations of recording sites were also noted by taking micrometer readings of their depth (2.860 - 3.940mm) below the dorsal surface of the medulla and by reading the locations of the microelectrode tracks. These locations were displayed on a diagrammatic unfolded DAO in the horizontal plane. This was produced by rostrocaudal reconstruction of horizontal transverse sections equally spaced by 0.250mm intervals (see later). In initial studies it was found that shrinkage of thin sections was less than 10%. Accordingly no allowance for shrinkage has been made in plotting recording sites and it is acknowledged that some errors may have resulted from this lack of correction.

CHAPTER III RESULTS

SECTION A: Respiratory Results

1. Patterns of breathing

1:1. Eupnoea

The pattern of spontaneous or fictive eupnoeic breathing was recorded as alternating efferent discharges of alpha and gamma motoneurones from the external (inspiratory) and internal (expiratory) intercostal nerve filaments as shown in channels 1 and 2 of Fig. 3, with their integrated versions shown in channels 3 and 4. Usually small and large spikes were present. The latter were attributed to the alpha motoneurones as identified by their strong periodicity, being confined to one or other phase of the cycle, and their low firing rate <20Hz (Sears, 1963; Anderson and Sears 1970). The small spikes were attributed to gamma motoneurones and had an amplitude of about one half to one fifth of the alpha spikes, a firing frequency of 2-10 times greater than that of the alpha spikes and their phasic discharge typically preceded that of the alpha spikes (Sears 1964 a,b,c; Eklund, von Euler and Rutkowski, 1964), as clearly illustrated in Figs. 10 and 13. The small spikes usually occurred throughout the respiratory cycle. They were either tonic, respiratory modulated or wholly periodic. An individual fusimotor unit could display all the three types of firing in response to elevation of CO_2

Fig. 3. Neurograms from a paralysed, fictively breathing animal at three different levels of CO_2. Channels 1 and 2: external (inspiratory) and internal (expiratory) intercostal nerve filaments. Channels 3 and 4: their respective integrated versions (time constant 100ms). F_ACO_2: 3.0%, 3.7% and 4.3% for panels A, B and C respectively.

Fig. 3.

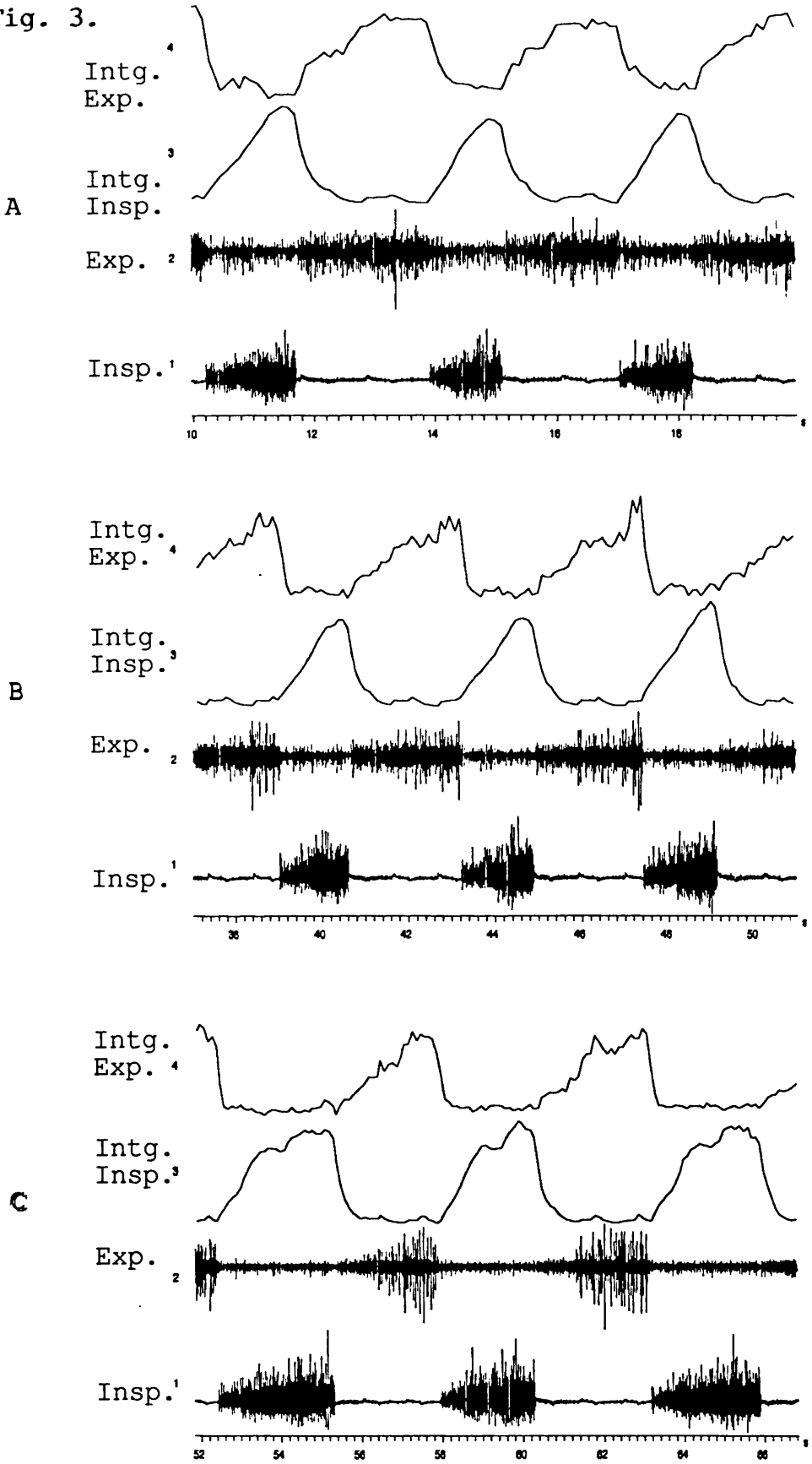
A
Intg. Exp. 4
Intg. Insp. 3
Exp. 2
Insp. 1
10
12
14
16
18
B
Intg. Exp. 4
Intg. Insp. 3
Exp. 2
Insp. 1
38
40
42
44
46
48
50
C
Intg. Exp. 4
Intg. Insp. 3
Exp. 2
Insp. 1
52
54
56
58
60
62
64
66

from apnoeic levels of 3.0% (panel A), through eupnoea at a level of 3.7% (panel B) to hypercapnia at a level of 4.3% as illustrated in panel C. The discharge for the alpha spikes was invariably periodic occurring in inspiration or expiration according to the filament of origin. The discharge frequency of both types of spikes was found to be dependent on the level of end expiratory F_ACO_2 (Fig. 3).

The integrated inspiratory intercostal nerve filament activity showed initially a ramp pattern of discharge leading to a plateau with abrupt termination (channel 3 in panel C). Differences in the slope and height of the plateau reflected the number of units recruited and their discharge rates. In the paralysed, artificially ventilated animal this integrated activity may be taken as reflecting the central inspiratory output, but there might, or might not be modulation at the higher rate of the respiratory pump, as seen at the higher level of CO_2. The integrated version of the expiratory filament activity (channel 4 in panel C) usually showed a slope with pump modulation and a plateau where full recruitment was seen for both alpha and gamma motoneurones at high CO_2 levels. For technical reasons (see i.e., sampling rates; Methods) only the integrated versions of the inspiratory and expiratory motoneurones activities will be illustrated in most of the figures and in particular when time compressed data was used for the purpose of demonstrating the sequence of events during the CO_2 titrations and cold blocking experiments (see later).

1:2. Hypocapnia

Under the normal experimental conditions, the eupnoeic levels of F_A CO_2 encountered in this work varied between 1.95 and 6.2% (mean = 3.52, $\pm$1.48% (SD), n = 40). To create hypocapnic apnoea, the preparations were hyperventilated by using a fast pump rate (40 - 60/min) and a small stroke volume (15 - 20ml) so that without the addition of CO_2, the F_A CO_2 fell to about 2.0% leading, most commonly, to a tonic expiratory alpha and gamma motoneurone discharge, or occasionally to a tonic inspiratory discharge, depending on whether the preparation is inspiratory or expiratory biased, (cf Bainton, Kirkwood and Sears, 1978). Figs. 4 and 5 illustrate typical recordings from a paralysed, fictively breathing expiratory biased preparation. In the control recordings (A of Fig. 4), the upper two traces display the original inspiratory and expiratory intercostal motoneurone activities, as recorded from their respective nerve filaments, with their corresponding integrals below. The inspiratory record contains both alpha and gamma activities which are reciprocally inhibited during expiration. The expiratory record is dominated by small gamma spikes, which discharge tonically and their activities only diminished during inspiration. The record also shows large alpha spikes firing mainly during the expiratory phase. The composite inspiratory and expiratory recordings showed some units firing in phasic bursts with each deflation and inflation phase respectively, of the respiratory pump at a rate of 59/min. This phasic

Fig. 4. Continuous titration of neural activity with reduction of chemical drive. A, illustrates recordings during the control period from a paralysed, fictively breathing, expiratory biased preparation. Upper two traces: inspiratory and expiratory intercostal neurograms, respectively; lower two traces: their corresponding integrated versions. Note that the composite inspiratory and expiratory recordings showed some units firing in phasic bursts with each deflation and inflation phase, respectively, of the respiratory pump at a rate of 59/min (best seen in their integrals). The dotted line represents the zero level of the integrator. F_ACO_2 = 4.5%. Horizontal bar = 2s. B, shows in a time compressed recording the whole sequence of events from eupnoeic breathing to hypocapnic apnoea. channel 1: expiratory, channel 2: inspiratory integrated intercostal motoneurone activities. CO_2 = 4.5%, 3.0% and 1.5% at start of recording, after 300s and 600s, respectively. For more details see Fig. 5.

Fig. 4.

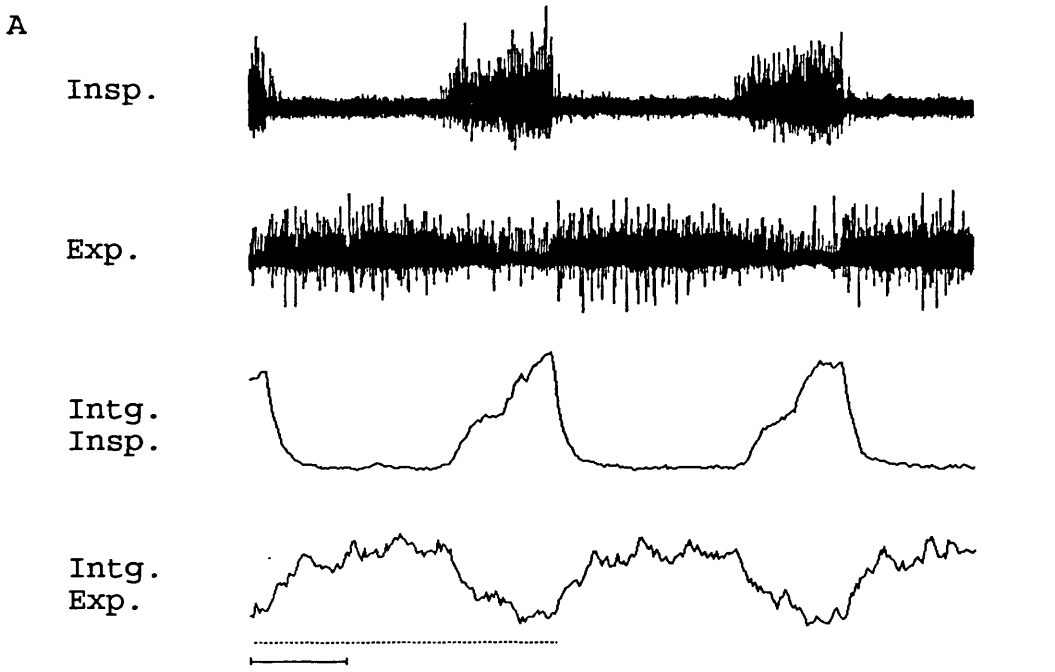
A
Insp.
Exp.
Intg.
Insp.
Intg.
Exp.

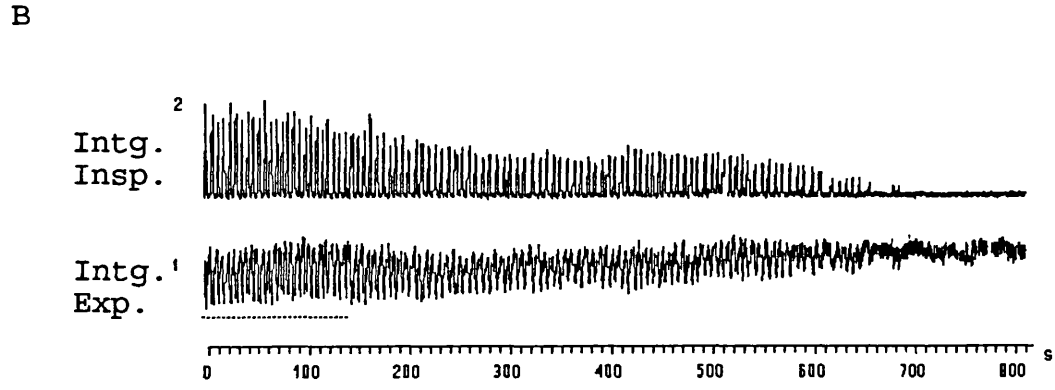
B
Intg.
Insp.
2
Intg.
Exp.
1
0
100
200
300
400
500
600
700
800
s

activation represents the chest wall 'deflation' and 'inflation' reflexes of the external and internal intercostal muscles (Sears, 1958, 1964d; Ramos and Mendosa, 1958). In contrast to the inspiratory integral (third trace), which comes to the baseline between bursts, the expiratory integral (fourth trace) stands well above the zero level (dotted line), this is because of the tonic gamma activity. Both filaments were strongly active at the elevated level of F_ACO_2 of 4.5% and a central respiratory rhythm occurred at 9/min. B shows the whole sequence of events from eupnoea to hypocapnic apnoea with channels 1 and 2 showing the inspiratory and expiratory intercostal motoneurone activities, respectively. The level of CO_2 was very gradually reduced in small increments of 0.5%, to reach 3.0% after 300s and 1.5% after 600s and maintained thereafter at the same level. The inspiratory activity progressively attenuated before it was completely abolished by 700s, during which time the expiratory activity was rendered tonic (note zero level of the integrator). This was due to the progressive reduction in phasic inhibition reciprocal to the declining action of the antagonist. This is best illustrated in Fig. 5, in which A, B and C show representative expanded sections from the data displayed in Fig. 4 B, taken at 0.0-100s, 400-500s and 700-800s, respectively. Channels 1 and 2 display the integrated expiratory and inspiratory activities, respectively. A shows the control recording at a CO_2 level of 4.5% when both activities were strongly rhythmic. When the CO_2 level was

Fig. 5, shows representative expanded sections from the data displayed in Fig. 4 B, taken at 0.0-100s in A, 400-500s in B and 700-800s in C. Channel 1 and 2 display the integrated inspiratory and expiratory activities, respectively. The dotted line under each expiratory record indicates the zero level of the integrator. A: control recording at CO_2 level of 4.5%. B: Intermediate state at CO_2 of 2.5%, note the gradual reduction of inspiratory activity and the subsequent decreasing inhibition of the expiratory activity. C: further lowering of CO_2 to 1.5%, resulted in slowing, disruption of rhythm and eventual loss of the inspiratory activity (end of record), subsequently the expiratory activity was rendered tonic with pump modulation representing the chest wall inflation reflex.

Fig. 5.

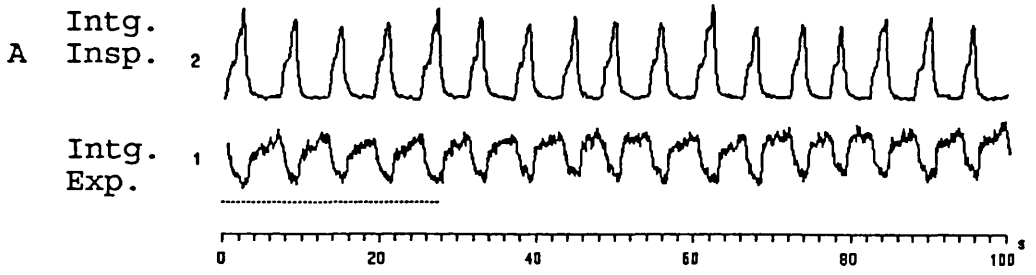
A
Intg.
Insp.
Intg.
Exp.
2
1
0
20
40
60
80
100
s

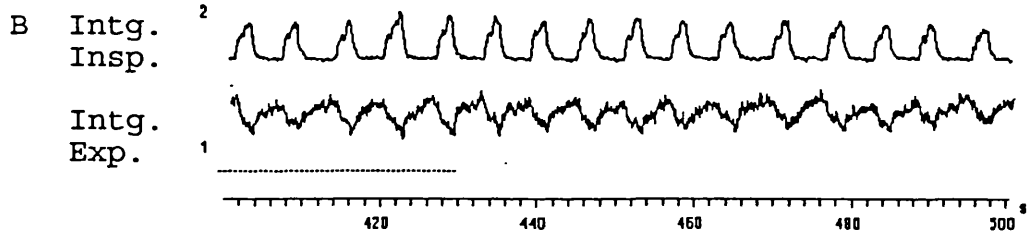
B
Intg.
Insp.
Intg.
Exp.
2
1
420
440
460
480
500
s

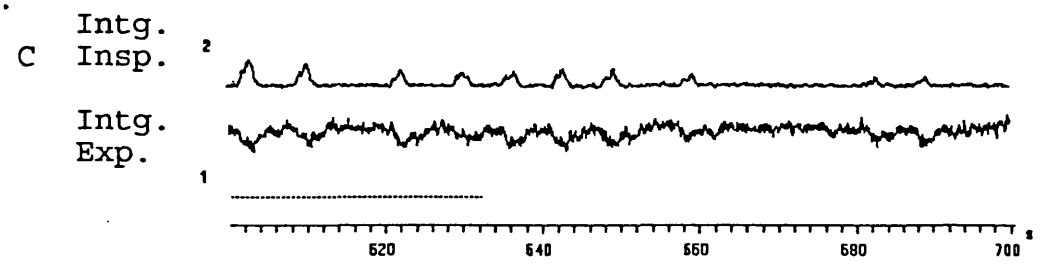
C
Intg.
Insp.
Intg.
Exp.
2
1
620
640
660
680
700
s

lowered to 2.5% as in B, the inspiratory activity gradually reduced and with this an accompanying reduction of the phasic inhibition of the expiratory activity and this represents an intermediate state. Further lowering of CO_2 to 1.5%, resulted in loss of the inspiratory activity (end of C), during which time the expiratory integrated activity was rendered tonic with pump modulation. The tonic component of activity which was due mainly to the gamma spikes was dependent on the prevailing CO_2 level. The pump modulation represents the chest wall inflation reflex of the internal intercostal muscles which is subserved by afferents from the muscle spindle primary and secondary endings which monosynaptically excite the internal intercostal motoneurones (Sears, 1964b; Kirkwood and Sears, 1974).

The central rhythmic respiratory drives to the inspiratory and expiratory motoneurones were established in several investigations to give reciprocal inhibition to their respective antagonistic motoneurones (Sears, 1964c, 1966; Aminoff and Sears, 1971). Similarly, the central tonic respiratory drives in hypocapnic apnoea, and that due to peripheral chemoreceptor drives were shown to manifest themselves also in a reciprocal manner (Bainton, Kirkwood and Sears, 1978). This was further confirmed in the present study by titrating the neural activities of the intercostal inspiratory and expiratory motoneurones with elevation of CO_2 level. Fig. 6A illustrates the recordings during the

control period, the upper two traces being the inspiratory and expiratory intercostal neurograms, respectively, with their corresponding integrated versions below. Fig 6B shows in a time compressed recording the entire sequence of events as CO_2 was slowly elevated from the state of hypocapnic apnoea to eupnoea. The upper trace shows the inspiratory activity while the lower trace illustrates the expiratory activity. Initially there was no activity of the inspiratory population at CO_2 level of 2.25% while the expiratory filament shows evidence of rhythmicity superimposed on a tonic discharge. This expiratory rhythmic activity was attributed to a subliminal inspiratory drive which periodically inhibits the tonic expiratory discharge, however, not sufficient enough to cause firing of the inspiratory motoneurones themselves (cf. Bainton et al., 1978). As CO_2 was progressively increased this tonic discharge of the expiratory motoneurones developed into the periodic discharge of eupnoea or (stimulating breathing) due to the progressively increasing periodic inhibition related to central respiratory generation. This is most obvious at a CO_2 level of 3.5%, when the inspiratory motoneurones became progressively active, the peak amplitude increasing rapidly with increasing CO_2 level (4.3%) and with this a progressive deepening of the periodic inhibition of the expiratory motoneurones. Such titrations were performed in most experiments to determine the threshold for rhythm generation for the sample populations of motoneurones and also to characterise the

Fig. 6. Continuous titration of neural activity with elevation of the chemical drive. A, illustrates recordings during the control period. Upper two traces: inspiratory and expiratory intercostal neurograms, respectively; lower two traces: their corresponding integrated versions. B, shows the whole sequence of events in a time compressed recording as CO_2 was slowly elevated from the state of hypocapnic apnoea to eupnoea. Upper trace, inspiratory activity; lower trace, expiratory activity. The level of CO_2 was slowly raised from 2.25% to 3.50% when rhythm started and by 4.3% it was fully restored.

Fig. 6.

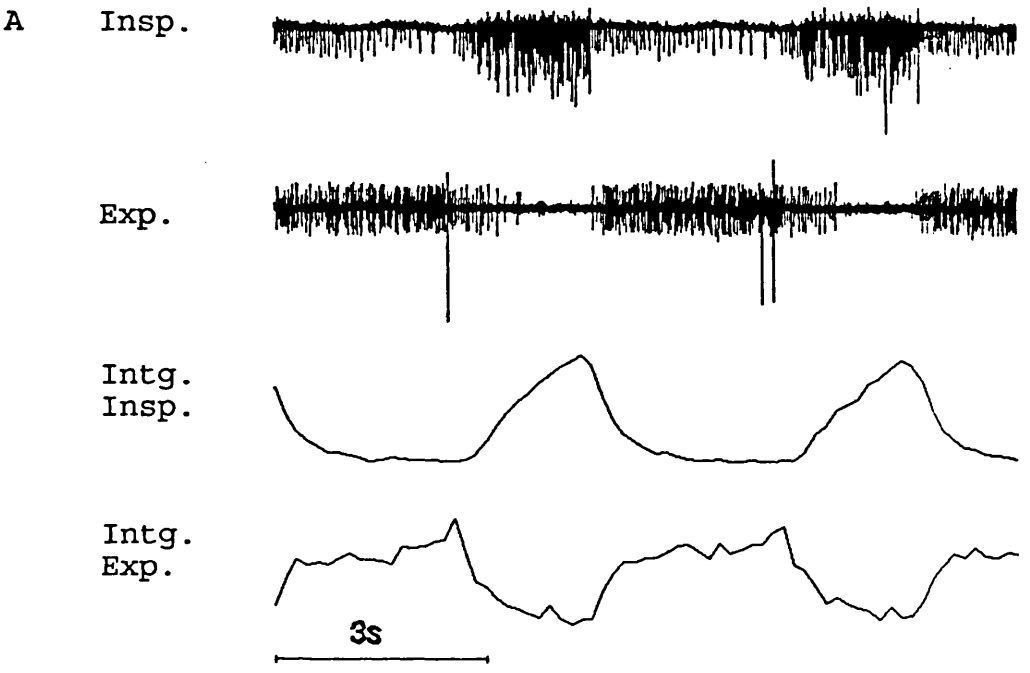
A
Insp.
Exp.
Intg.
Insp.
Intg.
Exp.
3s
B
2.25%
3.50%
4.3%
Intg.
Insp.
Intg.
Exp.
60s

state of the preparation as expiratory or inspiratory biassed.

1:3. Chest wall reflexes

Because the experiments involving the inferior olive (Section IIIB) depended on the detection of the proprioceptive inputs as judged by the reflex effects at spinal cord level, it was necessary to determine the phasing of the mass afferent activities during artificial ventilation. Such experiments are illustrated in Figs. 7 and 8 from different preparations artificially ventilated to create hypocapnic apnoea but with recordings made prior to paralysis. Channel 1 and 2 of Fig. 7, shows the mass afferent activity recorded from the peripheral stumps in the whole external intercostal nerve and a filament of the internal intercostal nerve, respectively, both being pure muscle nerves (Sears, 1964a). Their respective integrals are shown in channel 3 and 4; note that the expiratory neurogram is contaminated with sporadic EMG unit activity. Channel 5 illustrates the phasing of the artificial ventilation, as measured by the changes in airway pressure due to the respiratory pump. The low tidal excursions of pressure reflect the pattern of artificial ventilation adopted, i.e., fast rate, low tidal volume (see Methods). In panel A, the left dotted line shows the timing relationship between the maximum afferent activity in the external intercostal nerve and the deflation phase of the pump. The right dotted line shows that the peak afferent

Fig. 7. Demonstration of the relationship between the chest wall deflation and inflation reflexes and their respective afferent discharge in a hypocapnic, nonparalysed preparation. Channels 1 and 2 shows the mass afferent activity recorded from the peripheral stumps in the whole external, and a filament of the internal, intercostal nerves, respectively, with their integrals shown in channels 3 and 4. Channel 5 displays the airway pressure of the respiratory pump (cm H_2O). The left and right dashed lines in panel A shows the relation between the phasing of the pump and the deflation and inflation reflexes, respectively. Panel B shows the effect of stopping the pump at the end of its deflation phase (artifact on channels 1-4) on the afferent discharge. Ventilation rate 59/s.

Fig. 7.

A

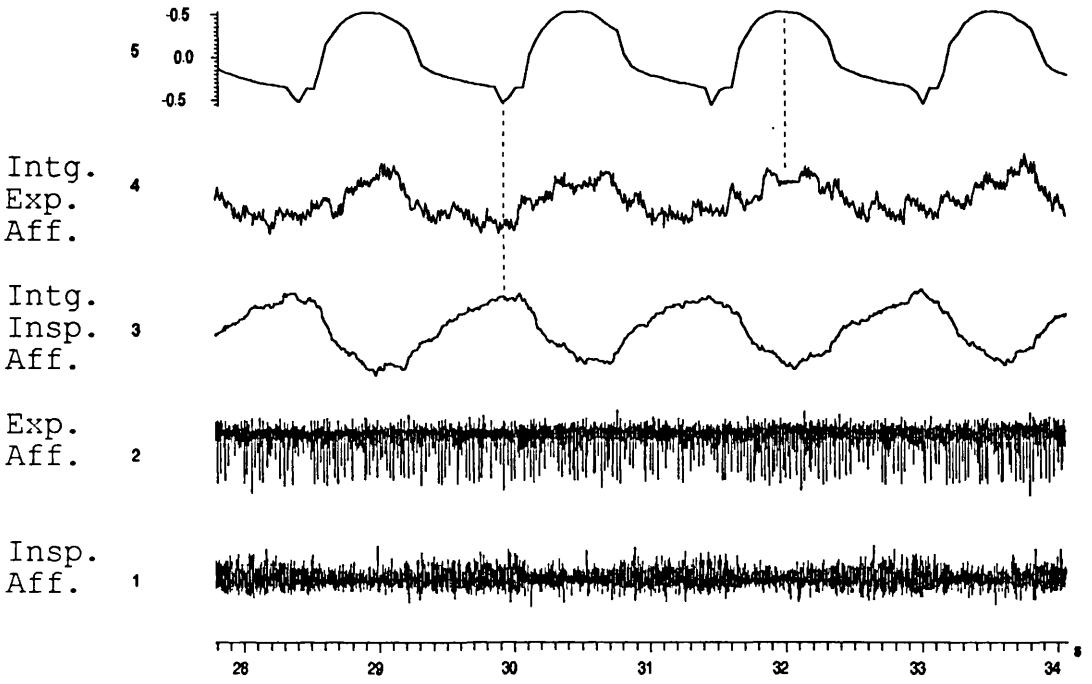
-0.5
0.0
-0.5
5
Intg.
Exp.
Aff.
4
Intg.
Insp.
Aff.
3
Exp.
Aff.
2
Insp.
Aff.
1
26
29
30
31
32
33
34
s

B

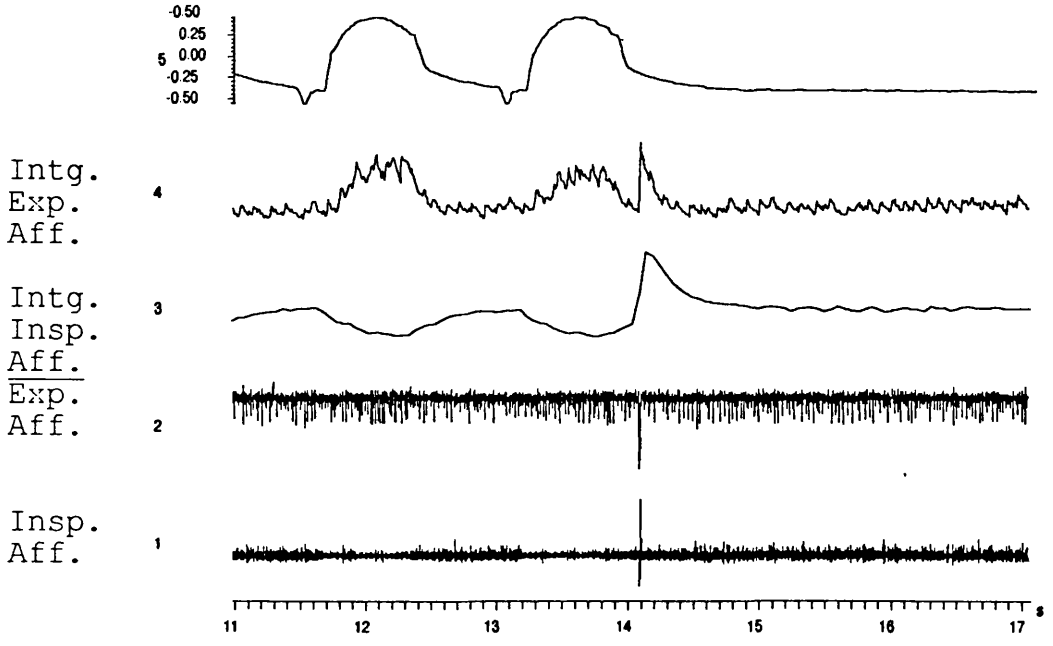
-0.50
0.25
5 0.00
-0.25
-0.50
Intg.
Exp.
Aff.
4
Intg.
Insp.
Aff.
3
Exp.
Aff.
2
Insp.
Aff.
1
11
12
13
14
15
16
17
s

activity in the internal intercostal nerve filament is in synchrony with the peak inflation phase of the pump. When the pump was stopped at the end of the deflation phase, as indicated by the mechanical artifact in channels 1-4 of panel B, the mass afferent discharge in the external intercostal nerve was abruptly rendered tonic, as clearly seen in the integral (channel 3), and that of the internal intercostal nerve filament became also tonic with loss of the pump-modulated activity.

In Fig. 8 the upper trace shows the integrated mass afferent activity in the external intercostal nerve at T6 segment, the middle trace shows the EMG recorded from the most proximal sector of the internal intercostal muscle at T7 segment and the lower trace shows the airway pressure. As for Fig. 7A, the left dotted line shows the relation between the maximum afferent activity in the external intercostal nerve and the deflation phase of the pump, The right dotted line shows that the peak EMG activity in the expiratory muscle is related to the peak inflation phase of the pump when the internal intercostal muscles would have been maximally stretched. When the pump was stopped at the end of the deflation phase, as indicated by the arrow and dotted line of panel B, the afferent discharge in the external intercostal nerve progressively increased, however, the EMG activity in the expiratory muscle ceased. By contrast, when the pump was stopped at the peak of inflation, as shown in panel C the expiratory activity was

Fig. 8, demonstrates other examples of the chest wall reflexes. Upper trace, integrated mass afferent activity in the external intercostal nerve; middle trace, integrated EMG activity in the internal intercostal muscle; bottom trace, output of the airway pressure of the respiratory pump. Panel A, the left dashed line shows the deflation-dependent phasing of the afferent discharge, the right dashed line shows the inflation-related discharge in the EMG. Panels B and C, the arrows indicate pump stop in deflation and inflation respectively. Ventilation rate 59/s. Horizontal bar 2sec.

Fig. 8.

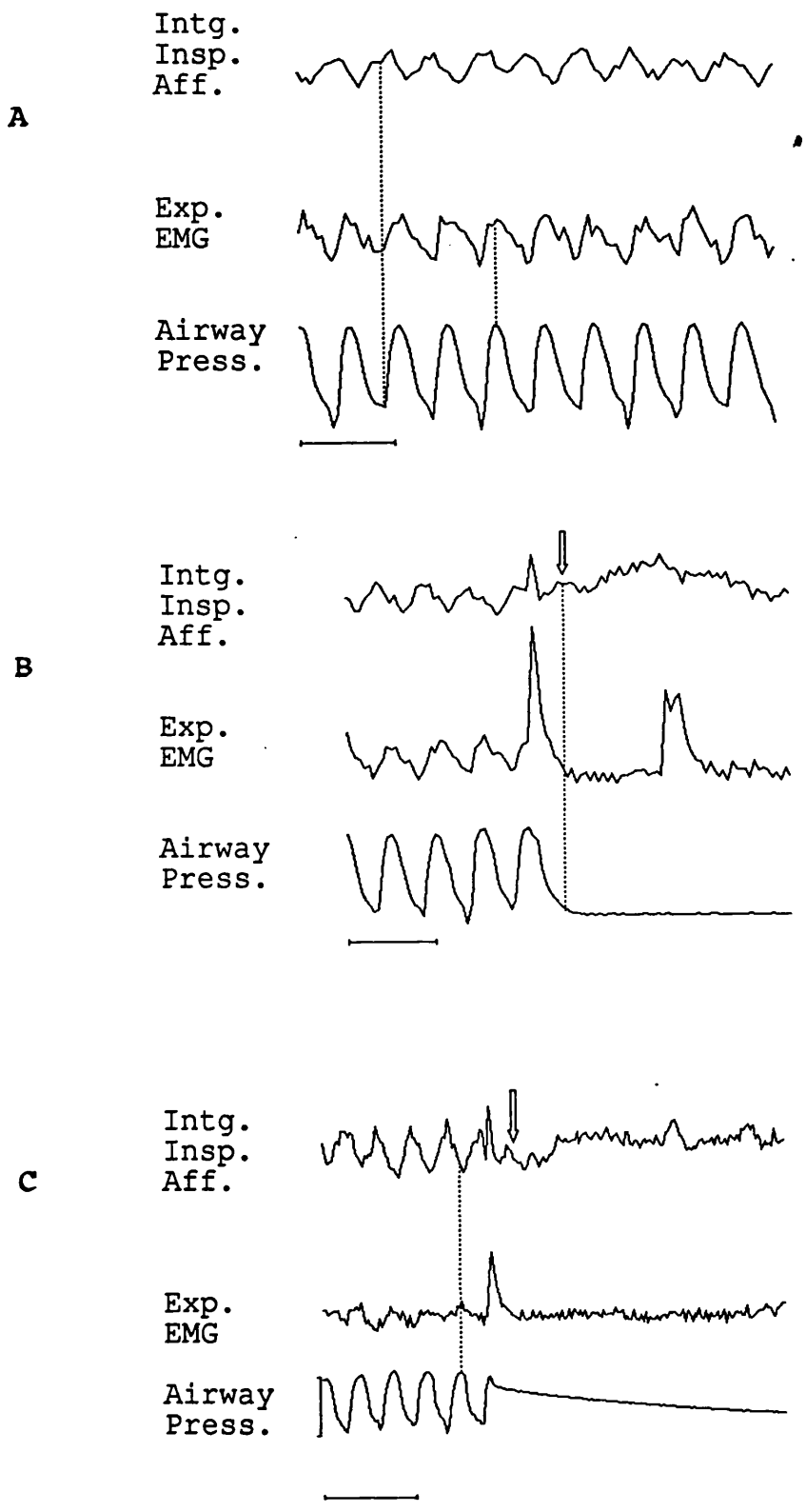
A
Intg.
Insp.
Aff.
Exp.
EMG
Airway
Press.
B
Intg.
Insp.
Aff.
Exp.
EMG
Airway
Press.
C
Intg.
Insp.
Aff.
Exp.
EMG
Airway
Press.

rendered tonic, while the afferent discharge in the external intercostal nerve became silent. This behaviour differs from that illustrated in panel B of Figs. 7 and 8; this because, as the ventilation was achieved in a closed system, the suction due to the CO_2 sampling pump resulting in a slow withdrawal of gas from the lungs resulted in a progressive fall of lung and chest wall volumes; consequently the expiratory muscles shortened, reducing the discharge of their spindles (as illustrated in Fig. 7) and hence reduced the level of reflex excitation of the expiratory motoneurones.

The behaviour of the chest wall reflexes at levels of CO_2 just at threshold for rhythm generation, is illustrated in Fig. 9, by continuous recordings from a different preparation. To the left the central respiratory drive is represented by two cycles of alternating inspiratory (upper trace) and expiratory (lower trace) activities at a rate of 17/min. However, as seen in the middle of the trace this changes to a burst of activity locked to the pump rate of 59/min, representing the deflation reflex of the inspiratory motoneurones and the inflation reflex of the expiratory motoneurones. The right third of the figure shows the reverse transition from the pump locked rhythm to that of the central respiratory rhythm, followed by a sustained period of the latter. This fluctuation in activity may be explained by the fact that when there is an appreciable liminal drive, this results in the central

Fig. 9.

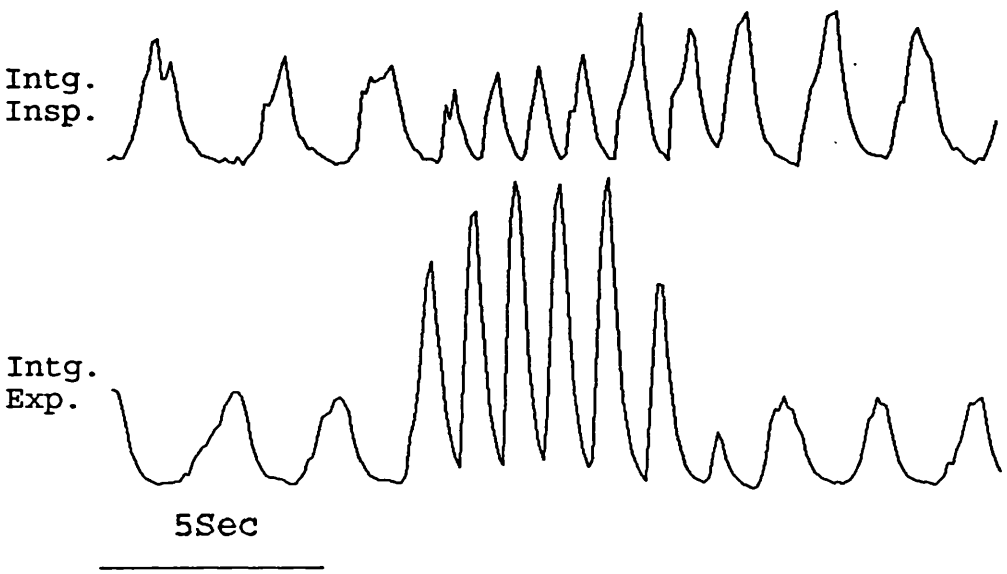

Fig. 9. Interaction between the central respiratory drive (left and right thirds) and the chest wall inflation and deflation reflexes (middle third of the continuous record) near threshold for central respiratory rhythm generation. Upper trace, integrated internal intercostal (inspiratory) and lower trace external intercostal (expiratory) neurograms. Horizontal bar 5s.

respiratory drive to dominate as shown in the left and right thirds of the figure with a reciprocal inhibition at segmental level of the deflation and inflation reflexes by central expiratory and inspiratory drives respectively. However in the middle third of the same figure such an inhibition did not occur, this may be due to the lack of an appreciable subliminal phasic drive to the corresponding respiratory motoneurones (Bainton, Kirkwood and Sears 1978).

2. Cold blocking of the spinal cord

It has long been recognized, that the main advantage of cooling methods is the ability to produce repeated, brief, local functional blockade which is reversible. In this study, blocking of the spinal cord was performed to examine its effects on the behaviour of respiratory motoneurones discharge during eupnoea, hypocapnia and reflex and other central activities evoked by the proprioceptive inputs. All experiments involving cold block of the spinal cord were made in paralysed artificially ventilated preparations with intact vagi. Under paralysis the movements are uniform as the positive pressure relieves the ribcage of the elastic recoil of the lung. Hence, the ribcage expands upwards and downwards along the passive lung volume chest wall pressure characteristic curve (see Campbell and Newsom Davis, 1970), or the corresponding rib cage configuration curve if appropriate measurements of chest wall and abdominal

diameters (cf. Konno and Mead, 1967) are made. All these parameters remain constant in the present work, as changes in chemical drives were made by adjusting the composition of the gases while rate and tidal volume were held constant.

Because the procedures of cold block and the following recovery take a considerably long time, the cooling thermode was first cooled to the desired temperatures (3-5°C) (Trendelenburg, 1910b) before being applied to the different aspects (i.e., dorsolateral, lateral and ventrolateral) of the second or third cervical segments.

2:1. Cold block in eupnoea

The following experiments were conducted at a level of CO_2 higher than the eupnoeic level to minimise the effect of spontaneous changes over the period of the experiment. Fig. 10 illustrates typical recordings from a preparation showing an inspiratory bias. The discharges of inspiratory and expiratory motoneurones are shown in the upper two traces with their respective integrated versions below. In the control recordings shown in panel A, the inspiratory and expiratory motoneurones are strongly active at the elevated CO_2 level of 4.85% and a central respiratory rhythm occurs at 9/min. The inspiratory record displays periodic large amplitude spikes due to alpha motoneurones accompanied by a tonic discharge of small amplitude spikes of gamma motoneurones, and the composite recording includes

Fig. 10.

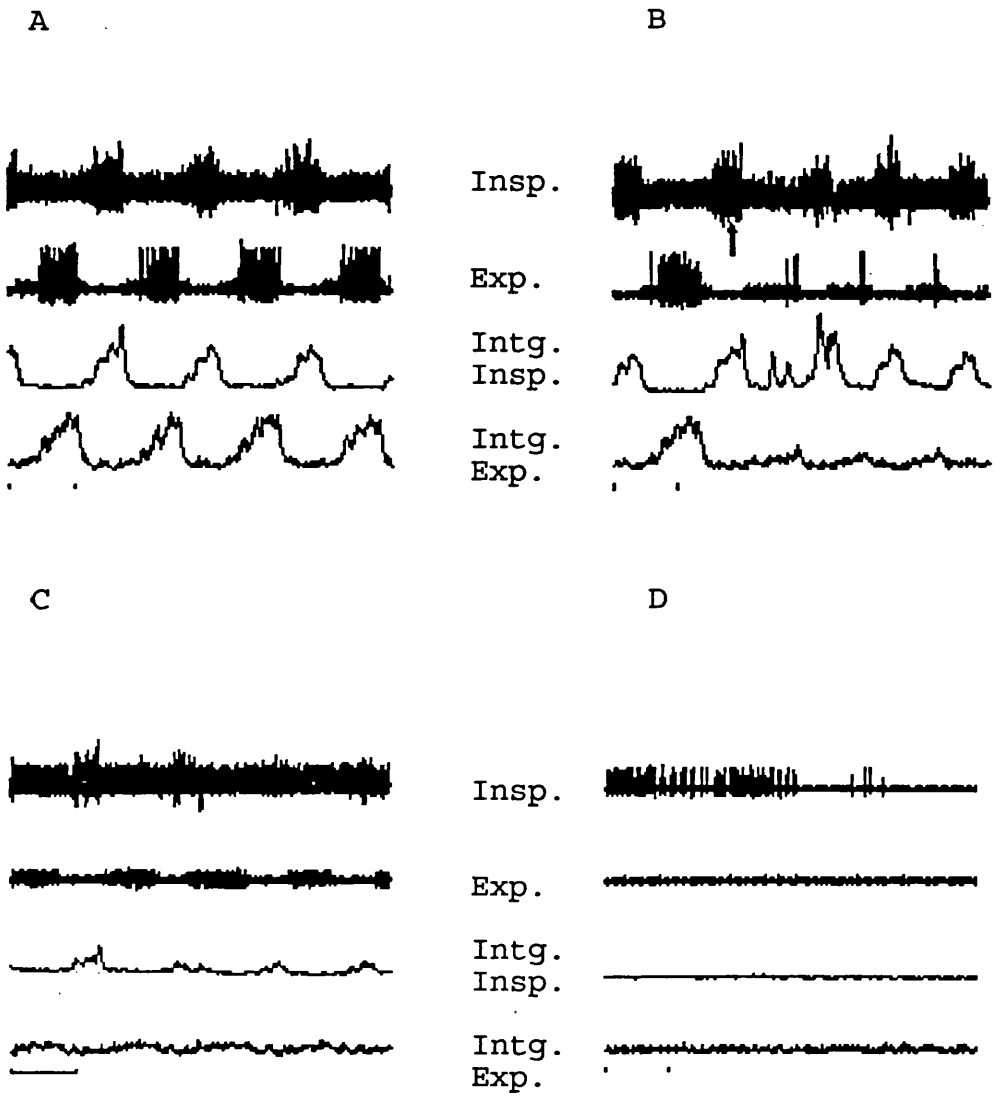

Fig. 10. Efects of cold block of the spinal cord (at C3 segment) during eupnoea. Upper two traces, recordings from external (inspiratory) and internal (expiratory) intercostal nerve filaments. Lower two traces, integrated versions of the upper two. Note that the composite inspiratory and expiratory recordings include units firing in phasic bursts with each deflation and inflation phase, respectively of the respiratory pump, as best seen in their integrals. Panel A, control recording; Panel B, during application of the thermode to the spinal cord (arrow); Panels C and D show the progression of events during blocking. F_ACO_2 was held constant at 4.85%. Horizontal bar = 5sec. For more details see text.

some larger units firing in phasic bursts with each deflation phase of the respiratory pump, at a rate of 59/min as best seen in the integral. As in the case of the inspiratory discharge, the expiratory recording is composed of large and small spikes which both show periodicity but with the latter showing a longer firing period within the cycle; it also shows some units firing in phasic bursts, but in this case firing with each inflation phase of the respiratory pump.

The thermode, at 3°C, was then applied to the ventrolateral surface of the spinal cord as indicated by the arrow in panel B. This resulted in an immediate potentiation of the rhythmic respiratory activity in reciprocal relationship, produced by the strong initial sensory stimulation of the spinal cord (Brooks, 1982). This is obvious in the inspiratory recording, best seen in the integral, manifested by four excitatory burst discharges. Interestingly these burst discharges occurred at a rate of 59/s, which was the set rate of the respiratory pump, corresponding to the deflation reflex of the internal intercostal muscle. With the progress of cold blocking, the periodic large inspiratory alpha spikes were abolished after 6min. The small gamma spikes however, persisted for a longer period (12min), with a progressive decrease in their number. Some of the latter showed evidence of central respiratory rhythm slowing from 8/min to 6/min before being rendered silent as shown in panel D. By contrast, over the

following 3 cycles after application of the thermode (panel B), the expiratory alpha motoneurones showed great reciprocal reduction in the number of their spike firing, with the surviving spikes occurring in phase with the inflation phase of the respiratory pump at the very end of the expiratory phase. Although the small gamma spikes were still active, their duration of discharge within each cycle was progressively shortened by the progressive loss of those firing early in the expiratory phase. The last surviving spikes corresponds here to the late expiratory phase, summated with the maximum peak inflation phase of the respiratory pump, and eventually completely blocked 2min after application of the thermode as shown in panels C and D. End expiratory CO_2 was held constant at 4.85% throughout this run.

To examine whether the pump modulation, encountered in the original control recordings of the inspiratory and expiratory motoneurone discharges as a result of thermode application (panels A and B of Fig. 10), was due to alpha or gamma motoneurones or both, the same data was subjected to further extensive analysis. This was done by selecting large and small spikes with the window discriminator and passing them through separate integrators. As shown in panel A of Fig. 11, channel 1 illustrates the original inspiratory record with its integral in channel 2. Channels 3 and 4 display as events per second, the mean rate of firing of gamma and alpha motoneurones, respectively. To

Fig. 11. Further analysis of the original inspiratory and expiratory recordings in panel A of data from the same recordings as illustrated in Fig. 10 showing the relation of the alpha and gamma motoneurone activities to the phasing of the respiratory pump. Panel A, illustrates the original inspiratory record in channel 1, with its integral in channel 2. Channels 3 and 4 display the discriminated gamma and alpha motoneurone discharges as mean rate, from 0-20 and 0-50 as events per second, respectively. Panel B, displays the original simultaneous expiratory record as channel 1, with its integral in channel 2. Channels 3 and 4 display the gamma and alpha expiratory motoneurones activity as mean rate, respectively. The dotted lines indicate the pump modulation of both the inspiratory and expiratory alpha and gamma motoneurone activities at a rate of 1/s. Panel C, shows the relationship between the phasing of the respiratory pump as airway pressure and the CO_2 meter output which lag behind the phasing of the pump.

Fig. 11.

A

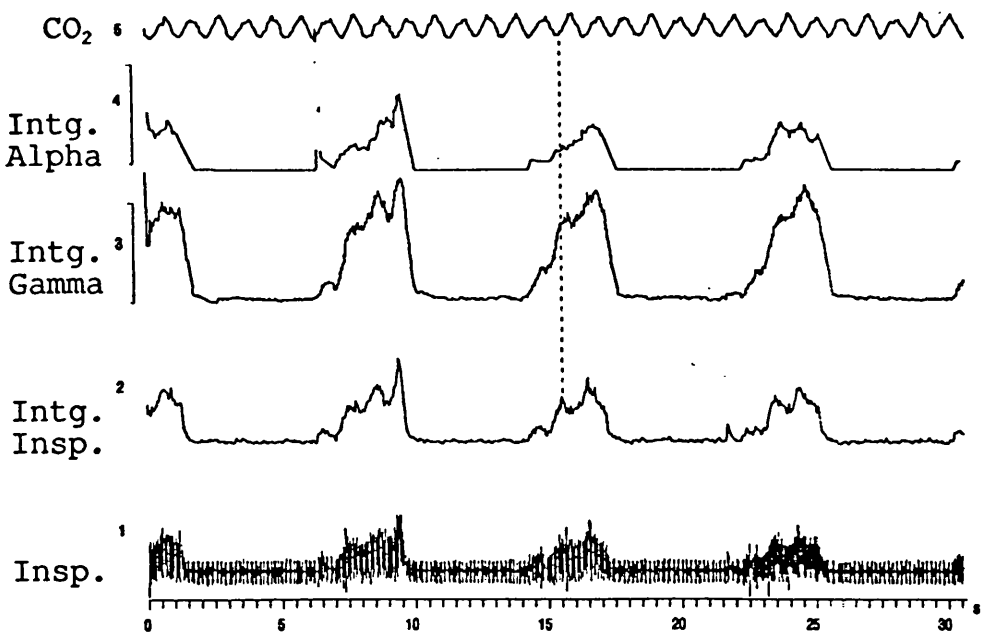
CO_2
Intg. Alpha
Intg. Gamma
Intg. Insp.
Insp.
0
5
10
15
20
25
30
s

B

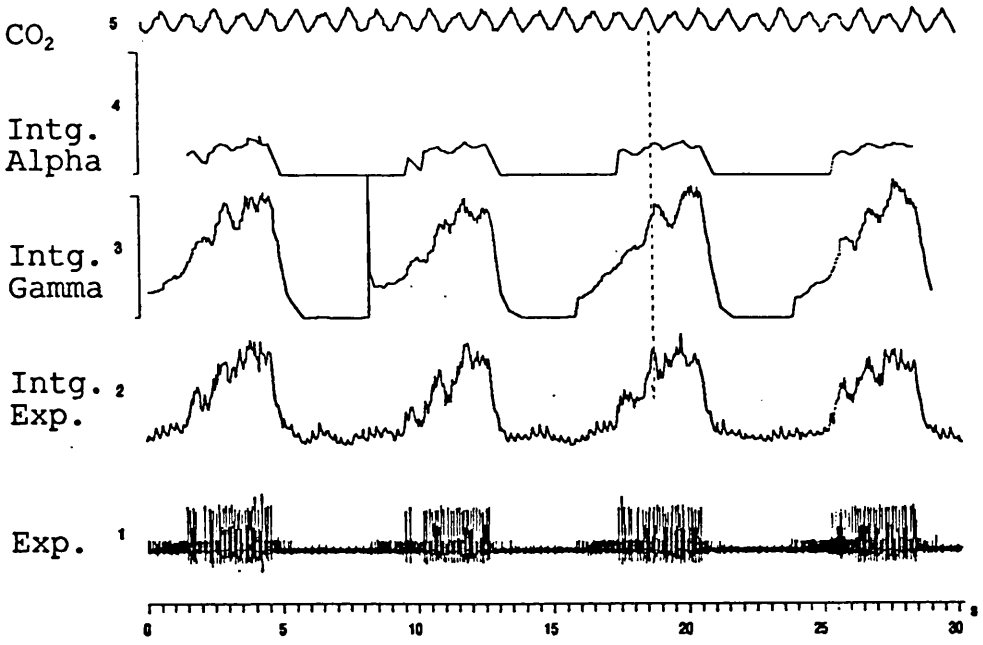
CO_2
Intg. Alpha
Intg. Gamma
Intg. Exp.
Exp.
0
5
10
15
20
25
30
s

C

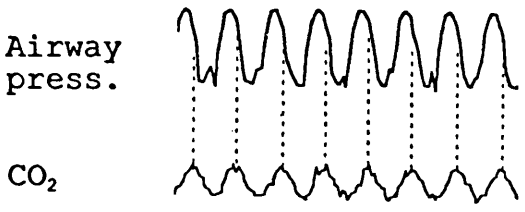
Airway press.
CO_2

examine the phasing of the alpha and gamma motoneurone bursts in relation to the respiratory pump, channel 5 is added to display the CO_2 meter output, which closely follows the phasing of the respiratory pump as shown separately in panel C, but with a short fixed delay attributed to the tubing system. Fig. 11. clearly demonstrates the pump modulation of both the inspiratory alpha and gamma motoneurones, corresponding to the deflation reflex (cf Eklund et al., 1963), as indicated by the dotted line, superimposed on the CRDP-like wave. Like the inspiratory discharge, the original expiratory record (second trace in panel A) is resolved into small (gamma) and large (alpha) spikes displayed in panel B of Fig. 11. Channel 1 shows the original data with its integral in channel 2, and channels 3 and 4 show the gamma and alpha motoneurone discharges, respectively, displayed as mean rate in events per second. As for panel A, channel 5 is added to display the CO_2 meter output. The alpha and gamma spikes show explicit pump locked activities (dotted line) corresponding in this state to the inflation reflex. Interestingly the source of this activity was found to come mainly from the gamma motoneurones with little input from the alpha motoneurones.

When the thermode was applied to the spinal cord as indicated by the arrow in Fig. 12, it was demonstrated in panel A, that the source of the four inspiratory burst discharges, was found to be induced mainly by the enhancement of the gamma motoneurones (channel 3), with

Fig. 12. The effect of cold block of the spinal cord on the discriminated inspiratory and expiratory alpha and gamma motoneurones activity, as obtained by further analysis of the original inspiratory and expiratory recordings in panel B of Fig. 10. Panel A, illustrates the inspiratory recordings with the same labelling and calibration of channels as for panel A of Fig. 11. Arrow indicates thermode application to the spinal cord. Note the enhancement of the gamma motoneurones activity as indicated by the 4 pump-locked excitatory burst discharges, corresponding to the deflation reflex (dotted line). Also, note the subsequent little effect on the alpha motoneurones activity. Panel B, illustrates the expiratory recordings with the same labelling and calibration of channels as for panel B of Fig. 12. Note the abrupt reduction of the alpha spike activity, with the surviving spikes occurring only with the maximum peak inflation phase but only at the end of the expiratory phase (channel 4). Note the progressive loss of the gamma spikes in the early expiratory phase (channel 3), with the surviving spikes showing clear pump modulation in phase with the inflation phase of the respiratory pump (dotted line).

Fig. 12

A

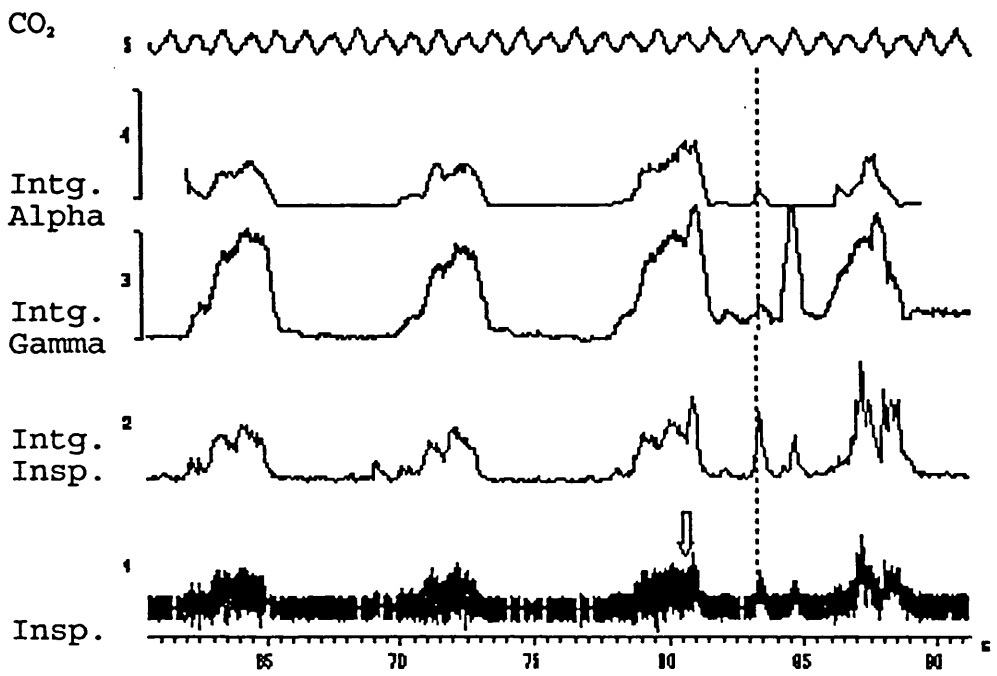
CO_2
5
4
Intg.
Alpha
3
Intg.
Gamma
2
Intg.
Insp.
1
Insp.
65
70
75
80
85
90
s

B

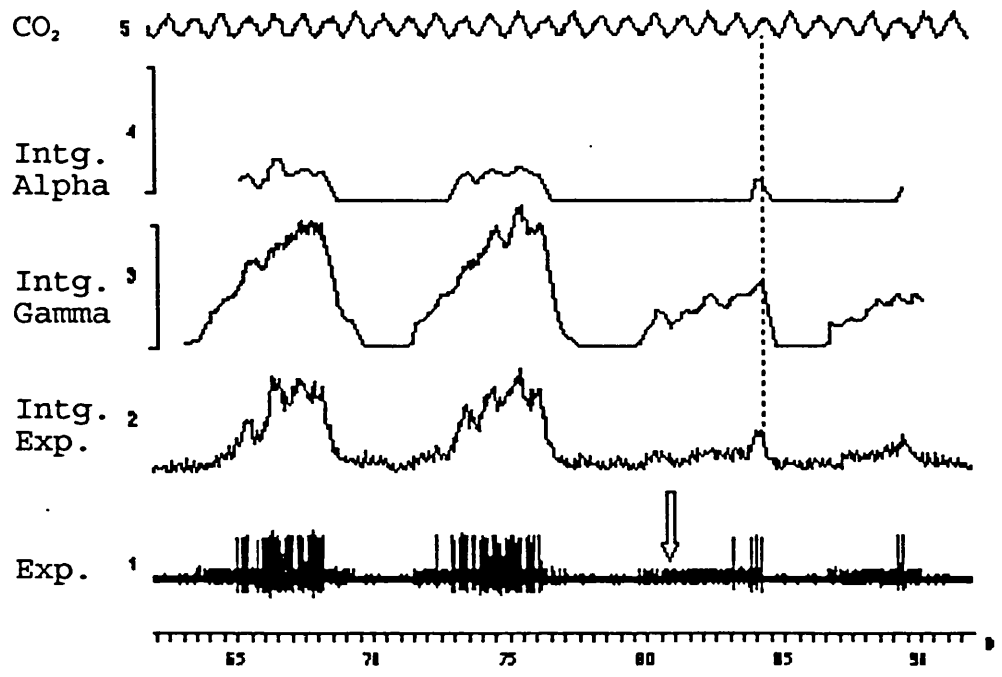
CO_2
5
4
Intg.
Alpha
3
Intg.
Gamma
2
Intg.
Exp.
1
Exp.
65
70
75
80
85
90
s

subsequent little input from the alpha motoneurones (channel 4). These bursts occurred in phase with the deflation phase of the respiratory pump as indicated by the dotted line. Meanwhile, in panel B the expiratory alpha spikes (channel 4) showed a concomitant reduction in number during the expiratory phase, with those surviving firing with the maximum peak inflation phase of the respiratory pump, but only at the very end of the central expiratory phase, superimposed on top of the CRDP-like wave as reflected in the integrated gamma activity. The duration of discharge of the expiratory gamma motoneurones (channel 3) within each cycle was progressively shortened by the progressive loss of those firing early in the expiratory phase. However, they showed a clear modulation in phase with the inflation phase of the respiratory pump superimposed on top of the CRDP like wave.

2:2. Recovery from cold block in eupnoea

Fig. 13 illustrates the restoration of activity during the recovery period following removal of the thermode (note that labelling is the same as for Fig. 10). The small inspiratory gamma spikes recovered 30s later, with a tonic pattern of discharge as illustrated in panel A, then progressively diminished to be completely abolished after 80s, as shown in panel B (see below). Panels C (4 min) and D (5 min) show the progressive and full restoration of full rhythmic gamma and alpha motoneuronal activities later. Sixty seconds after lifting the thermode, the small spikes

Fig. 13.

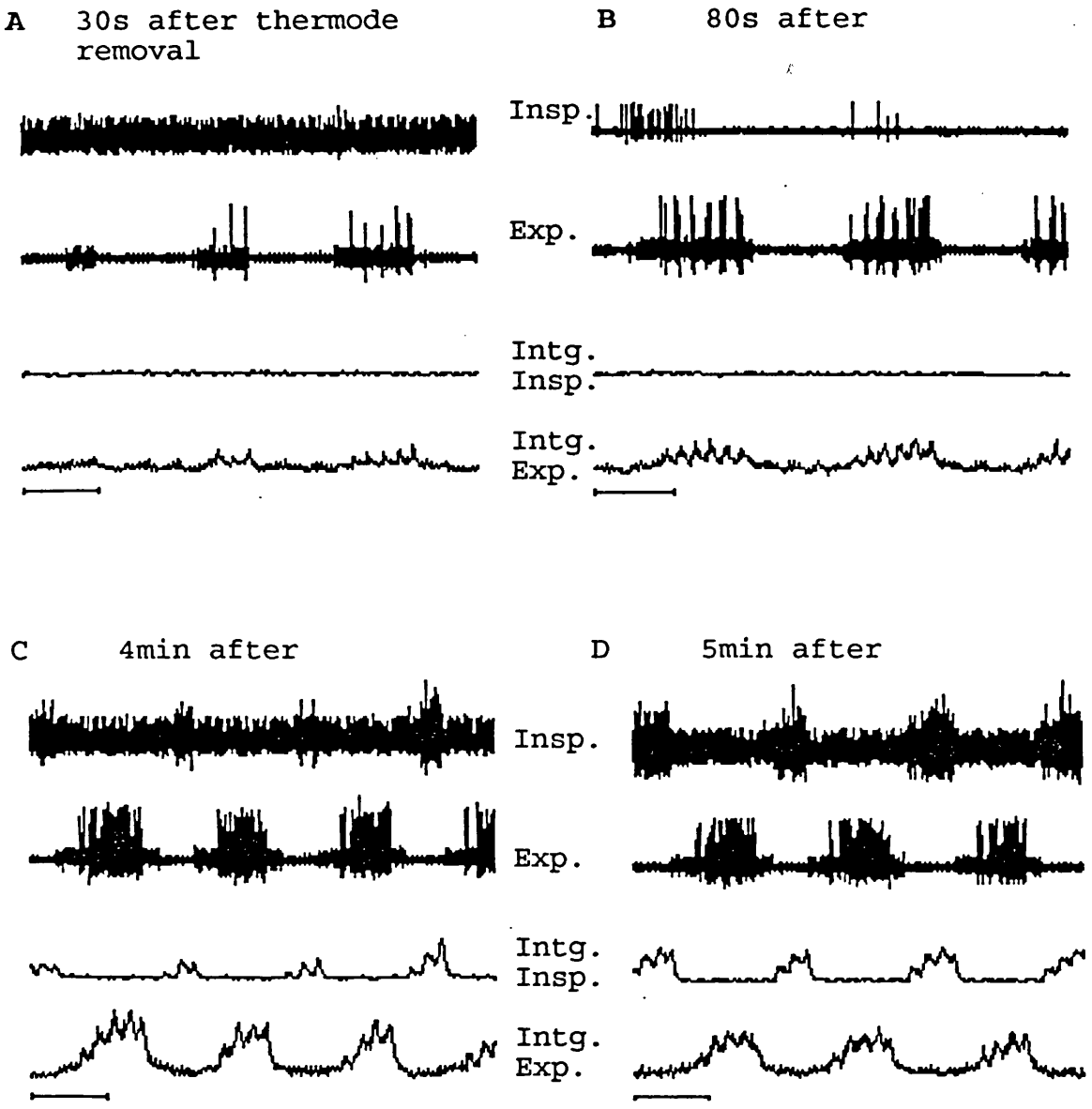

Fig.13, The progression of events during the recovery period in eupnoea after removal of the thermode. Recordings as in Fig. 10. Panel A, recovery of both inspiratory and expiratory activities. Panel B, subsequent reduction of inspiratory activity with reciprocal enhancement of expiratory activity. Panels C and D, progressive restoration of both activities. F_ACO_2 was held constant at 4.85%. Horizontal bar = 5sec. For more details see Figs. 15 and 16.

firing in expiration before blocking reappeared first in late expiration -2.5sec duration- and gradually earlier, the firing eventually occupied the whole expiratory phase -7sec duration- (Panels A and B). The large alpha spikes were firstly restored in late expiration and with further recruitment they occupied most of the expiratory phase, discharging only intermittently with each inflation phase of the pump, at a rate of 59/min (Panels A and B). Four minutes later progressive and full restoration of full rhythmic expiratory gamma and alpha motoneuronal activities occurred (panels C and D).

The original inspiratory and expiratory recordings in each of panels A and B of Fig. 13 were further analyzed and illustrated as Figs. 14 and 15, respectively. They display the selected gamma and alpha spikes as mean rate, as described above for Fig. 11, with the aim of showing if their responses to the deflation and inflation of the thoracic wall induced by the respiratory pump, is altered or not. Each of Figs. 14 and 15, displays simultaneously the inspiratory (panel A) and expiratory (panel B) activities with the same labelling and calibration of channels as for Fig. 11.

Thirty seconds after removal of the thermode, most of the inspiratory gamma units (channel 3 in panel A of Fig. 14) fired in phasic bursts with each deflation as inferred from the CO_2 trace and indicated by the dotted line, while others

Fig. 14, illustrates the simultaneous restoration of inspiratory (panel A) and expiratory (panel B) activities recorded 30s after removal of the thermode, to show the relation of their alpha and gamma motoneurone activities to the phasing of the respiratory pump. Labelling and calibration of channels as for Fig. 11, channel 5 displays the CO_2 meter output. Panel A, shows pump-locked activity of the restored inspiratory gamma units (channel 3) in phase with the deflation phase of the CO_2 meter (dotted line). The alpha units (channel 4) shows very little activity just above the zero. Panel B, shows the restoration of the expiratory alpha (channel 4) and gamma (channel 3) motoneurones activities. Note that both activities reappeared in late expiration and gradually occupied the whole expiratory phase with clear pump modulation corresponding to the inflation reflex.

Fig. 14

A

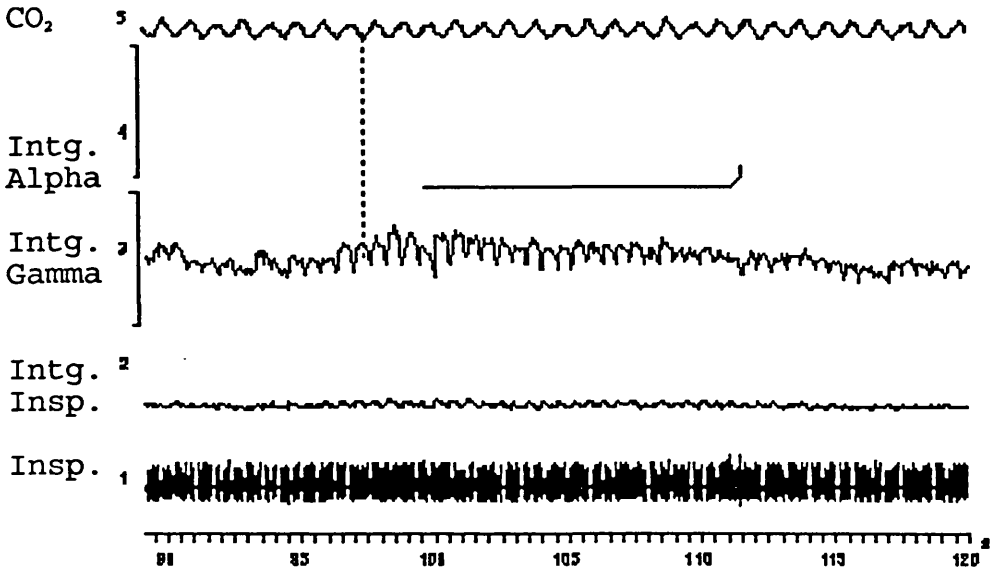
CO_2
5
Intg.
Alpha
4
Intg.
Gamma
3
Intg.
Insp.
2
Insp.
1
90
95
100
105
110
115
120
s

B

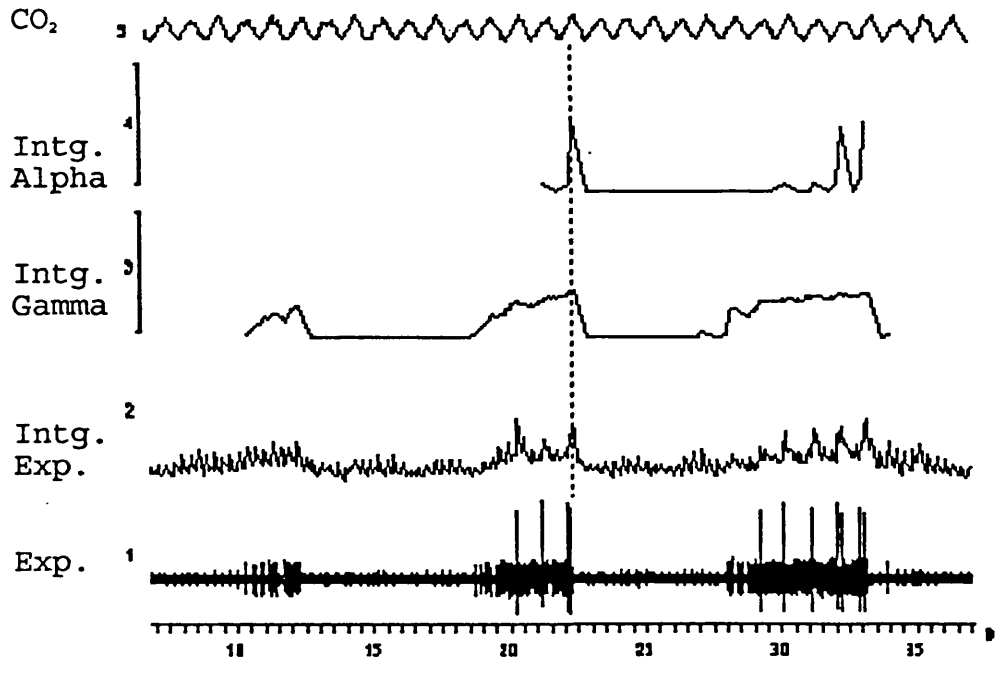
CO_2
5
Intg.
Alpha
4
Intg.
Gamma
3
Intg.
Exp.
2
Exp.
1
10
15
20
25
30
35
s

fired tonically, although also already rate modulated with the respiratory pump, while the alpha units showed very little recovery. At this time the expiratory gamma motoneurones (channel 3 in panel B of Fig. 14) allowed three observations to be made. Firstly, they initially reappeared in late expiration and their firing gradually recovered earlier until eventually it occupied the whole expiratory phase with a concomitant shortening of the inspiratory periods (see also Fig. 13 panels A and B). Secondly, they showed clear pump modulation corresponding to the inflation reflex (dotted line). Thirdly, they clearly showed that the smooth CRDP-like wave is dependent on their continuous activity during the expiratory phase. In contrast, the firing of the expiratory alpha motoneurones (channel 4) which is locked to the inflation phase of the pump, is insufficient to form the smooth, truly CRDP-like wave. Nevertheless, their occurrence in this phase demonstrates the existence of a subliminal, central expiratory drive (see below).

The recordings illustrated in Fig. 15 were recorded 80 seconds after removal of the thermode and showed fluctuations in the respiratory activity. So that with the progressive enhancement of the expiratory alpha and gamma motoneurone activity (channels 3 and 4 of panel B, respectively), there was a concomitant reduction of the inspiratory gamma motoneurone activity, with loss of the pump modulation (channel 3 of panel A). The latter was then

Fig. 15, illustrates restoration of inspiratory (panel A) and expiratory (panel B) activities recorded 80s after removal of the thermode, to show the fluctuation of their discriminated gamma and alpha motoneurones. Labelling and calibration of channels as for Fig. 11. Panel A: progressive reduction of inspiratory gamma motoneurone activity, with loss of the pump modulation (channel 3), the alpha motoneurone activity disappeared completely. Panel B: subsequent progressive enhancement of expiratory gamma and alpha motoneurones activity (channels 3 and 4, respectively) with clear pump modulation locked to inflation (dotted line). Note that although the intermittent pump-locked firing of the alpha units was increased, their integral after each initial rise returns to the base line so that no CRDP-like wave develops.

Fig. 15

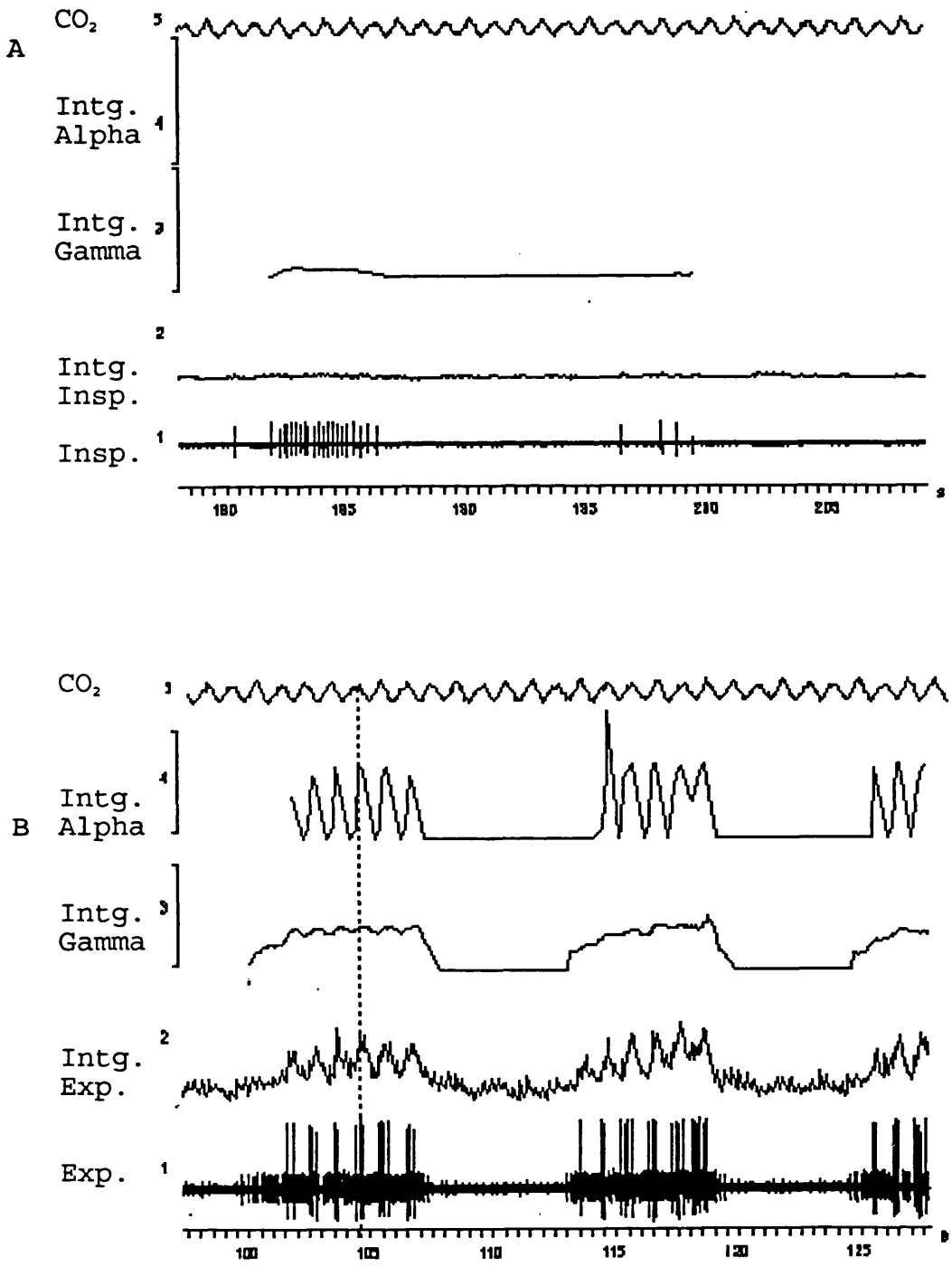
A
CO_2
Intg. Alpha
Intg. Gamma
Intg. Insp.
Insp.
B
CO_2
Intg. Alpha
Intg. Gamma
Intg. Exp.
Exp.

completely abolished. The expiratory gamma units, while occupying the whole expiratory phase to form the CRDP-like wave, showed a clear pump modulation locked to the inflation phase as indicated by the dotted line. Although their firing rate was increased, the expiratory alpha units did not show a CRDP-like wave in their integrated trace. This was because their intermittent, pump-locked discharge occurred relatively synchronously, so that after each initial rise the integral had time to reach the base line.

Interestingly, in the early recovery period, the respiratory rate was at its lowest value during the entire procedure, this being at 5/min, then gradually increased to 8/min close to the control rate.

The whole sequence of events due to blocking in eupnoea is illustrated in Fig. 16. The upper and lower traces display the integrated expiratory and inspiratory activities, respectively (note the different scale). Panels A and B are repeat experiments from the same preparation as in Figs. 10 and 13, but with application of the thermode to different positions on the spinal cord, namely a ventrolateral position in A and a dorsolateral position in B. Panels C and D, are from different preparations, with a dorsolateral position of the thermode in C and a lateral position in D. The left arrow in each panel indicates the thermode application to the spinal cord while the right arrow indicates the removal of the thermode. For all experiments

Fig. 16. Continuous time compressed recordings of integrated expiratory (upper trace) and inspiratory (lower trace) activities in each of panels A, B, C and D, to show whole sequence of events due to blocking in eupnoea. Panels A and B are from the same preparation with a ventrolateral and a dorsolateral position of the thermode, respectively. Panels C and D, are from different preparations, with a dorsolateral position of the thermode in C and a lateral position in D. The left-hand arrow in each panel indicates thermode application to the spinal cord, the right-hand arrow indicates thermode removal. The lower case letters a-d divide each panel into four sections: a, transition from eupnoea to the stimulating effect produced by the thermode; b, restoration of activity after removal of thermode; c, fluctuation in activity after recovery; d, restoration of full rhythmic activity. The bottom arrow in C shows restoration of both inspiratory and expiratory activities following an arousal stimulus. For all experiments the CO_2 levels were held constant throughout at 4.85%, 4.15%, 4.6% and 6.0% for panels A, B, C and D, respectively. Horizontal bar: under C = 300s for A, B and C; under D = 100s.

Fig. 16.

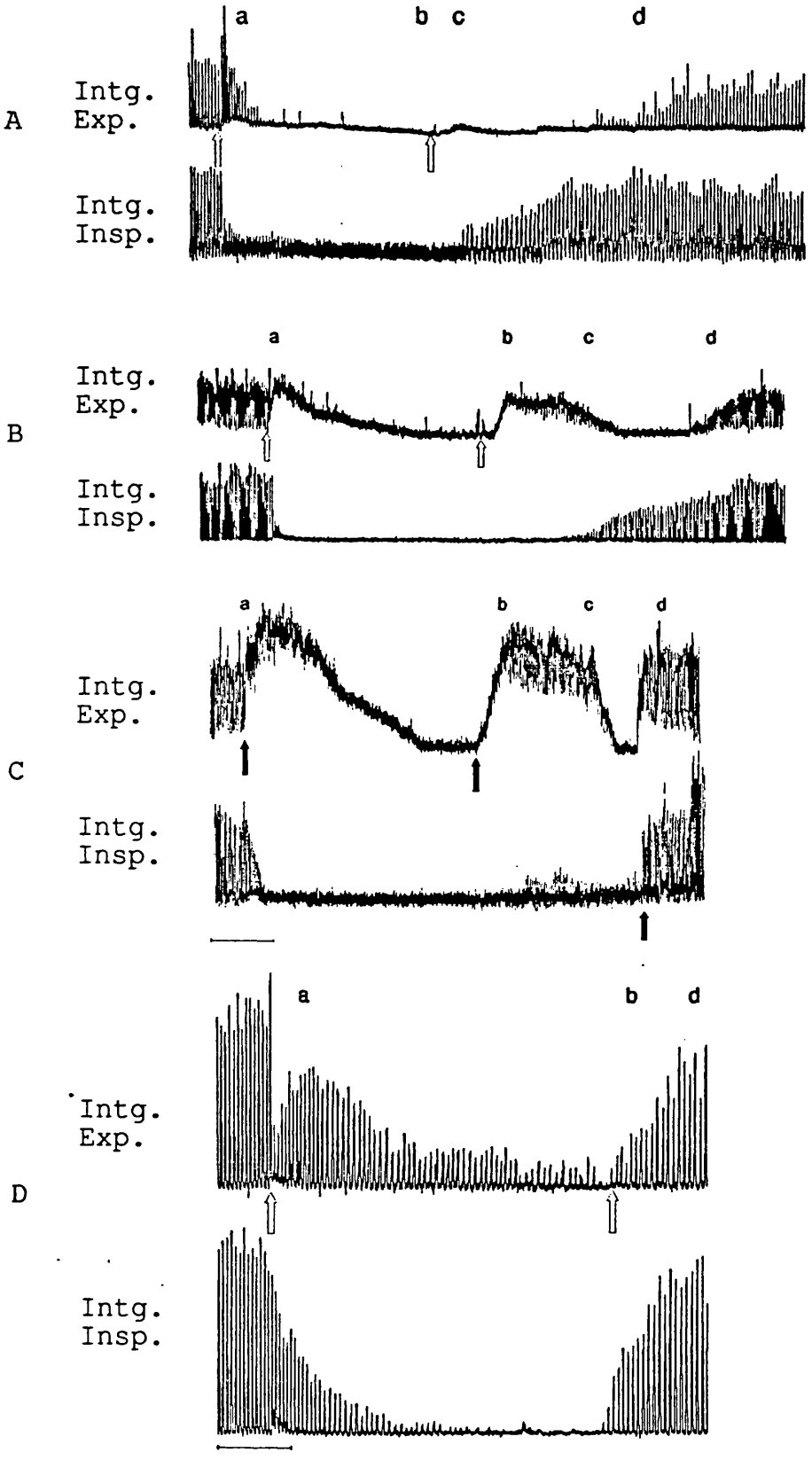
a
b c
d
A
Intg.
Exp.
Intg.
Insp.
a
b
c
d
B
Intg.
Exp.
Intg.
Insp.
a
b
c
d
C
Intg.
Exp.
Intg.
Insp.
a
b
d
D
Intg.
Exp.
Intg.
Insp.

Fig. 17. Recordings as in Fig 16 illustrating expanded forms from sections a, b, c and d of panel B.

Fig. 17.

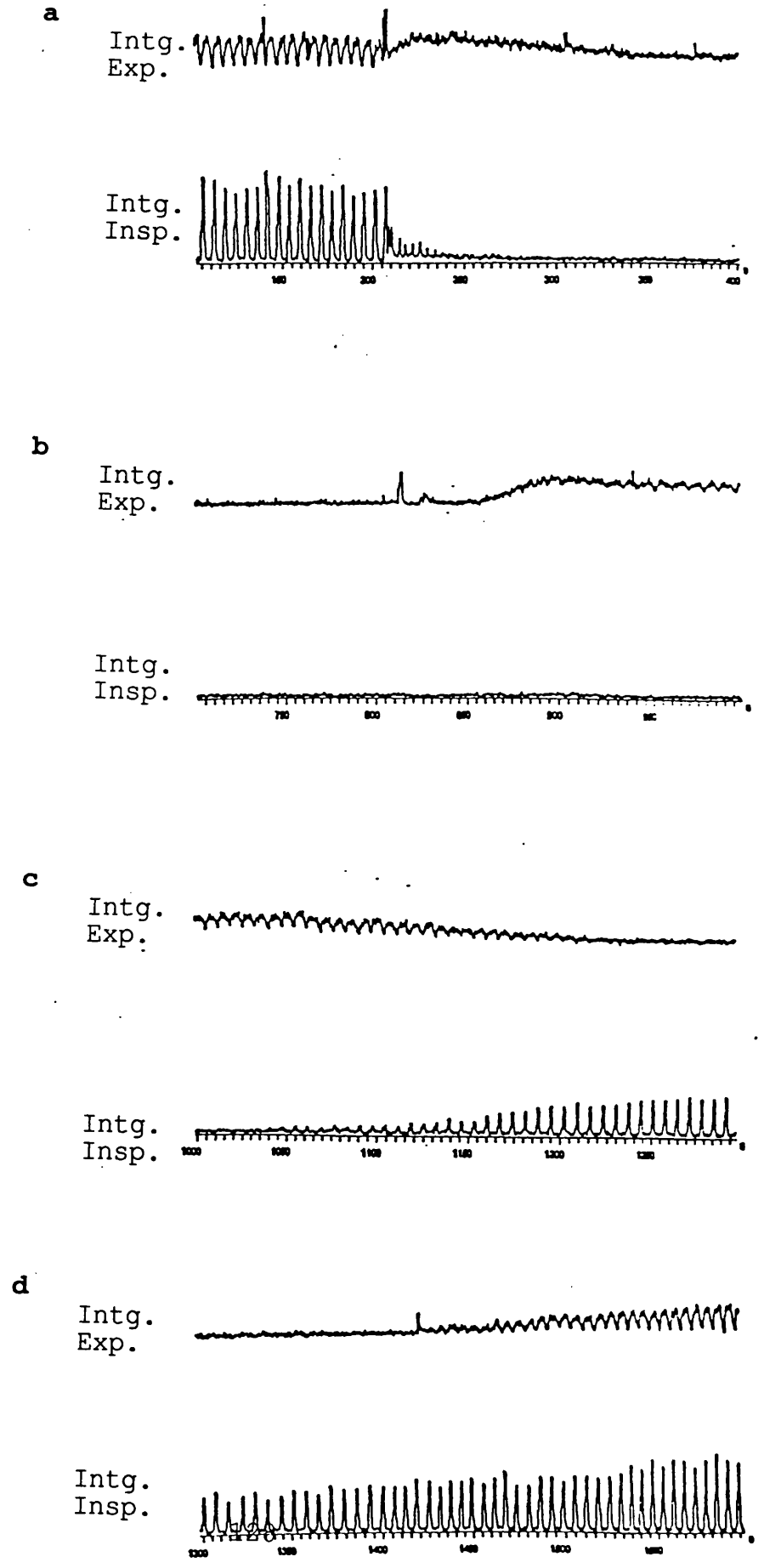
a
Intg.
Exp.
Intg.
Insp.
b
Intg.
Exp.
Intg.
Insp.
c
Intg.
Exp.
Intg.
Insp.
d
Intg.
Exp.
Intg.
Insp.

the CO_2 levels were held constant throughout the runs at 4.85%, 4.15%, 4.6% and 6.0% for panels A, B, C and D, respectively. For ease of explanation and comparison each panel is also divided into 4 sections a-d. Time-expanded versions of these sections from panel B are presented collectively in Fig. 17. Section a in each shows the transition from the control eupnoeic state to the initial and immediate potentiation of rhythmic activity produced by the system response to the strong sensory stimulation of the spinal cord (see above). Hence, section a of panels B, and C in Fig. 16 and in Fig. 17a, shows that, after a brief inspiratory burst as reflected in the elevated base line of the integrator, the peak inspiratory activity progressively diminished before being totally abolished in nearly 100s. In striking contrast, the expiratory activity showed an obvious initial increase in tonic activity and a concomitant loss of the reciprocal inspiratory-phased periodic inhibition, Then this activity gradually declined before eventually being completely blocked in nearly 650s in B and 700s in C of Fig. 16, as shown by the base line plateau.

When the thermode was removed as shown in section b in panels B and C of Fig. 16 and in Fig. 17b, the rhythmic activity recovered first in the expiratory motoneurones with the peak integrated activity rising above the peak of the control and to about the same level of the immediate, excitatory response produced by the application of the

thermode to the cord. The expiratory activity, then gradually declined to reach the base line but without the loss of rhythm (section c), this is more obvious in the expanded version in Fig.17c. Meanwhile the inspiratory activity reappeared and progressively augmented as shown in sections c and d of Fig. 16 panel B, and in Fig.17c and d. The expiratory activity spontaneously reappeared again (section d in panel B and Fig. 17d) with a progressive phasic inhibition parelling the augmenting phasic inspiratory discharge. In Fig. 16 panel C both the expiratory and inspiratory activities failed to recover again after their decline, but did however abruptly recover in response to pulling the forelimb as indicated by the bottom arrow.

With the ventrolateral position of the thermode, a different behaviour was obtained (Fig. 16, panel A). Whereas the rhythmic expiratory activity disappeared first and rapidly (within 1.5min) a tonic discharge of the small inspiratory spikes was maintained for a longer period after the loss of the phasic inspiratory activity. Because of the time compressed recording of this figure, it is difficult to clearly demonstrate the events following removal of the thermode. However with reference to Fig. 13, panels A and B, apparently showed that when the thermode was lifted the activity appeared first in the inspiratory motoneurones (panel A), to disappear again when the expiratory activity fully recovered before final restoration of rhythm in both

(Figs. 13, panels C and D and section d of Fig. 16).

With a lateral position of the thermode (Fig. 16 panel D, section a), both the inspiratory and expiratory motoneurone activities showed an initial decrease. Whereas that of the inspiratory activities progressively declined to zero over 4min, the expiratory motoneurones showed a secondary increase before itself eventually declining to zero over approximately 8min. Section b showed that rhythm is present in both motoneurone populations just after removal of the thermode and they progressively augmented to simulate the control recording (section d), without showing that fluctuation of activities observed in panels A, B and C.

2:3. Cold block in hypocapnic apnoea

Fig. 18 shows recordings of the whole sequence of events from phasic respiration to the induction of hypocapnic apnoea, the production of cold block of the spinal cord during hypocapnic apnoea and the recovery. The upper and lower traces show the integrated expiratory and inspiratory activities, respectively. Starting from the left, this figure is divided into 8 sections A - H. Expanded versions of these sections are shown separately as Fig. 19, with the following description applied for both figures. Section A shows control recordings of the alternating rhythmic expiratory and inspiratory activities at an initial F_ACO_2 level of 4.15%. Section B shows the sequence of events when

Fig. 18.

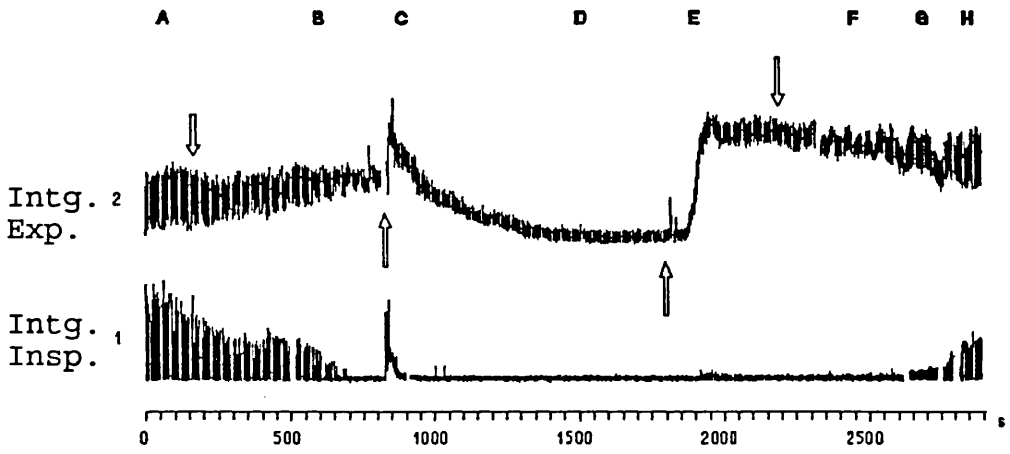

Fig. 18. Demonstration of the whole sequence of events from eupnoea A, through hypocapnia B, cold blocking of the spinal cord in hypocapnia C and D, recovery from blocking in hypocapnia E, to eupnoea again in F, G and H. Upper trace, integrated expiratory, and lower trace, integrated inspiratory neuronal activities. Note that following removal of the thermode the tonic expiratory activity (E) was the first to recover, and within nearly 3min reached the same peak level it had shortly after the thermode was applied to the cord (C). F_A CO_2: 4.15% for A, 2.35% from B to the beginning of F and 4.5% for G-H. Downward arrows: reduction (left), and increase (right) of CO_2 level. Upward arrows: left, application and right removal of thermode.

Fig. 19, shows representative parts from sections A-H of Fig 18, displayed in expanded forms. Upper trace, integrated expiratory and lower trace, integrated inspiratory motoneuronal activities. Sections have the same specifications as for Fig. 18. Horizontal bar 5sec.

Fig. 19

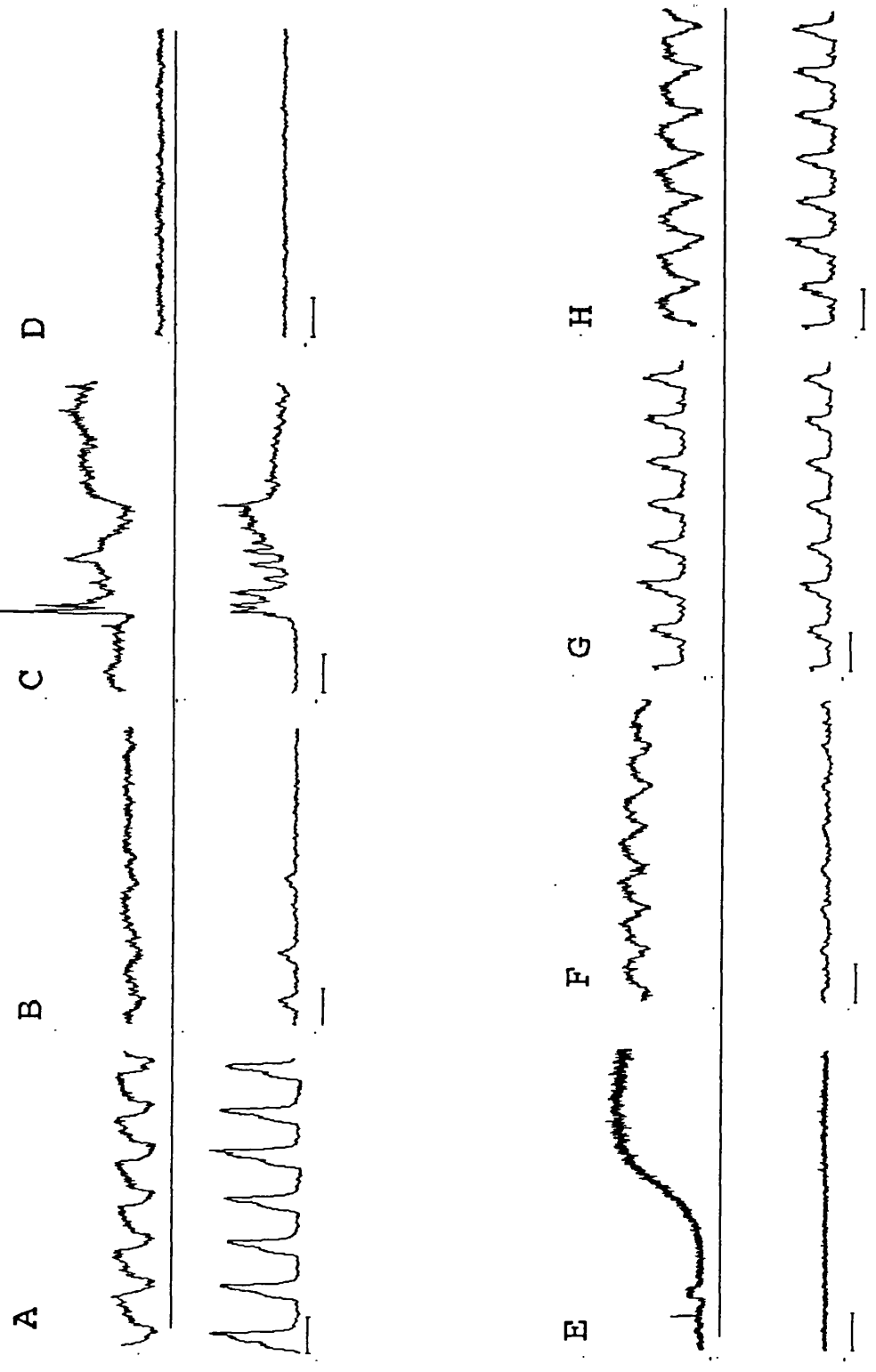

CO_2 was reduced gradually to 2.35% (left downwards arrow) to induce hypocapnic apnoea, and maintained at the same level until section F when CO_2 was restored to eupnoeic levels (right downwards arrow). In section B the peak inspiratory activity progressively diminished and was eventually abolished whereas the expiratory activity was rendered tonic through the gradual reduction of the inspiratory-phased inhibitory component (cf. Bainton et al., 1978).

As for cold block in eupnoea (section a in panels B and C of Figs. 16 and 17), application of the cold thermode to the dorsolateral surface of the spinal cord (section C of Fig. 18 - left upwards arrow, and Fig. 19), evoked a transient reciprocal reflex burst activity of the inspiratory and expiratory motoneurones. This burst activity was locked initially to the respiratory pump rate of 59/min, and lasted for nearly 75sec. Whereas the inspiratory burst activity occurred in an already silent inspiratory motoneurone, the expiratory burst occurred in an already tonically discharging expiratory motoneurones. With this added burst, the expiratory activity attained double that of the control level and persisted for nearly the same period as the cold-activated inspiratory burst. Subsequently, the inspiratory motoneurones again became inactive as in the control (apnoeic) period, and the tonic expiratory activity gradually declined to be virtually abolished after 10min. The initial excitatory effects were attributed to the sudden stimulating effect of cooling on

the spinal cord prior to blocking (see Brooks, 1982). The residual tonic activity in the integrated record was due to the low level 'gamma' spikes which was attributed to the spinal mechanisms (cf. Eklund et al., 1963; Sears, 1963)

2:4. Recovery from cold block in hypocapnic apnoea

When the thermode was removed as shown in section E (right upward arrow), the tonic expiratory activity was the first to recover, and progressively increased eventually to reach the same peak level it had shortly after the thermode was applied to the cord. This tonic activity persisted for nearly 6min during which time the inspiratory recording remained silent except for some low level gamma activity as indicated by the increasing baseline noise and slight elevation of the integrated activity. The CO_2 was then slowly increased (section F, right downward arrow) and this led to central rhythm generation as expressed by the periodic inhibition of the tonic expiratory activity associated with an overall slow decline of the expiratory activity and a concomitant a small but definite increase in the inspiratory activity, which became more conspicuous at the onset of rhythm generation as seen in sections G and H at CO_2 level of 4.5%.

2:5. Cold block of the spinal cord and chest wall reflexes

Fig. 20 illustrates recordings in a preparation in which F_ACO_2 was reduced to 2.90% to cause hypocapnic apnoea. In A, the expiratory filament recording (upper trace) showed

alpha and gamma spikes. The single unit alpha spike discharged in phasic bursts of 4-5 spikes at 8 - 10Hz with each inflation phase of the pump (rate = 59/min) while the individual gamma spikes fired tonically at rates >20/sec. At this level of CO_2 the inspiratory activity was completely abolished (not shown; cf. Bainton et al., 1978). End tidal CO_2 was maintained at the same level throughout the cooling procedure, which typically took 9min for blocking to be complete. With its temperature adjusted to 5°C, the thermode was applied to the dorsolateral surface of the spinal cord causing the large units gradually to decrease in number and eventually to disappear completely after 90s. The last spikes to disappear were the ones which fired at the peak of each inflation (B and C). The firing rate of the small spikes also progressively reduced with time (B and C) to disappear completely after 300s (D). Thirty seconds after removal of the thermode, the small spikes recovered first (not shown) and their firing rate steadily increased with time. The large spike recovered after a period of 60s (E) and its firing rate increased after 90s (F). Interestingly, the recovery of the large spike occurred as a reverse sequence of its disappearance in blocking (E and F), with its firing occurring at the summit of each inflation phase of the pump and with their traces forming a mirror image (C and E).

Fig. 20. The effect of cold blocking of the spinal cord on chest wall inflation reflex as obtained from expiratory motoneurone activity during hypocapnic apnoea. Upper trace, internal intercostal filament neurogram, lower trace end tidal CO_2 fraction. A, control recordings, B, C and D, representative sections taken 60s, 90s and 300s, respectively, after application of the thermode; E and F taken 60s and 90s after lifting the thermode. End tidal CO_2 fraction was held constant at 2.90% during the whole procedure.

Fig. 20.

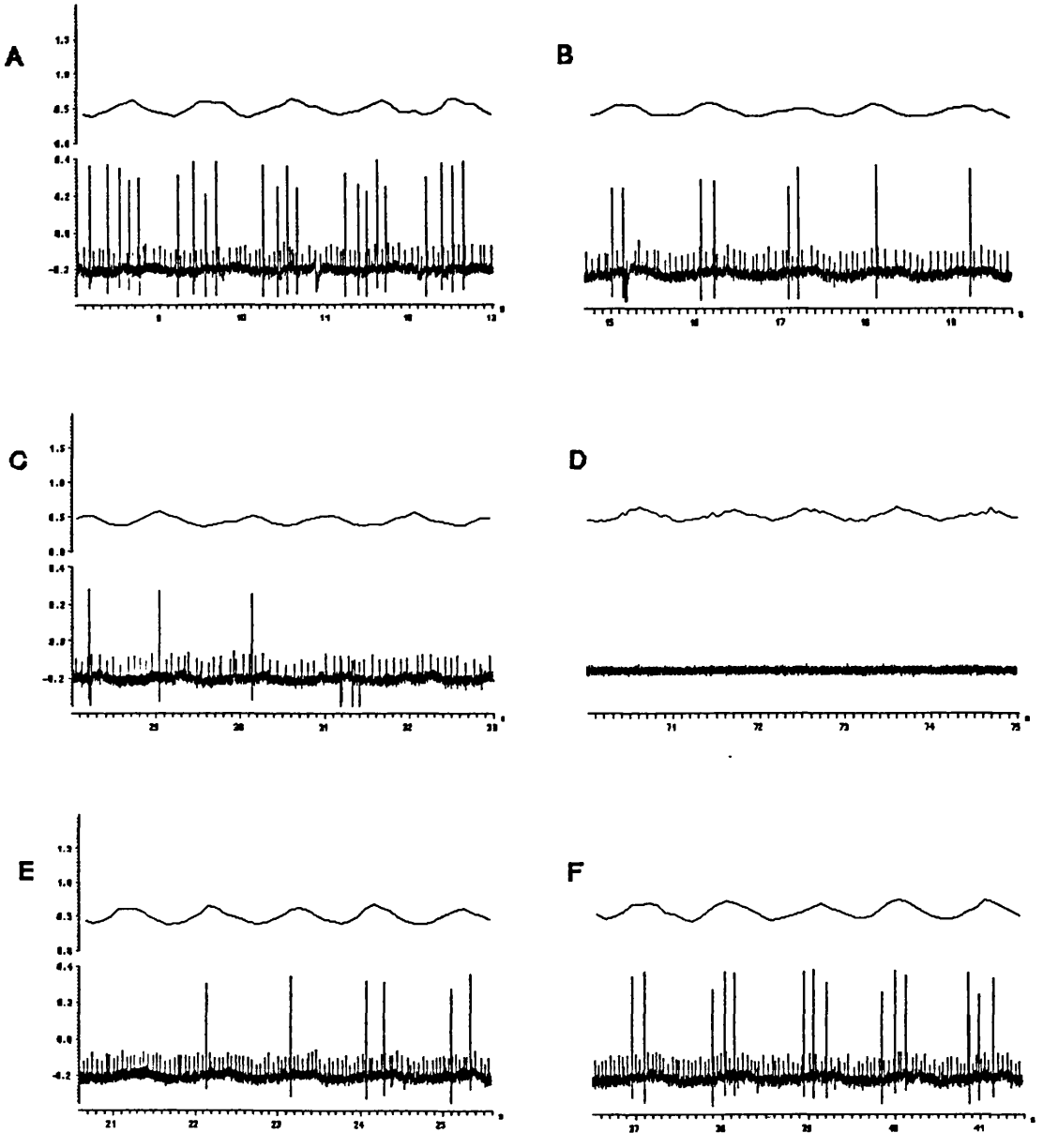

3. Discussion of respiratory results

It has long been recognized, that the main advantage of cooling methods in acute studies is the ability to produce repeated, brief, local reversible functional blockade without the compensatory neural reorganization that can occur after permanent lesions. With regard to the present work, the effects of cooling on respiration goes back to the turn of the century when Stefani (1985) and Degnello (1900) used cold-block techniques which were further developed by Trendelenburg in the year 1910, as cited in the extensive review by Brooks (1983). Trendelenburg repeatedly cooled the carotids of etherized rabbits which resulted in a fall of arterial blood pressure followed later by slowing and then cessation of respiration. In order to localize the areas that control these functions he used iced saline at 4°C to cool the spinal cord at the level of the second cervical segment and thus to interrupt the descending pathways between bulbar and spinal respiratory 'centres', but avoiding cooling of the phrenic nerve. The rabbit was vagotomized to diminish reflex changes of blood pressure and respiration. The cold block resulted in a depression of blood pressure and abolished thoracic and diaphragmatic respiratory movements; however it did not affect the movement of the nares, leading to the suggestion that the respiratory rhythm is generated at the medullary level (Trendelenburg 1910b). Similarly, with the vagi intact, the above results were obtained by gradual

cooling of the spinal cord at the same segmental level, but at starting temperatures higher than 20°C, in this case however, depression without excitation of blood pressure and respiration was observed.

In the present study, blocking was performed with a different technique (see methods). The cooling thermode was first cooled to the desired temperatures (3-5°C) (Trendelenburg, 1910b) before being applied to the different aspects of the second or third cervical segments, to examine its effects on both 'central' and reflex behaviour of respiratory motoneurones under different conditions, i.e. eupnoea, hypocapnic apnoea, and reflex and other central activities evoked by the proprioceptive inputs. From our experience with cold block experiments at this range of temperatures, thermode application (e.g. when repositioning of the thermode on the appropriate aspect of the spinal cord surface) usually results in an exaggerated reciprocal response on both intercostal motoneurone populations. This cold stimulus was strong enough to evoke burst activity in an already silent intercostal motoneurone (see below). For better understanding of these effects, discussion will first be focused in the normal operating mechanisms of the intercostal motoneurones during the above conditions prior to block.

3:1. Operating mechanism of the intercostal motoneurones

3:1:1. Eupnoea

In the intact animal the rhythmic pattern of respiratory motoneurones discharge is principally determined by the final balance between the supraspinal phasic and tonic inputs, segmental proprioceptive inputs and two interdependent inhibitory mechanisms acting at medullary and segmental levels (Bainton et al. 1978). So that during inspiration, there is excitation of inspiratory bulbospinal neurones with an associated reciprocal inhibition of the expiratory bulbospinal neurones (Merrill, 1974). Correspondingly, at segmental level there is excitation of the inspiratory motoneurones and reciprocal inhibition of the expiratory motoneurones, which latter also inhibits the inflation-induced stretch reflexes of the internal intercostal muscles that otherwise would occur (Sears, 1964c,d).

During the expiratory phase the expiratory bulbospinal neurones are disinhibited and assume a discharge rate proportional to the prevailing chemical drive from peripheral and central chemoreceptors assuming hyperoxic conditions of excitation. This expiratory bulbospinal discharge, monosynaptically depolarizes the expiratory motoneurons, now also released from the inhibition linked to the inspiratory bulbospinal activity to cause the depolarising phase of CRDP which may or may not reach firing threshold (Sears, 1979). The CRDP in summation with segmental and other propriospinal inputs, determines the overall shape of the CRDP and hence the firing pattern of

the individual motoneurons. Such reciprocal pattern of inspiratory and expiratory motoneuron discharge, which reflects interaction between the central respiratory drive and reflex inputs, is shown in this study (e.g. see Figs. 3, 4A, 6A and 10 panel A). In panel A of Fig 10, both the inspiratory and expiratory alpha and gamma motoneurons are strongly active at an elevated level of CO_2, with some units discharging with each deflation and inflation phase, respectively of the respiratory pump. The inspiratory record showed that the gamma activity continues also during the expiratory phase but lacks the pump modulation. Differentiation of the inspiratory and expiratory recordings into alpha and gamma spikes was performed to show the behaviour of their discharge through the respiratory cycle (Fig. 11). Our findings are similar to the previous results obtained by Sears (1962); and those of Eklund et al. (1963, 1964). Thus it was revealed that the inspiratory alpha and gamma motoneurones discharge maximally during inspiration (see the integrals) and together with the summation of the segmental deflation reflex caused the depolarising phase of CRDP. The deflation reflex was inhibited during expiration, this is because of the conductance changes associated with the postsynaptic inhibition induced by the expiratory bulbospinal drive which specifically reduces the efficacy of synaptic transmission from inspiratory muscle spindle afferents, (Kirkwood and Sears,1973), thus preventing the reflex contraction of the inspiratory muscles during expiration

(see below). As in the case of the inspiratory recordings, the expiratory alpha and gamma motoneurones discharge maximally in late expiration as indicated by their integrals, with the inflation reflex superimposed on top of the CRDP-like wave. The chest wall inflation reflex, which is caused by the internal intercostal muscle spindle afferents discharge, is normally inhibited during the inspiratory phase, a period corresponding to the hyperpolarizing phase of the CRDP.

3:1:2. Hypocapnia

It was revealed by many authors, that lowering the CO_2 level in preparations under artificial ventilation results in hypocapnic apnoea, a state characterized most commonly by a tonic expiratory alpha and gamma motoneurone discharge, and less frequently by a tonic inspiratory discharge (Sears, 1964; Bainton et al. 1978). In this work re-examination of these results at segmental level was performed, with the intention to show the behaviour of respiratory motoneurones during cold blocking of the spinal cord. It was shown here, (Figs. 4B and 5B,C) in an expiratory biased preparation, after hyperventilating the preparation, the inspiratory activity ceased leading to a tonic discharge of the expiratory motoneurones which are now released from their 'central' inspiratory linked-inhibition. This was revealed by Bainton and Kirkwood (1979) in their study of the expiratory bulbospinal neurones. They showed very clearly that those expiratory

bulbospinal units which were phasic in eupnoea were the ones which were rendered tonic during hypocapnia. Since bulbar inspiratory neurones are silenced in hypocapnia (cf. Cohen, 1966), there would be no inspiratory bulbospinal drive to the spinal cord and hence no reciprocal inhibition of the expiratory motoneurones. Conversely there is reciprocal inhibition of the inspiratory motoneurones and this is proportional to the now tonic expiratory bulbospinal drive. Such an expiratory mechanism could mediate the control of end-expiratory volume or, through changes in rib cage and abdominal configuration, optimize the mechanical performance of the diaphragm under different postural conditions (Da Silva, Sayers, Sears and Stagg, 1977).

3:1:3. Chest wall reflexes

Studies on the afferent and efferent innervation of the intercostal muscle spindles have revealed an important role of this receptor and its reflexes in breathing. It was previously established that passive movements of the chest wall induced by artificial respiration elicits reflex activity in both alpha (Ramos and Mendosa, 1959; Sears, 1958, 1963) and gamma motoneurons which persists in the spinal preparation (Critchlow and Euler, 1963; Corda, Von Euler and Lennerstrand, 1965). During hypocapnia, it is shown that (Fig. 7), the deflation phase of the pump, resulted in a maximum afferent discharge in the external intercostal nerve, while the peak afferent activity in the

internal intercostal nerve filament was in synchrony with the peak inflation phase of the pump. When the pump was stopped at the end of the deflation phase, (panels B of Figs. 7 and 8), the afferent discharge in the external intercostal nerve progressively increased while that of the inflation reflex ceased. By contrast, when the pump was stopped at the peak of inflation, Fig. 8C the expiratory activity was rendered tonic, while the afferent discharge in the external intercostal nerve became silent. As the nerves recorded from are entirely muscular in distribution, these afferent discharges in the external intercostal nerve and internal intercostal nerve filament are attributed to the muscle spindles in their respective muscles when they were stretched. So those movements resulting from artificial or normal respiration are usually enough to act as stimuli (cf. Ramos and Mendosa, 1959). Also, by using intracellular recording Eccles, Sears and Shealy (1962) and Sears (1964) found that EPSPs are evoked monosynaptically in the thoracic motoneurones by the excitation of low threshold afferents that give rise to group Ia component of the afferent volley recorded at the root entry zone. This is because the intercostal motoneurons were proved to receive both monosynaptic and polysynaptic connections from primary and secondary muscle spindles in homonymous nerves of the same and adjacent segments (Sears, 1964; Kirkwood & Sears, 1974; Kirkwood & Sears, 1981); and their responses disappeared after section of the corresponding dorsal roots.

The behaviour of the chest wall inflation and deflation reflexes at levels of CO_2 just at threshold for rhythm generation showed fluctuation in activity with the central respiratory drive (Fig. 9). This may be explained by the fact that when rhythm generation was present, the central respiratory drive dominates as shown in the left and right thirds of (Fig. 9) with a reciprocal inhibition, at segmental level, of the deflation and inflation reflexes by the alternating central expiratory and inspiratory drives respectively. However in the middle third of the same figure central rhythm generation ceased and such alternating inhibition did not occur. However, the tonic drives were sufficient to facilitate the chest wall reflexes indicating a measure of coexistence as proposed by Sears, (1990). Hence, these results support the view that the normal functional operation of the inhibitory phase of the CRDP is to prevent reflex excitation of the antagonistic muscle contraction as discussed above.

3:2. Effects of cold block of the spinal cord in eupnoea

3:2:1. Dorsolateral cold block

With a dorsolateral position of the thermode (section a of panel A and B of Figs. 16 and 17), the inspiratory activity ceased after a brief burst. The expiratory activity however, showed an obvious initial rhythm superimposed on an exaggerated tonic activity, which attained a higher level than the peak level it had before application of the

cold thermode. This enhancement lasted for approximately 60s in panel B and 150s in panel C. This initial enhancement was attributed to the system response to the strong initial stimulation of the dorsal horn ascending fibre system (Brooks, 1983), and those of the thoracic tendon organs which ascend in the lateral column (Shannon, 1982). Stimulation of the latter was observed to inhibit inspiration and extends the expiratory time, by delaying the inhibition of medullary expiratory neurones by medullary inspiratory neurones. The overall process would be expected to result in the release of the expiratory motoneurones from their antagonistic inhibition.

With the progression of cold blocking, the expiratory activity although gradually declining, persisted for nearly 12min before eventually being completely blocked. The results could be most simply explained by the fact that blocking had interrupted the inspiratory bulbospinal axons and abolished, at segmental level, the inspiratory-linked reciprocal inhibition of the expiratory motoneurones (Sears 1964). Such disinhibition thus reveals the existence of a tonic excitatory drive to the expiratory motoneurones which potentially persists throughout the respiratory cycle (Bainton et al. 1979). This result is possible because at C3, the segmental level of these blocking procedures, the inspiratory bulbospinal axons are known to be mainly concentrated dorsolateral to the expiratory axons although with some axons descending among those of the latter

(Newsom Davis and Plum, 1972; Merrill 1974). Hence, the chance of inspiratory bulbospinal axons being blocked before all the descending expiratory axons is greater. The persistence of the initial rhythmic expiratory activity may be explained by the as yet not blocked portion of the inspiratory bulbospinal axons which were located more ventrally between the expiratory axons. The other possibility is that, the expiratory bulbospinal neurones themselves remained rhythmic, and that this rhythmic activity summated at segmental level with the now disinhibited tonic drive to provide the overall but progressively diminishing 'expiratory' drive to the spinal motoneurones. This explanation could thus summate the conclusions reached by Anderson and Sears (1970) on the basis of stimulating the 'respiratory centres' as defined by Pitts et al. (1939a), namely that the respiratory motoneurones could be in receipt of tonic as well as phasic drives, such summation occurring at segmental levels. The above explanation takes no specific account of the possibility that the alpha and gamma intercostal motoneurones contributing to the 'integral', might be subject to very different and indeed independent controls, but such differences would best be analyzed electrophysiologically. The above results are similar to the findings obtained by cooling (Budzinska, von Euler, Kao, Pantaleo and Yamamoto, 1985c) and lesioning experiments of the medulla (Bainton et al., 1978). In the first instance, focal cooling of rostral areas in the

medulla led to tonic activity in expiratory muscles with a strong inhibition of inspiratory activity. These 'release phenomena' were also associated with corresponding increments in the discharge rate of expiratory neurones in the caudal nucleus retroambiguus and Botzinger complex, which also send their axons to their counterparts in the thorax (Budzinska, et al. 1985c). In the second instance, the result is consistent with the work of Bainton et al. (1978) in which lesions were performed in the midline extending from the obex to 2- 3mm rostral, with the aim of interrupting the inspiratory bulbospinal axons, all of which in the cat decussate at this level (Merrill, 1974). Such lesions led to total loss of diaphragmatic and external intercostal muscle activity whilst the expiratory activity persisted throughout virtually the entire cycle but without alteration in its phase peak intensity. However, the present work showed that in the early stage of cold block the expiratory activity may attain a higher peak intensity as seen in Fig. 16, panel C. This is probably due to the different sites of interruption of the inspiratory bulbospinal axons, so the additional activity may be attributed to a tonic non-respiratory source (see later), or to the effect of 'disinhibition' being greater in the cold block preparation.

3:2:2. Recovery from dorsolateral cold block

After removal of the thermode, the expiratory rhythmic activity recovered first, with its peak intensity rising

above its control level and to about the same level of the immediate excitatory response produced by the application of the thermode to the cord (section b of panels B and C of Figs. 16, and 17). This would not be surprising, as the expiratory bulbospinal axons are located more ventrally, between the tip of the ventral horn and the ventral surface of the spinal cord, so their chance of earlier recovery is much greater. However, their release alone from cold block does not explain that additional activity. So this 'release phenomenon' certainly indicates that there is/are other source/s included (see below). The expiratory activity gradually declined again with the onset and gradual recovery of the inspiratory motoneuron activity indicating the release from block of the inspiratory bulbospinal axons (section c of panels B and C of Figs. 16, and 17). This led to an overall inspiratory bias in the pattern of respiratory motoneuron activation, accompanied by a concomitant reciprocal phasic reduction of the expiratory motoneuronal discharge as can be recognized by the declining base line of the expiratory integral until with further elevation of the CO_2, it increased in activity pari passu with increasing activity of inspiratory motoneurones. Although the temperature in the spinal cord was not directly measured, it appears from this sequence of events, that there is a range of temperature during which the balance of inspiratory and expiratory bulbospinal drives to the respiratory motoneurones shifts from one group to the other, and with this the corresponding reciprocal

inhibitions, before full recovery occurs at near normal temperatures (Fig. 16Bd and 17d). The situation during partial recovery would be thus similar to that which occurs during hypocapnic apnoea, when one central respiratory drive dominates throughout with tonic activity (Bainton et al.,1978); or, at levels of CO_2 subthreshold to rhythm generation the two drives can coexist as tonic, co-activation of inspiratory and expiratory motoneurones. At higher levels of CO_2, rhythm is expressed as a periodic, reciprocal inhibition of these tonic activities (Bainton et al., 1978; Sears et al., 1982; Sears 1990).

3:2:3. Ventrolateral cold block

In the following paragraphs discussion is directed with more details towards the effect of cooling on alpha and gamma motoneurones activity. In the control recordings (panel A of Fig. 10) both the inspiratory and expiratory activities were strongly active with some inspiratory gamma units firing althrough. Both records showed clear pump modulation of their selected gamma and alpha units corresponding to the inflation and deflation reflexes, respectively (panel A of Fig. 11). The inflation reflex of the expiratory motoneurones was abolished during the inspiratory phase (panel B of Fig. 11), corresponding to the hyperpolarising phase of the CRDP, whereas it was facilitated during expiration. Conversely the deflation reflex of the inspiratory motoneurones was abolished during expiration but facilitated during inspiration (panel A of

Fig. 11).

The immediate enhancement of the inspiratory alpha and gamma motoneurone activities following application of the thermode to the ventrolateral surface of the spinal cord (panels B of Fig. 10 and A Fig. 12), was attributed on the one hand, to the system response to the strong initial stimulation of the dorsal horn ascending fibre system (see before), and to the release of the inspiratory motoneurones from their antagonistic inhibition, on the other (see below). This enhancement of the inspiratory motoneuronal activities was accompanied by a concomitant reciprocal reduction of the expiratory alpha and gamma motoneuronal activities (panel B of Fig. 10 and Fig. 12). With the progression of cold blocking, the expiratory activity was abolished altogether in 2min, while the inspiratory alpha and gamma motoneuronal activities persisted for a prolonged period before eventually completely blocked. From the above, it was assumed that cold block had interrupted the descending axons conveying the expiratory activity. Of these axons, the expiratory bulbospinal, because of their more ventral location, were the first to be affected (see above). Furthermore, cold block might have affected those axons which convey the depolarizing phase of the CRDP. Accordingly, there would be low drive to the expiratory alpha and gamma motoneurones, and hence reduction of the mean level of their membrane potentials. This explanation accounts for the pattern of the reduction in number of the

expiratory alpha and gamma units (panel B of Fig. 12). Thus, the late surviving alpha spikes occurred only at the very end of central expiratory phase, and then only in phase with the inflation phase of the respiratory pump. Consequently, the overall amplitude of the inflation reflex discharge was reduced, and it then only occurred at the peak of the CRDP-like wave in the integral. Hence, it can be concluded that the late apparently reflex firing of expiratory alpha motoneurones is due to summation of the reflex input with the depolarising phase the of CRDP, which had been rendered sub-threshold for causing firing itself, due to the blocking of the expiratory bulbospinal axons. Meanwhile, the period of phasic discharge of the expiratory gamma motoneurones was also progressively shortened by the progressive loss of those firing early in the expiratory phase which would correspond to the early part of the CRDP (Sears, 1964), and is explained in the same way as for the loss of the alpha spikes (see above).

As discussed above, the initial reduction of the expiratory activity, was accompanied with a subsequent reciprocal enhancement of the inspiratory motoneurones activity, particularly of the gamma component and also that of the pump-modulated deflation reflex which occurred during the inspiratory phase (panel A of Fig. 12). With the progression of cold blocking, whereas the inspiratory alpha motoneurone activity was lost (after 6min) with the loss of respiratory modulation, the tonic gamma motoneurons

activity persisted for nearly 12min before being completely abolished (Fig. 10C). This may indicate that there is another non-respiratory drive to the gamma motoneurones which survived cold block after the block of the inspiratory bulbospinal drive. This may correspond to the tonic gamma motoneurone activity in the absence of respiratory rhythm (Sears, 1964c; Critchlow and von Euler, 1963; Eklund et al., 1964), which was found to be most prominent in those muscles with the highest proportion of muscle spindles, the rostral external intercostals, as observed from EMG recordings by Duron and Marlot, (1987) - this corresponds to the same area for our recording procedures-. The role of this tonic activity was suggested to serve a primarily postural role with respiratory modulation only at higher levels of drive (Sears,1964c; Duron, 1973).

3:2:4. Recovery from ventrolateral cold block

As expected, with the removal of the thermode the inspiratory activity was the first to recover (panel A of Figs. 13 and 14). This is because the inspiratory bulbospinal axons are located dorsolateral to the expiratory axons (Merrill, 1974) so their chance of earlier recovery is greater than that of the expiratory axons. With the later onset and gradual recovery from block of the expiratory bulbospinal axons, as indicated by the progressive increase in expiratory gamma and alpha motoneuronal activity, the inspiratory gamma activity

gradually declined, leading to an overall rhythmic expiratory activity (panel B of Figs. 13 and 14). This rhythmic expiratory activity was possibly due to recovery of those inspiratory bulbospinal axons contained within the same compartment as the expiratory bulbospinal axons, and which although not sufficiently active to drive the inspiratory motoneurons, provided reciprocal inhibition of expiratory motoneurons. This fluctuation in activity of both the inspiratory and expiratory motoneurons may be attributed to the effect of temperature on their descending bulbospinal axons following removal of the thermode(see above). In the early recovery period the smooth CRDP-like expiratory phased wave is determined by the firing of the gamma motoneurones which also showed the pump modulation locked to the inflation phase of the respirator. The alpha spikes only occur with each inflation as indicated by their integrals which after each initial rise decline to the base line. This suggests that the recovering expiratory drive was sufficient to cause continuous firing of the gammas, whereas the alphas were in receipt only of a subliminal drive as indicated by their intermittent firing (see above). Recovery appeared to be complete within 8min when the rhythmic activation of expiratory and inspiratory motoneurons had recovered to its control values.

3:3. Effects of cold block in hypocapnic apnoea

As for the effects of cold stimuli in eupnoea (section a in panels B and C of Figs. 16 and 17), application of the cold

thermode to the dorsolateral surface of the spinal cord in hypocapnic apnoea (section C of Figs. 18 and 19) evoked transient reciprocal reflex burst activity of both inspiratory and expiratory motoneurone populations. Whereas the expiratory burst activity occurred in an already tonically discharging expiratory motoneurones to attain double that of the control level, the inspiratory burst activity occurred in an already silent inspiratory motoneurones. As discussed above these evoked burst activities were attributed to the system response to the strong initial stimulation of the dorsal horn (Brooks, 1983) and lateral column (Shannon, 1982) ascending fibre systems. Also, the peak intensity activity of the expiratory motoneurones could be explained by same reasoning as for (section a in panels B and C of Fig. 16 and Fig. 17) mentioned above. Alternatively this additional activity may be attributed to the tonic non-respiratory source. This because single or double ipsilateral hemi section of the spinal cord, resulted in an abnormal pattern of respiratory discharge with more discharge of the expiratory motoneurones accompanied with a stronger modulation by the respiratory pump (Kirkwood, Sears and Westgaard, 1984). They attributed this added activity to the tonic non-respiratory source but partly proprioceptive in origin (see below). With progression of cold blocking the inspiratory motoneurones were rendered silent, whereas the expiratory motoneurones still showed some residual tonic activity in the integrated record which was

maintained for a long period before eventually being completely blocked. This was expected to be due to the low level 'gamma' spikes attributed to the spinal mechanisms (cf. Eklund et al., 1963; Sears, 1963) caused by the interruption of the inspiratory bulbospinal axons as a result of blocking, which would abolish at segmental level reciprocal inhibition of the expiratory motoneurones (Sears 1964).

3:4. Restoration of activity in hypocapnic apnoea

A constant finding in 4 hypocapnic preparations was that following the recovery from blocking there was an exaggerated tonic activity of the expiratory motoneurones. For example section E of Figs. 18 and 19 above, shows that this activity was double that before blocking and at the same level of the excitatory response produced by the cold thermode when firstly applied to the spinal cord. The simplest explanation of this additional activity would be that, the effects of cold thermode could have aroused the preparation and over the time scale involved (nearly 30min), led to a lighter level of general anaesthesia which would favour the expiratory bias state of the preparation. Otherwise, to relate this additional activity to the expiratory bulbospinal neurones following Bainton and Kirkwood (1979), and also bearing in mind they are monosynaptically connected to the expiratory motoneurones (Kirkwood and Sears 1973), this activity should be at the same level as before blocking, or blocking had released the

expiratory bulbospinal neurones themselves from other inhibitory sources. Alternatively, this additional tonic activity must represent an additional input, which suggests that a release process was involved. An interesting possibility could be that, this exaggerated expiratory activity could have resulted from postsynaptic potentiation induced by accumulation of synaptic transmitter following cold block of the expiratory bulbospinal drive. Termination of repetitive stimulation (at high frequencies) of synapses concerned in monosynaptic activation of motneurones and neuromuscular motor end plates, results in a sudden liberation of transmitter (Eccles and Rall, 1951). This liberation runs at a maximum attainable rate under the now, resting conditions causing maximum drainage of transmitter from the presynaptic terminals. Such a mechanism results in accumulation of 'available' transmitter (the amount of transmitter that is liberated by a given size of presynaptic impulse) above the resting level (Eccles, 1964). Consequently, a testing impulse would cause a potentiated post tetanic EPSP. The availability of the transmitter and hence, the post tetanic potentiation were found to correlate with the frequency rather than the number of impulses of the conditioning teteni. Such that, the higher is the frequency, the more is the transmitter liberation and post tetanic potentiation (Hubbard and Schmidt, 1963). The latter also, was found to be much more prolonged, lasting for minutes after long conditioning teteni of synaptic transmission than after brief tetani,

lasting only for seconds (Hubbard and Schmidt, 1963). Interestingly, it seems that there are much greater similarities between the factors that cause transmitter release (and hence subsequent post synaptic potentials) in neuromuscular synapses and those concerned in monosynaptic activation of motoneurones, on the one hand, and the factors concerned in activation of expiratory motoneurones, on the other. Namely, the expiratory bulbospinal axons monosynaptically excites the expiratory motoneurons (Kirkwood and Sears, 1974) at a peak firing rate of more than 120/s (Merrill, 1974), which is approximately equivalent to the post tetanic stimulation mentioned above. Furthermore, this physiological excitation occurs day and night throughout life whether the animal is breathing spontaneously or artificially ventilated and under anaesthesia with or without paralysis. Moreover in this particular experiment, cold block was performed in hypocapnic apnoea, so that tonic excitation was maintained for more than 12min. and the following resting period lasted for nearly 6min. It would therefore be expected that, after cessation of this long high frequency expiratory bulbospinal tetanus, there would be an accumulation of available transmitter therein above the resting level, as a consequence, restoration of activity would cause an increased liberation of transmitter so giving that observed potentiated tonic expiratory activity. Alternatively this potentiation would have followed chemoreceptor stimulation as it was shown that such

stimulation results in a persisting effect long after the original stimulus (Eldridge and Millhorn, 1981).

Another possibility could be that, this additional activity may be due to another system whose activity was released by blocking. One candidate for this would be the reticulospinal fibres arising from the nucleus reticularis gigantocellularis. Because sustained stimulation within the medial reticular formation causes a sustained activation of expiratory motoneurons and reciprocal inhibition of inspiratory motoneurons (Andersen & Sears, 1970). This activity persisted after sagittal brainstem lesions which interrupted the bulbospinal respiratory axons and appeared to represent a separate ipsilateral reticulospinal projection to the thoracic level in support of the anatomical findings of Pitts (1946). Furthermore, the reticulospinal fibres are located most medially on the medial border of the ventral horn (Bush, 1960), so that their chance of earlier recovery is greater than that of the bulbospinal expiratory axons regardless of the position of the thermode. Also, the long reticulospinal fibres were proved anatomically to send terminals to the thoracic motoneurones (Wilson, Yoshida and Schor, 1970). Although not carrying an input with a respiratory rhythm to the respiratory motoneurones (Salmoiraghi and Burns, 1960), the reticulospinal projections nevertheless could actually have an important role in the regulation of breathing. Specifically, this could be concerned with the adjustment

of a steady excitatory bias on the intercostal alpha and gamma motoneurones, with reciprocal inhibitory biasing of the antagonists (Andersen & Sears, 1970), these adjusting the operating point of the CRDP (Sears, 1967). Hence, it is proposed that such added tonicity of discharge arises from released traffic in the reticulospinal and expiratory bulbospinal axons.

The significant of the tonic activity in the origin of respiratory rhythm remains controversial. Duron (1973) has emphasised that tonic activities without respiratory modulation occur in the EMG of those muscles with the highest concentration of muscles spindles i.e. mainly the rostral external intercostal muscles, which corresponds to the area where efferent activity was obtained in this study. He has suggested that these tonic activities may be more important in determining the posture of the thorax, influencing thoracic movements and 'pulmonary distribution' or helping to determine the functional residual capacity of the lungs; as in stabilizing the shape of the rib cage. Furthermore these tonic activities were found to play an important role in the efficient operation of the diaphragm (Da Silva et al., 1977). von Euler (1983, 1986) has cast doubt on whether the response of tonic activity in hypocapnic apnoea, after sagittal incision and following cold block, represents genuine respiratory activity. Rather, he suggested that it represents a release of tonic activity in the systems mediating behavioural and non

respiratory functions of the internal intercostal and abdominal motoneurones.

3:5. Effects of cold block on chest wall reflexes

During hyperventilatory hypocapnic apnoea, the expiratory intercostal motoneurones showed alpha and gamma spikes (Fig. 20A In A). The single unit alpha spike occurring in phasic bursts with each inflation phase of the pump, while the individual gamma spikes fired tonically. This can be explained by the fact that the system is left in a state of expiratory apneusis (Sears, 1977). The rhythmic changes in the excitability of the expiratory motoneurones has been abolished not only, because of loss of reciprocal inhibition of the expiratory motoneurones at segmental level, but also because of loss of periodicity of the expiratory bulbospinal system at medullary level (Sears, 1964c; Bainton et al., 1978; Bainton and Kirkwood, 1979). Hence, the discharge pattern of the expiratory motoneurones is now simplified and can be explained in terms of their known supraspinal and proprioceptive inputs. This excitatory bias allowed the segmental chest wall inflation reflex to be seen uncomplicated by the rhythmic inhibition of these motoneurones.

With application of the cold thermode to the dorsolateral surface of the spinal cord, the alpha spikes gradually decreased in number before completely abolished. Eventually the cold block had interrupted the descending supraspinal

drives (see above) and subsequently brought the mean level of the membrane potential of the expiratory alpha motoneurones to its resting level. Thus the loss of these inputs at segmental level specifically reduces the efficacy of synaptic transmission from expiratory muscle spindle afferents due to the conductance changes associated with this postsynaptic inhibition. Although not pump modulated, the tonic discharging gammas reduced in number with the progress of cooling, This seems to be one of the sources facilitating the inflation reflex as their reduced firing reduced the amplitude of the reflex (for the significance of the tonic activity see above). Furthermore, there was evidence from Sears (1958) and Ramos and Mendosa (1959), that during hypocapnia expiratory motoneurones receive a tonic facilatatory mechanism that favours their activation by stretch reflexes induced by lung inflation.

3:6. Restoration of chest wall reflex activities

With the removal of the thermode, conduction in the descending axons including the expiratory bulbospinal was progressively restored. It was assumed these drives progressively depolarized the expiratory alpha motoneurones resulting in the gradual reappearance of alpha spikes with each inflation phase of the respiratory pump in reverse order of their loss, i.e., last to block, first to recover (Fig. 20E and F).

SECTION B: Olivary Results

In the experiments described in this section of Results extracellular recording through glass-coated tungsten electrodes was used to search for respiratory-related activities in the DAO. Inspiratory and expiratory motoneurone activities were recorded from the external and internal intercostal nerve filaments at eupnoeic or elevated levels of CO_2. Three principal types of respiratory related activities were encountered; 1), respiratory phased mass activity; 2), respiratory phased, low frequency activity; and 3), respiratory pump locked activity. The preparations were then subjected to changes in the chemical drive to look for any changes in behaviour of the olivary discharges that might indicate their spinal or supraspinal origin and this was also examined through reversible cold blocking of the spinal cord. The last part of the Results finishes with the description of a category of monophasic mass respiratory discharges encountered within the territories of the DAO and the Section concludes with a discussion of these Results.

1. Respiratory phased high frequency activity

Examples of this type, which could be in phase with either inspiration or expiration, are shown in A of Figs. 21 and 22 (from different locations). In each figure the lower trace displays the firing of neurones recorded from within

the inferior olive of the same preparation, together with the integrated neurograms recorded from an external intercostal nerve filament as an index of the central respiratory drive (upper trace). The recordings in Fig. 21 were made early in the experiment while those in Fig 22 made at the end of the experiment when the pattern of breathing had changed. In Fig. 21A, the olivary activity is in phase with central inspiration, and consists of low amplitude (200uv), mainly single, and diphasic spikes of 1.5ms duration, as shown in expanded form in B, with a firing rate augmenting from 25-40/s within each cycle. Individual spikes often fire in couplets. In contrast the firing of the other example of high frequency olivary activity, is in phase with central expiration as shown in Fig. 22A. The spike shape as shown in expanded form, is similar to that in Fig. 21 B, being diphasic 180uv in amplitude and of 2ms duration with a peak frequency of 50/s. The figure also shows an envelope of low amplitude 'mass', inspiratory-phased activity which is absent during the expiratory half of the cycle. The discharge pattern of olivary neurones in Figs. 21 and 22, is similar to that of the mass inspiratory or expiratory bulbospinal activity in the ventral respiratory group as described by Merrill (1970, 1974) and many others, but in this latter case the mean and peak firing rates were much higher (Kirkwood, 1995; Bainton and Kirkwood, 1979). The single units shown above were isolated from the mass activity by adjustment of electrode position and the use of fine electrodes.

Fig. 21

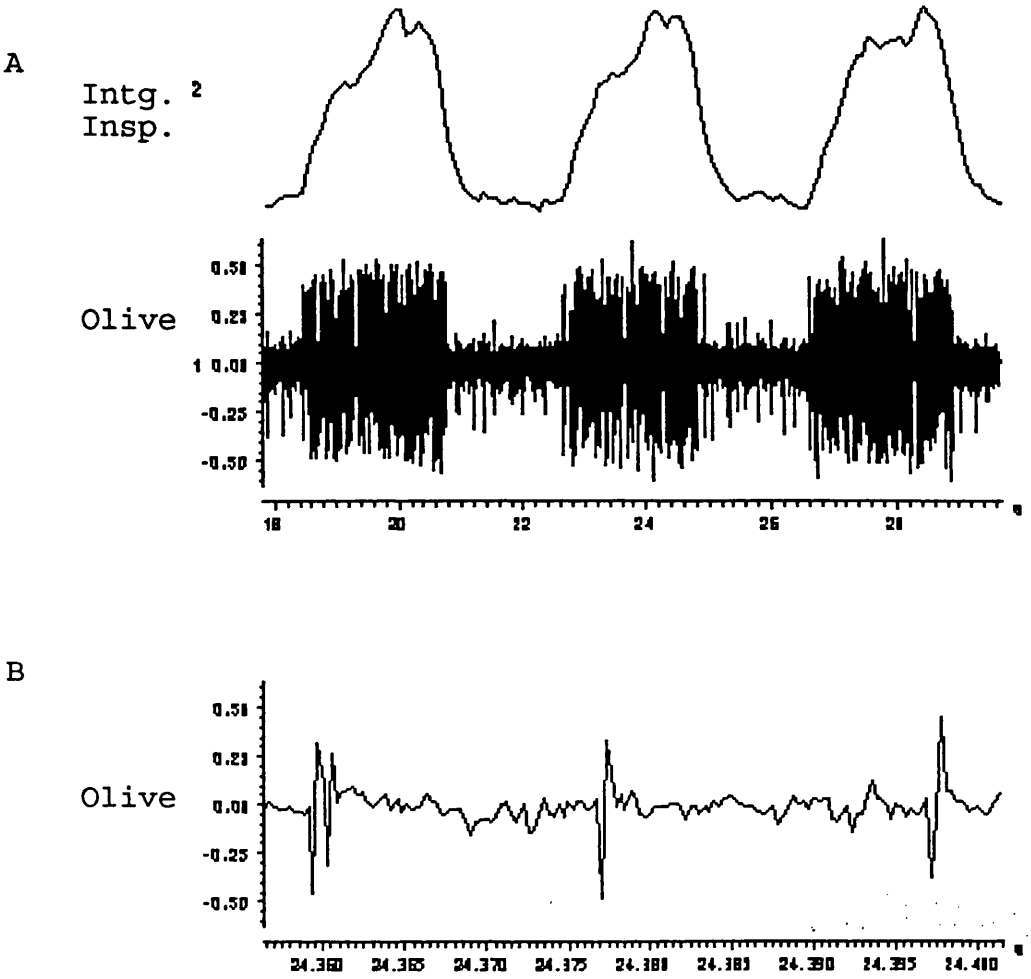

Fig. 21. A, extracellular recording from a paralysed fictively breathing preparation illustrating an inspiratory phased activity in the inferior olive (channel 1), with its respective integrated neurogram recorded from external intercostal (inspiratory) nerve filament (channel 2) B, spike shape in a fast sweep display which is of low amplitude (200uv), diphasic and of 1.5ms duration, note the burst of 2 spikes on the left. Vertical calibration in mv.

Fig. 22

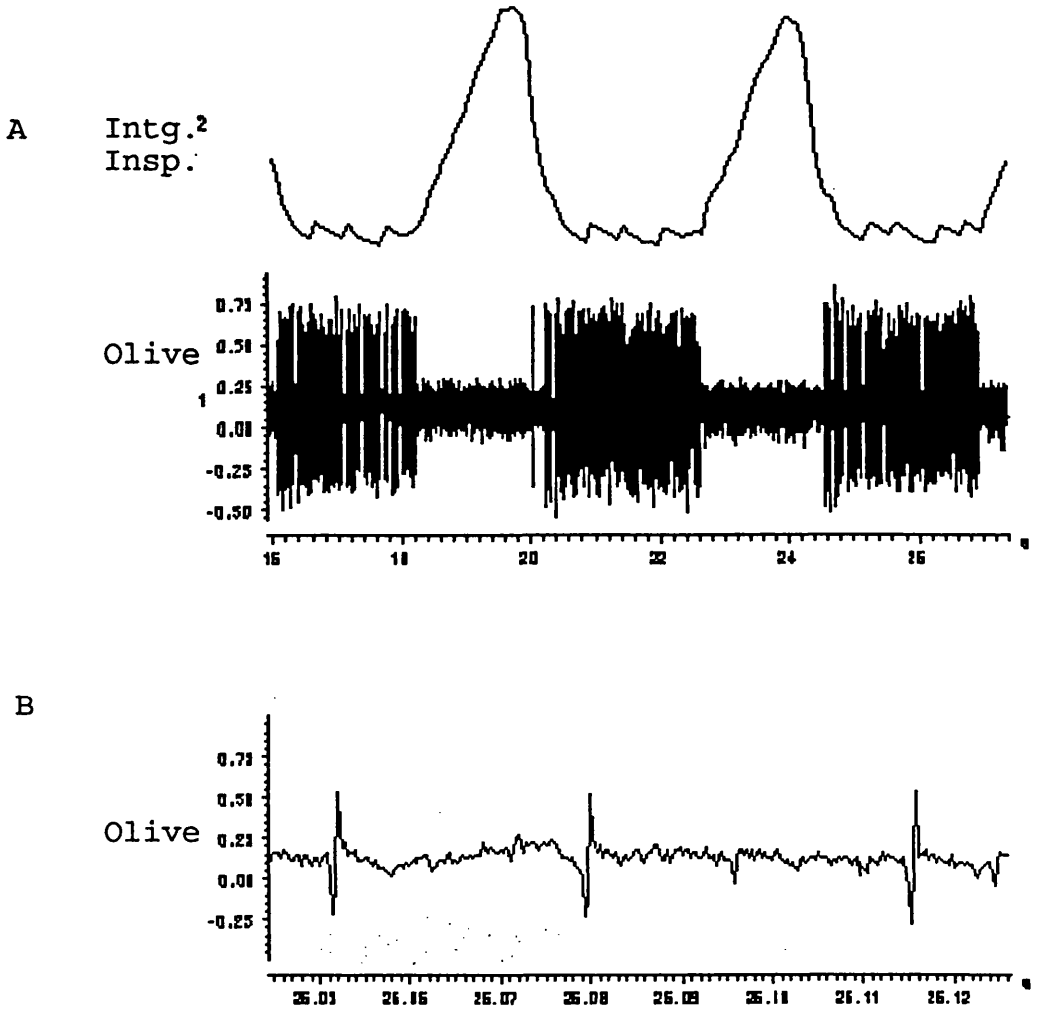

Fig. 22. A, extracellular recording from the same preparation as in Fig. 21 illustrating expiratory phased activity in the inferior olive (channel 1), with its respective integrated neurogram recorded from an inspiratory nerve filament (channel 2); B, spike shape in a fast sweep display. Vertical calibration in mv.

2. Respiratory phased low frequency activity

This type of respiratory activity consists of diphasic, single or complex spikes of moderate to high amplitude (300uv - 1.0mv), and from 1.5 - 5ms duration. The spikes discharge singly but, more typically, occur repetitively at low frequencies ranging from 2 - 15/sec, in phase with either central inspiration (Fig. 23 and 24) or expiration (Fig. 25). Channel 1 in Fig. 23, shows the original olivary single unit recording, together with its instantaneous frequency and rate in channels 4 and 5. Channels 2 and 3 show the integrated neurograms of the inspiratory and expiratory motoneurone activities, respectively. The unitary olivary activity is in phase with central inspiration, and consists of moderate amplitude (300uv), diphasic spikes with an overall duration of 5ms obtained by spike triggered averaging of 200 spikes in 23 inspiratory half cycles as shown in Fig. 23B. This unit has a firing rate varying from 5 and 12/s within the respiratory half cycle. This figure also shows two more important features of the olivary activity when examined as rate. The first is that the rate was found to be modulated during inspiration with a period approximately of 1s which corresponds to 60/min which is the frequency of the respiratory pump. The movements of the pump or the resulting airway pressure are not illustrated in this particular figure, but their phase can however be inferred from channel 2 in which the integrated inspiratory

Fig 23. A single olivary unit firing at low frequency during inspiration. A, Channel 1 shows the original olivary activity together with its instantaneous frequency and rate in channels 4 and 5, respectively. Channels 2 and 3 show the integrated neurograms of inspiratory and expiratory motoneurone activities, respectively. Average spike shape is shown in B.

Fig. 23.

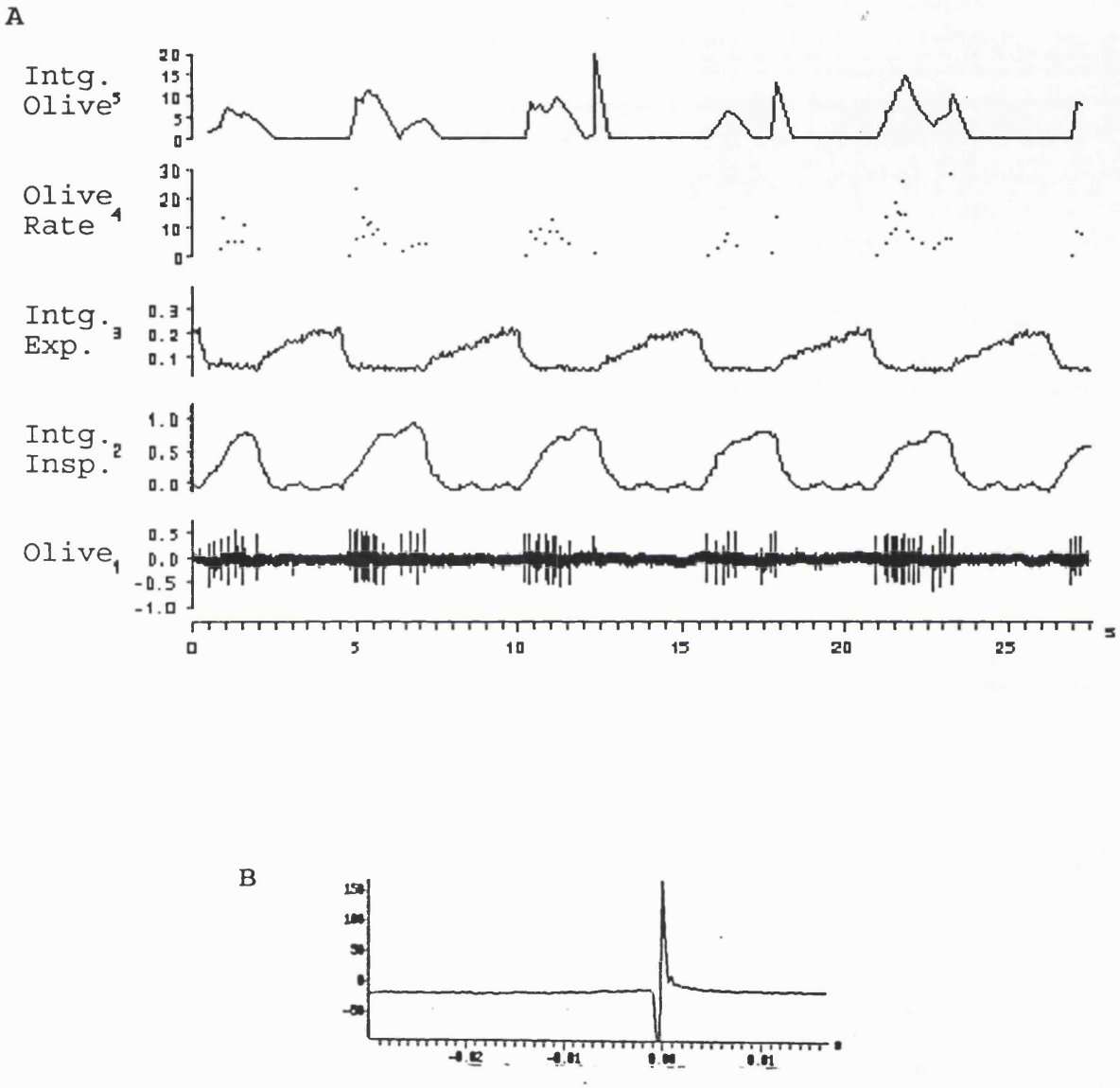

intercostal motoneurone discharge shows modulation at the same rate.

As described earlier (section III:A) stretch of the external intercostal muscles spindles induced by deflation of the chest wall, reflexly excites the inspiratory intercostal motoneurones during the inspiratory phase of the 'central respiratory drive'. Hence, the pump modulated inspiratory phased olivary activity, in channel 5 can be seen to occur in phase with the pump-locked deflation reflex discharge of the inspiratory intercostal motoneurones. The second important feature is obtained by comparison of the integrated 'central' inspiratory motoneurone activity (channel 2) with that of the olivary activity (channel 5) in terms of rate. Both display a CRDP-like wave of activity. However, when the former is augmenting, the latter is decrementing, to form a mirror image. For the former, this was confirmed by further analysis of the number of occurrences of olivary discharges in the first and second halves of the inspiratory half cycle. As shown in Table 1, the number of discharges in the first half varied between 5.00 and 16.00 (mean = 11.45, SD^{+}_{-} = 2.39, n = 20), while their number in the second half varied between 4.00 and 13.00 (mean = 7.50, SD^{+}_{-} = 2.40, n = 20). The ratio of the mean firing in the first half to the second half was found to be 1.63.

In the same preparation following partial cerebellectomy

Table 1.

Half cycle No.	A No. of spikes in the 1st half	B No. of spikes in the 2nd half	Ratio A/B
1	10	7	1.43
2	5	5	1.00
3	14	6	2.33
4	11	9	1.22
5	10	7	1.43
6	10	7	1.43
7	13	10	1.30
8	14	9	1.56
9	12	5	2.40
10	8	6	1.33
11	12	8	1.50
12	10	7	1.43
13	11	5	2.20
14	11	13	0.85
15	12	9	1.33
16	16	12	1.33
17	13	7	1.86
18	12	5	2.40
19	11	4	2.75
20	14	9	1.56
Mean	11.45	7.50	1.63
SD	2.39	2.40	0.52
Maximum	16.00	13.00	2.75
Minimum	5.00	4.00	0.85

Table 1. Relationship between the number of olivary spikes in the first and second halves of 20 inspiratory half cycles, to show the decrementing firing of an olivary neurone discharging at low frequency.

including the posterior lobe and the cerebellar nuclei, a high amplitude (600uv) single unit was recorded discharging apparently at low frequency (4-6/s) and in phase with central inspiration (Fig 24A, channel 1). However, as shown on a fast time base in Fig. 24B, each discharge consisted of a burst of up to 7 brief duration impulses discharging at high frequency (400-500/sec). The figure (B) also revealed low amplitude complex spikes of 3-4 impulses picked by the microelectrode probably from remote olivary neurones, possibly in the same ensemble (cf Foster et al., 1986). Such 'burst' activity was not dependent on the use of paralysis, as similar recordings were obtained in non-paralysed intact preparations as illustrated for the unit shown in Fig. 25. Here an apparent single unit of high amplitude (1.0mv) discharged at about 4 - 6/s, during the expiratory phase (panel A). However, as seen on a fast time base each discharge consisted of a brief duration high frequency (400-500/sec) burst of 1-7 impulses (panel D). The bursting pattern of discharge in these olivary units in response to normal physiological stimuli (the central respiratory drive) is similar to the characteristic bursting discharge of olivary neurones evoked by single-shock electrical stimulation of peripheral nerves (Armstrong et al. 1968, Crill 1970) but with the difference that the bursting pattern was summated for the entire expiratory phase. The data in the second example was subjected to more extensive analysis of all discharges occurring within 20 expiratory half cycles as illustrated

Fig. 24

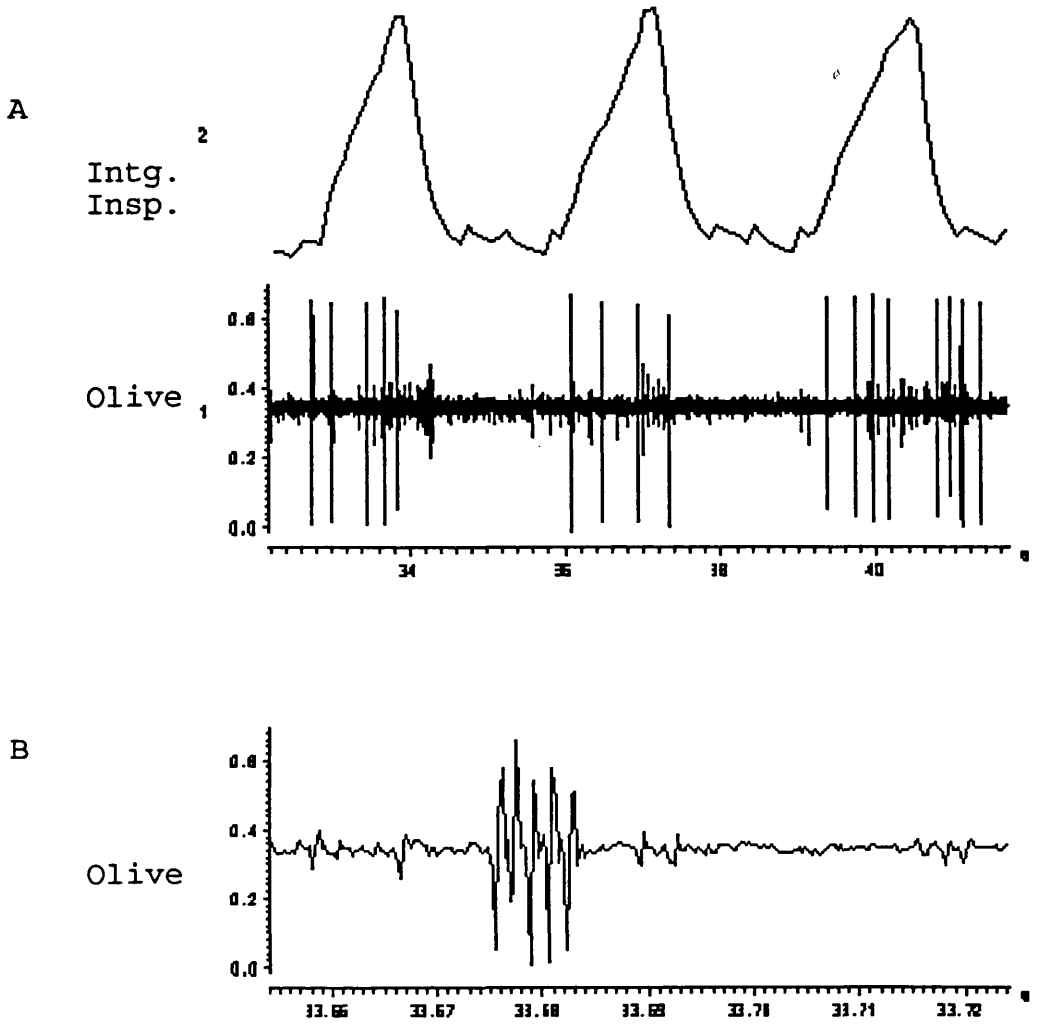

Fig. 24. A: An example of a high amplitude single unit discharging repetitively at low frequency (4-6/s) recorded from the same preparation as in Fig. 23 (after partial cerebellectomy), and in phase with central inspiration (channel 1). Channel 2 shows the integrated neurogram of central inspiratory activity. B: shows on a fast time base that one discharge consists of a burst of 5 brief duration impulses discharging at high frequency of 500/sec. Note the low amplitude complex spikes of 3-4 impulses on the background. Vertical bar in mv.

Fig. 25

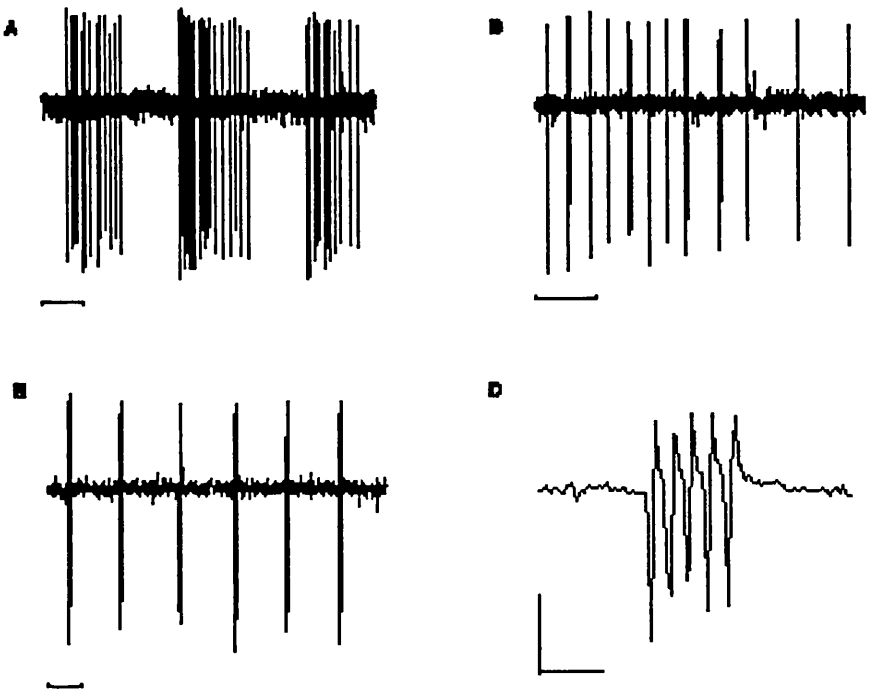

Fig. 25. Another example from an non-paralysed (anaesthetized) preparation showing a high amplitude single unit discharging repetitively at low frequency (4-6/sec), in phase with central expiration (panel A). Panels B, C and D are shown on a fast time base. Each discharge was found to consist of a brief duration high frequency (400-500/sec) burst of 1-7 impulses (panel D). Horizontal bar = 2, 0.5, 0.1 and 0.01s for A, B, C, and D respectively. Vertical bar = 300uv.

in Fig. 26. This was done to determine the relationship, if any, between the number of wavelets in each discharge and the period of the subsequent interval, on the basis that the number of high frequency spikes might influence, if not actually determine, the duration of the resulting afterhyperpolarization, as in the case of Purkinje cell burst activity (cf. Campbell and Hesslow, 1986a and b). It is apparent from this figure that the symbols fall into 3 main clusters. The first cluster represents olivary discharges that consist of 3 wavelets following the initial spike, the subsequent periods of each burst being found to range from 60 - 200ms. The second cluster, which is more prominent consists of 4 wavelets/discharge with their subsequent periods between 75 and 300ms. The third cluster consists of 5 wavelets/discharge and subsequent interval periods of 100 - 400ms. This figure indicates that there is a strong tendency for an increase in the interval between burst discharges whenever there is an increase in the number of wavelets within the preceding burst discharge, which tendency is also applicable to the scattered symbols shown in the figure.

As in the case of the inspiratory unit shown in Fig. 23, the expiratory unit of Fig. 25 was also found to have an overall decrementing pattern of firing. Hence, a similar analysis was performed on same data (Table 2). It was found that the number of discharges in the first half of the

Fig. 26.

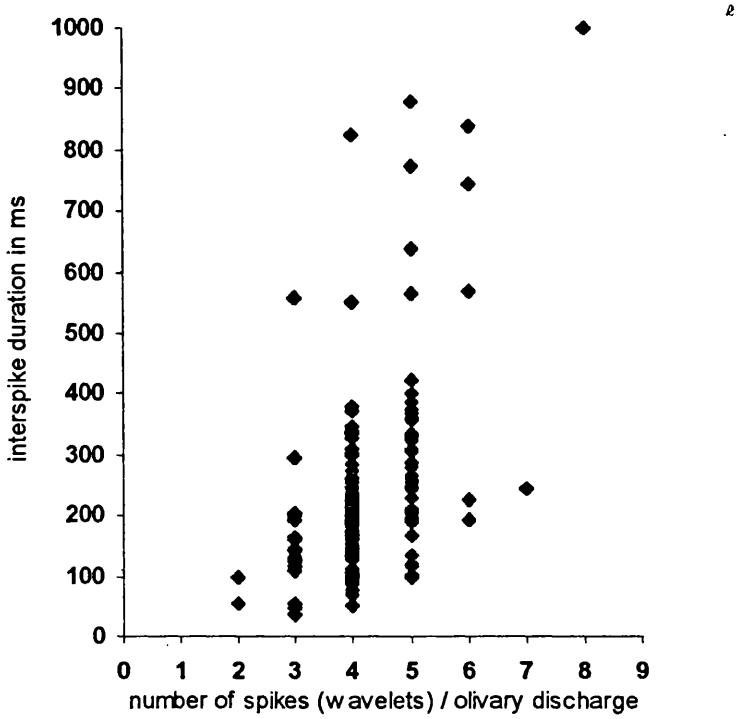

Fig. 26., shows the relationship between the number of wavelets/olivary discharge and the subsequent interspike duration, obtained from olivary discharges occurring in 20 expiratory half cycles (from the same section of data as in Fig. 25). Note that the symbols fall into 3 main clusters; the first represents olivary discharges with a burst of 3 wavelets/discharge and a subsequent interspike period of 60 - 200ms, the second consists of 4 wavelets/discharge and a subsequent interspike period of 75 - 300ms and the third cluster consists of 5 wavelets/discharge and a subsequent interspike period of 100 - 400ms. Note also, the tendency for the increase in interspike period whenever there is an increase in the number of wavelets within a preceding discharge.

Table 2.

Half cycle No.	**A** No. of discharges in the 1st half	**B** No. of discharges in the 2nd half	Ratio **A/B**
1	13	7	1.86
2	12	6	2.00
3	14	8	1.75
4	10	5	2.00
5	5	3	1.67
6	12	7	1.71
7	8	4	2.00
8	9	5	1.80
9	8	5	1.60
10	8	4	2.00
11	12	5	2.40
12	12	7	1.71
13	7	4	1.75
14	8	3	2.67
15	10	5	2.00
16	9	4	2.25
17	3	6	0.50
18	6	4	1.50
19	5	3	1.67
20	7	2	3.50
Mean	8.90	4.85	1.92
±SD	2.97	1.60	0.56
Maximum	14.00	8.00	3.50
Minimum	3.00	2.00	0.50

Table 2. Relationship between the number of olivary discharges in the first and second halves of 20 expiratory half cycles, to show the decrementing firing of an olivary neurone discharging at low frequency. Data obtained from continuous recording as in Fig. 25. Note that the mean number of discharges in the first half is nearly twice that of the second half.

expiratory phase, varied between 3.00 and 14.00 (mean = 8.90, SD^{+}_{-} = 2.97, n = 20), whereas their number in the second half varied between 2.00 and 8.00 (mean = 4.80, SD^{+}_{-} = 1.60, n = 20). The ratio of the mean firing in the first half to the second half = 1.92, which clearly indicates that the total number of discharges fired by this unit in the first half is nearly twice that during the second. Hence, unlike the typical augmenting pattern of the expiratory motoneurones, this analysis confirms the decrementing firing pattern of this olivary unit. This is further supported by Fig. 27, which shows the sequence of interspike durations in the first 8 of the above 20 expiratory half cycles, arranged consecutively along the abscissa, plotted against their relevant periods as ordinate in A and B. It is evident that within each cycle the period increases towards the end of each half cycle indicating the decrementing frequency of firing of this olivary unit.

Another feature of the low frequency discharge of olivary neurones is their firing at the peak of a specific phase as illustrated in channel 1 of panels A and B in Fig. 28 recorded in different preparations. Panel A, shows an example of olivary activity at end inspiration, and in panel B the activity is superimposed on the summit of an envelope of mass inspiratory activity. Channel 2 shows the integrated neurogram of the external intercostal nerve at T3.

Fig. 27.

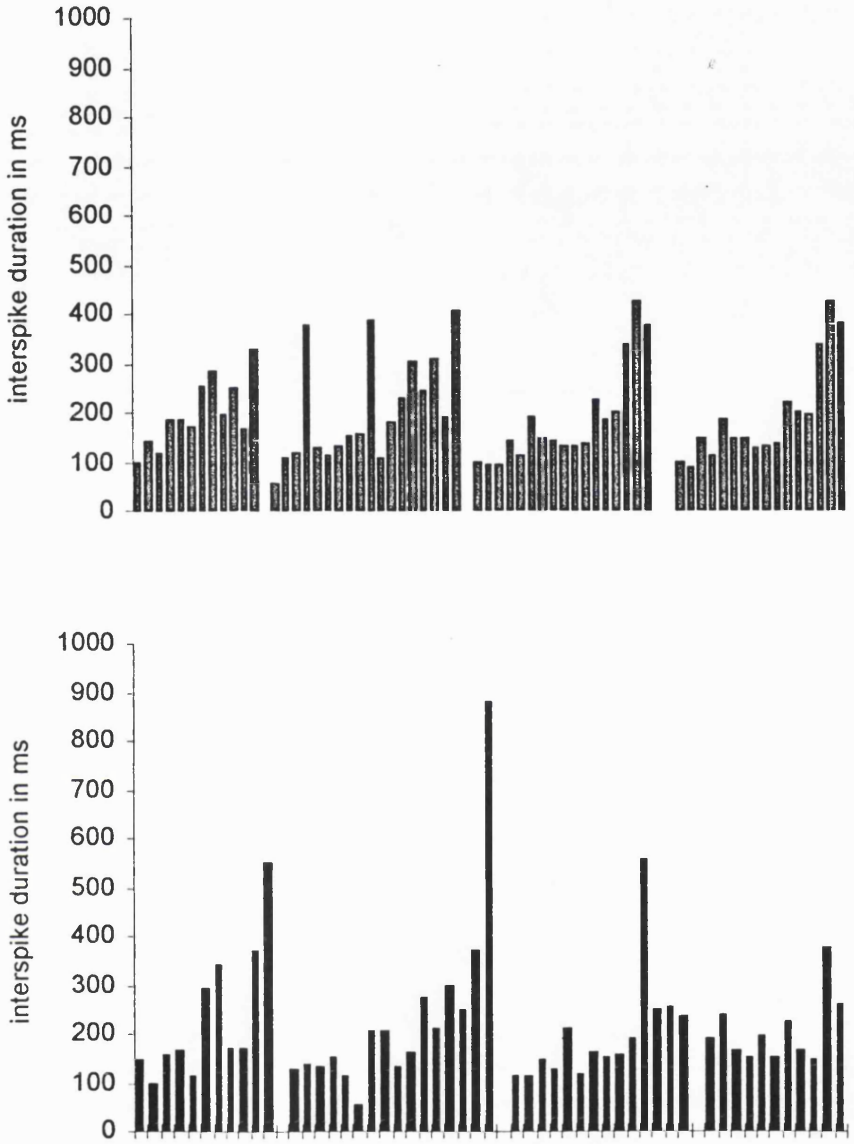

Fig. 27, shows the decrementing frequency of firing of the expiratory olivary unit shown in Fig. 25, as obtained from the sequence of interspike intervals in the first 8 half cycles. The individual interspike intervals are arranged consecutively along the abscissa, plotted against their relevant periods as ordinate. Note that these periods are increasing towards the end of each half cycle.

Fig. 28.

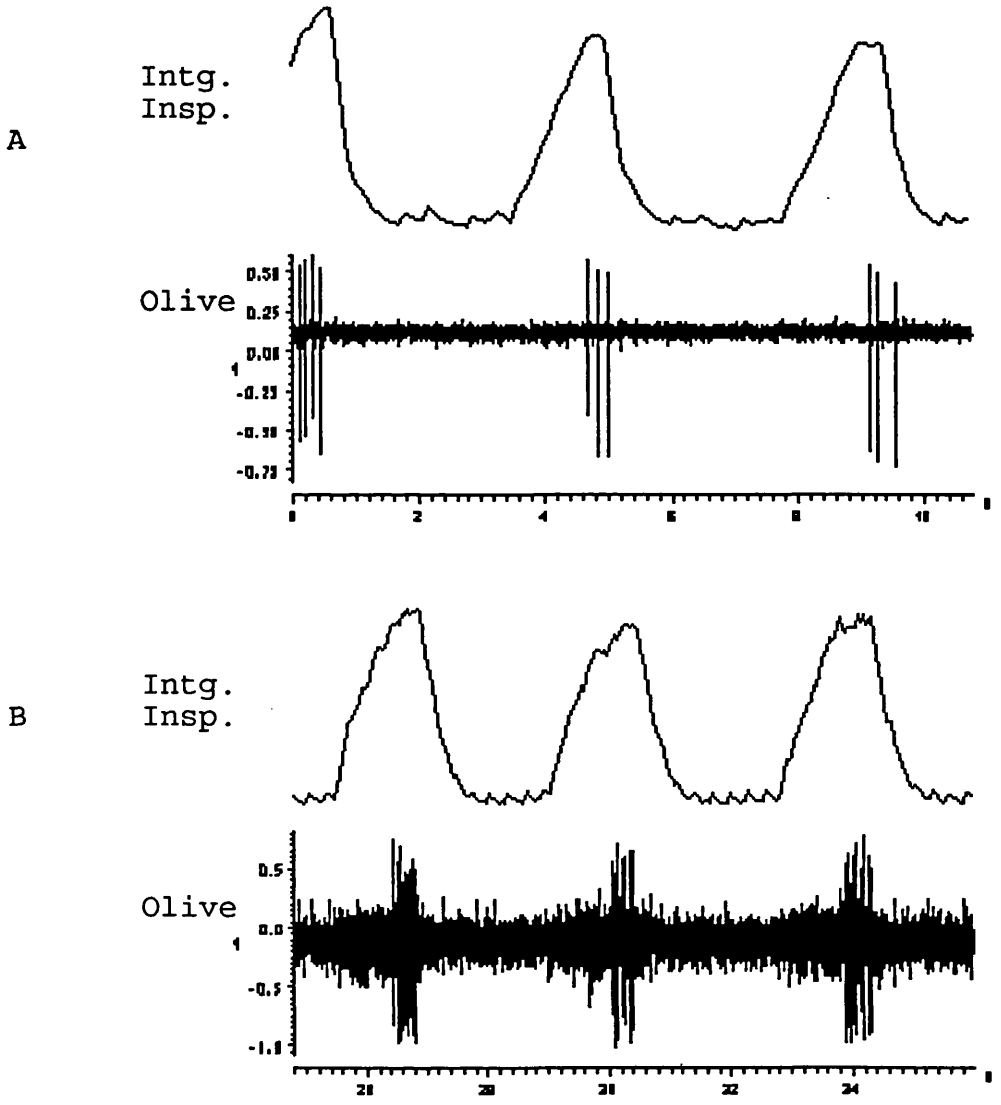

Fig. 28. shows other variants of the low frequency pattern of olivary neurones recorded from different preparations discharging at end inspiration (channel 1). Panel A: at the submit of central inspiration, Panel B: superimposed on top of an envelope of mass inspiratory activity. Channel 2 shows the integrated neurogram of central inspiratory activity. Vertical calibration in mv.

3. Pump modulation of the olivary phasic activity

For much of the work, eupnoeic or moderately elevated levels of respiratory drive were utilized to search for respiratory-phased olivary activity. Frequently, it was difficult to characterize clearly the phasing of the olivary discharge due to the occurrence and sporadic nature of intermittent discharges throughout the respiratory cycle. However, the situation was greatly clarified, when searching was performed during hypocapnic apnoea or at levels of CO2 near threshold for rhythm generation. The above type of low frequency discharging neurone was then found to display respiratory pump modulated activity concomitant with the segmental reflex activation of either the internal intercostal motoneurones during inflation of the chest wall or the external intercostal motoneurones during its deflation. Fig. 29 shows simultaneous recordings from the olive and the external (inspiratory) and internal (expiratory) intercostal nerve filaments. This preparation is showing spontaneous transitions from central rhythm generation to apnoea. The upper trace shows the olivary activity which consists of high amplitude (500 uv), diphasic spikes of 5ms duration and a firing rate varying from 5 - 12 /s. Integrals of the inspiratory and expiratory motoneurone activities are shown in the middle and lower traces. During central rhythm generation the olivary neurone discharged sporadically but mainly during the inspiratory phase of the cycle (extreme left and right of

Fig. 29.

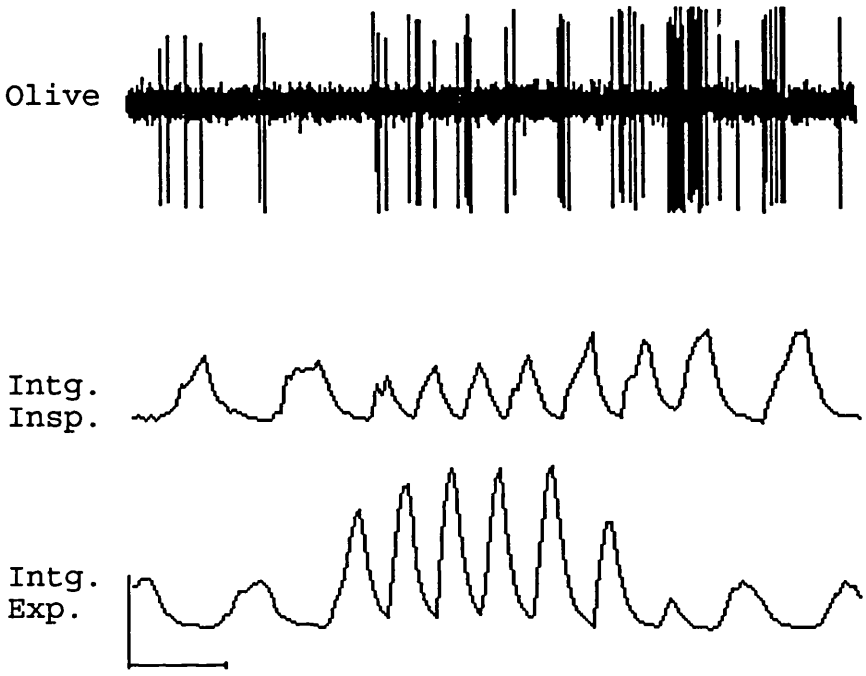

Fig. 29. Continuous recordings from DAO (upper trace) and external (inspiratory) and internal (expiratory) intercostal nerve filaments displayed as integrated neurograms in the middle and lower traces, respectively. Note the spontaneous transitions from central rhythm generation (left 2 cycles) to proprioceptive phasing of activities (middle of figure) and central phasing again (see text). Horizontal bar = 2s. Vertical bar = 250uv.

the upper trace). However, during apnoea (middle section) its discharge became clearly locked to the deflation phase of the pump and concomitantly there is reflex activation of the external intercostal motoneurones. When the central rhythm generation resumed, the overall olivary discharge was restricted to the central inspiratory phase including that of the reflex component seen in the integrated inspiratory record.

Other examples of pump locked activity from different preparations in phase with either the deflation or inflation phase of the pump are illustrated in Figs. 30 and 31, respectively. In Fig. 30 the olivary recording is displayed in channel 1 with its corresponding integral in channel 2; channel 3 depicts the phasing of the respiratory pump. As shown in the control recording in panel A, this olivary activity, which consists of regular bursts of spikes occurring at intervals of one second corresponding to rate of the respiratory pump, is superimposed on an underlying low-voltage inspiratory phased mass activity, best seen in the integral. The regular bursts of activity correspond to the deflation phase of the respiratory pump, as indicated by the dotted line, and they occur in synchrony with the chest wall movements produced by the respirator. Panel B shows the effect of stopping the respiratory pump (arrow), which resulted in progressive augmentation and prolongation of the inspiratory activity,

Fig. 30. Example of pump-locked activity in the DAO in-phase with chest wall deflation. The olivary recording is displayed in channel 1 with its corresponding integral in channel 2; channel 3 displays the CO_2 record which reflects the phasing of the respiratory pump. Panel A, control recording. The dotted line shows the association of the regular, olivary bursting with the peak deflation phase of the respiratory pump. Panel B, the effect of stopping the respiratory pump (arrow). Note the progressive augmentation and prolongation of the inspiratory-phased mass activity and the associated loss of the deflation pump-locked component. Panel C, shows the behaviour of the olivary activity as a result of turning on the respiratory pump.

Fig. 30.

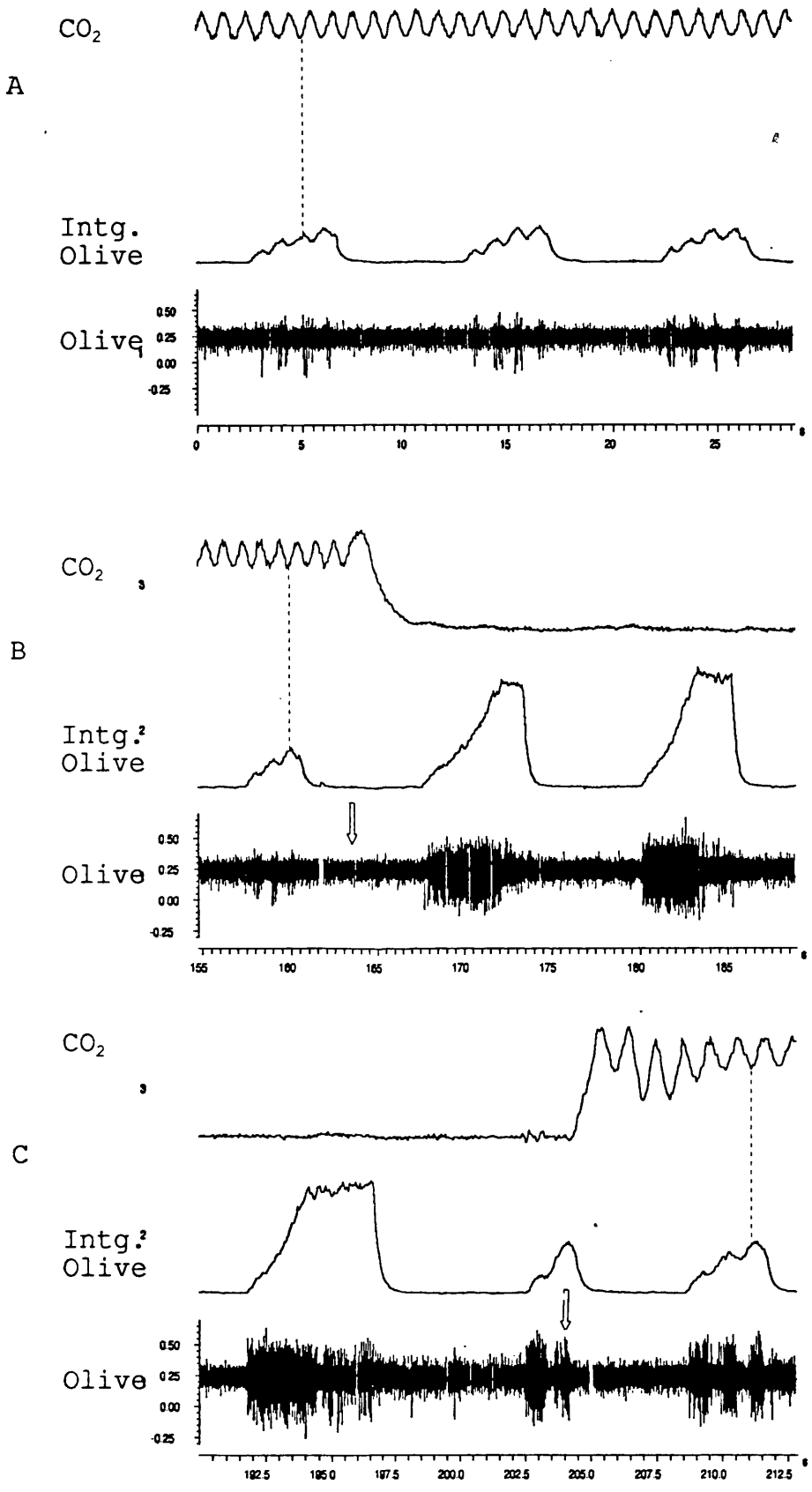
A
CO_2
Intg.
Olive
Olive
0.50
0.25
0.00
-0.25
0
5
10
15
20
25
B
CO_2
Intg.^{2}
Olive
Olive
0.50
0.25
0.00
-0.25
155
160
165
170
175
180
185
C
CO_2
Intg.^{2}
Olive
Olive
0.50
0.25
0.00
-0.25
192.5
195.0
197.5
200.0
202.5
205.0
207.5
210.0
212.5

with subsequent loss of the deflation phase pump-locked component. Panel C shows the behaviour of the olivary activity as a result of turning on the respiratory pump which led to gradual restoration of the olivary activity towards the control recording as manifested by the resumption of the deflation bursts superimposed on the low voltage mass inspiratory activity. Fig. 31 illustrates an olivary recording consisting of mass inspiratory-phased activity augmenting towards the end of the half cycle, alternating with an expiratory phased activity (lower trace). The integral of this olivary activity is displayed in the middle trace. Close examination of the olivary inspiratory activity revealed that it contains some units firing at a rate of 1/s which is the set rate of the respiratory pump. The expiratory-phased olivary bursts also occurred at the same rate. Neither the movements of the pump or the resulting airway pressure were recorded in this experiment, but the phasing of these pump-locked olivary bursts can however be inferred from the CO_2 traces which closely follow the phasing of the respiratory pump and which have been added with correct phasing to panels A and B. The inspiratory pump-locked olivary units were found to occur with each deflation phase of the respiratory pump, best seen in the integral as indicated by the left hand dotted line in panel A and the right hand line in panel B. The expiratory-phased olivary bursts occurs in synchrony with peak inflation phase as indicated by the right hand dotted line in panel

Fig. 31. Inspiratory and expiratory-phased central modulation of olivary activity evoked by deflation and inflation of the chest wall. Olivary recording displayed in the lower trace with its integral in the middle trace, the upper trace depicts the phasing of the respiratory pump. Note that: 1), the mass olivary activity which is in phase with central inspiration contains some units firing with each deflation phase of the respiratory pump, best seen in the integral (left and right dotted lines in panels A and B, respectively); 2), the olivary expiratory phased activity occurs in synchrony with the peak inflation phase of the respiratory pump (right and left dashed lines in panels A and B, respectively). When the pump was turned off (arrow in panel A), the inflation and deflation related activities immediately ceased and resumed when the pump was turned on (arrow in panel B), whereas the inspiratory central activity showed a slight but definite increase.

Fig. 31

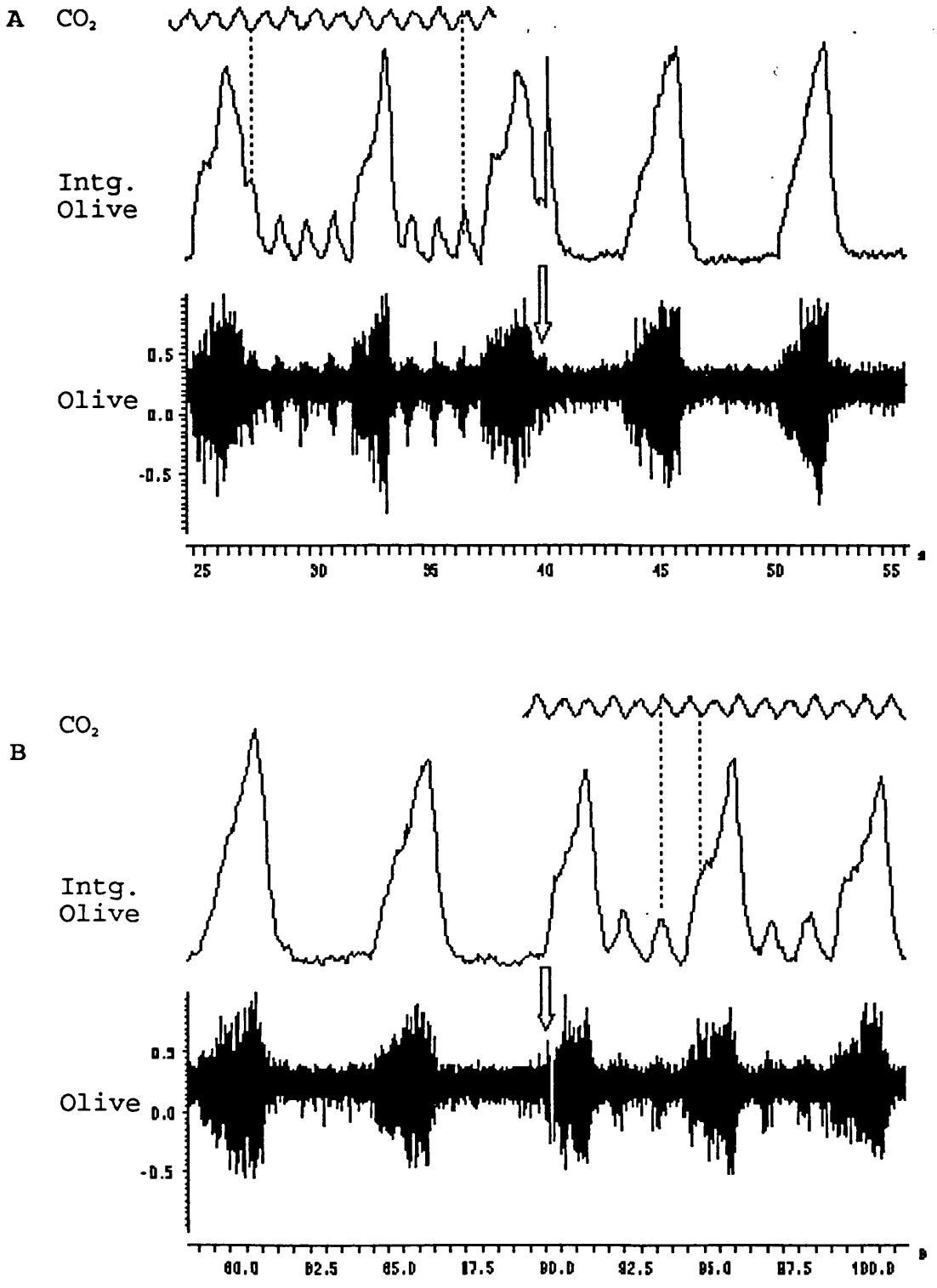
A
CO_2
Intg.
Olive
Olive
0.5
0.0
-0.5
25
30
35
40
45
50
55
B
CO_2
Intg.
Olive
Olive
0.5
0.0
-0.5
80.0
82.5
85.0
87.5
90.0
92.5
95.0
97.5
100.0

A and left hand line in panel B. Eventually this olivary recording is mixed with components in synchrony with the chest wall deflation and inflation as produced by the respirator and its modulation by the central rhythm generation corresponds with the inflation and deflation reflexes. When the pump was turned off (arrow in panel A), the activity due to the inflation and deflation reflexes immediately disappeared and resumed when the pump was turned on (arrow in panel B), whereas, the central inspiratory drive showed augmentation as obtained from measures of the integrand inspiratory wave forms.

The experimental basis of the attribution of the pump-locked activation of the intercostal motoneurones to chest wall reflexes is dealt with in section IIIA. The pump-phased olivary activity, is here also provisionally attributed to muscle spindles in the external and internal intercostal muscles. However, it was thought necessary to check the phasing of the afferent discharges from these two sets of muscles under the specific circumstances of the present experiments. Recordings were simultaneously made of olivary activity and the afferent discharges in the external and individual branches of the internal intercostal nerve. Fig. 32 shows recordings from a paralysed, expiratory-biased preparation during artificial ventilation without the addition of CO_2, and with the pump rate held at 80/min so that F_ACO_2 was 1.5%. Channels 1 and 2 illustrate the original recordings of the olivary

activity and the mass afferent activity in the cut distal branches of the external intercostal nerve with their respective integrals in Channels 3 and 4. Channel 5 shows the airway pressure (scale cmH_2O). From panel A it is apparent that the two activities are out of phase, such that, the olivary activity occurs with the inflation, and the mass afferent activity with the deflation, phases of the respiratory pump, indicating the strong likelihood that the olivary activity is due to muscle spindles in the internal intercostal muscles. This conclusion is further supported by the response to switching off the respiratory pump at the end of its inflation phase. This is illustrated in panel B to show the whole sequence of events in a time compressed recording obtained from section of data immediately following that shown in panel A. When the pump was stopped, the afferent discharge in the external intercostal nerve showed an initial increase followed by a decline, best seen in the integral (channel 4). This initial rise and decline in afferent discharge was accompanied by a reciprocal decrease and increase of the olivary activity, respectively. The afferent discharge was then rendered tonic and progressively increased several fold over its original activity. The olivary activity however, showed a gradual decline reciprocal to the afferent discharge. With the pump switched on the reverse of activity was resumed, such that whereas the afferent discharge was decrementing the olivary activity was

Fig. 32. Simultaneous recordings of olivary and internal intercostal nerve mass afferent activities from an inspiratory biased preparation during hypocapnic apnoea induced by artificial ventilation (Pump rate = 60/minute; FA CO_2 = 1.5%). Channels 1 and 2 illustrate the olivary and mass afferent discharge. Their respective integrals are shown in Channels 3 and 4, while Channel 5 depicts the airway pressure (cmH_2O). Panel A, control recording; Panel B, shows the whole sequence of events in a time compressed recording from control through pump stop to pump on again. Note that the initial rise and decline in afferent discharge following pump stop, was accompanied by a respective reciprocal decrease and increase of the olivary activity. Note that the latter afterwards showed a gradual decline reciprocal to the several fold increase in the afferent discharge. With the pump switched on the reverse of activity was resumed.

Fig. 32

A

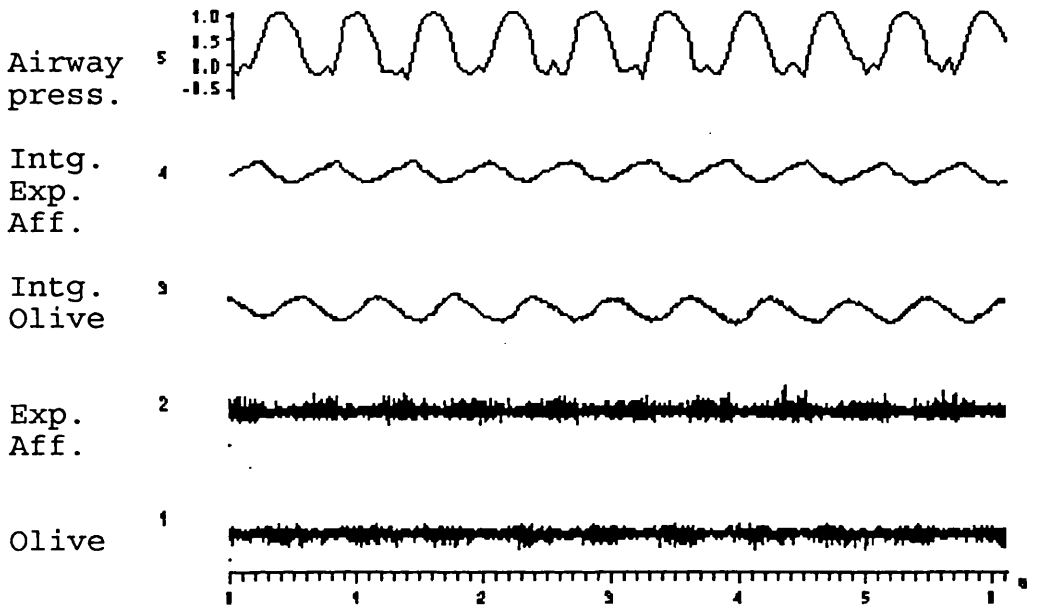
Airway press.
Intg. Exp. Aff.
Intg. Olive
Exp. Aff.
Olive

B

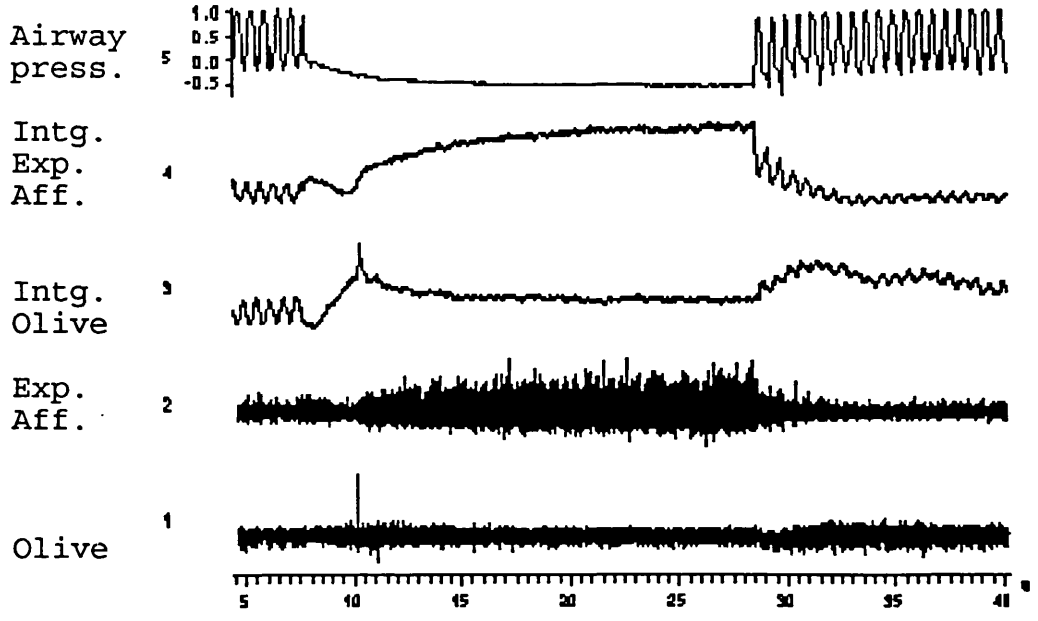
Airway press.
Intg. Exp. Aff.
Intg. Olive
Exp. Aff.
Olive

enhanced in a reciprocal manner. Because a closed ventilatory system was used, a progressive deflation of the chest wall occurred due to the suction created by the sampling pump of the CO_2 meter and this caused a progressive increase in the inspiratory intercostal afferent activity which was accompanied by sustained mass activity in the olive. When the respiratory pump was turned on both the olive and external intercostal nerve afferent resumed their phasic pump-locked discharge.

4. The effect of chemical drive on respirator-phased olivary activity

The carbon dioxide tension, via central and peripheral chemoreceptors, exerts the most important chemical stimulus to breathing (see introduction), hence, we investigated the effect of CO_2 on olivary neurone activity as illustrated in Fig. 33. The lower trace shows a single unit discharging at low frequency (5 - 12/s) and in phase with central inspiration with its rate in the uppermost trace. The upper and lower of the two middle traces illustrate the integrated neurograms of the expiratory and inspiratory motoneurone discharges, respectively. The control recordings shown in panel A were made at an initial CO_2 level of 4.75%. When CO_2 was reduced to 2.5%, the olivary activity gradually reduced and eventually ceased all together, at a time the alternating rhythmic inspiratory and expiratory activities persisted althrough with

Fig. 33.

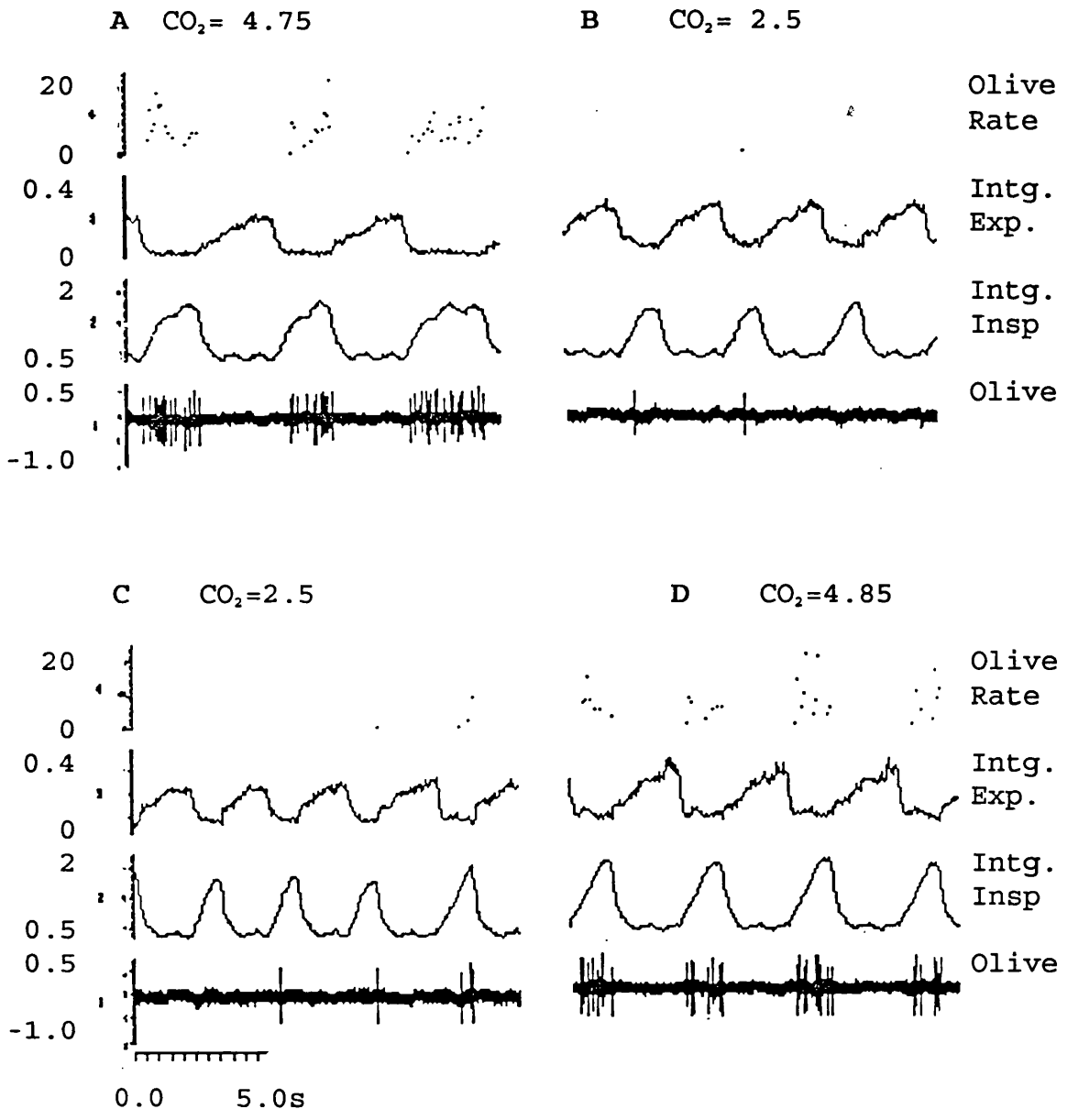

Fig. 33. The effect of chemical drive on respiratory phasic olivary discharge recorded from the same experiment as for Fig. 23. The original olivary recording is displayed in the lower trace and as rate in the uppermost trace. The upper and lower of the two middle traces illustrate the integrated neurograms of the expiratory and inspiratory motoneurone discharges, respectively. The control recordings is shown in panel A at an initial CO_2 level of 4.75%. Panels B and C recorded at a reduced CO_2 level of 2.5%. Panel D recorded at just above the control level of CO_2 (4.85%). Note that the olivary activity was reduced during reduction of chemical drive and increased during its elevation.

diminished activity of the former, and increased activity of the latter (panel B). In this case the CO_2 was not further reduced to abolish central rhythm generation, instead, the CO_2 level was increased in small increments to the same initial control level. At 4.85% the same single unit reappeared and its activity progressively increased occupying the entire inspiratory phase as before together with the pump modulation as evident in panels C and D.

5. Cold block of the spinal cord

5:1. Effects on phasic olivary activity

The purpose of these experiments utilizing cold block of the spinal cord was to examine if the respiratory modulation encountered in the olive originated from supraspinal levels or was evoked by ascending inputs from the spinal cord. Hence, recordings were made from the inferior olive of paralysed artificially ventilated cats, and the spinal cord at C3 was cooled to temperatures ranging from 3-5°C in order reversibly to block conduction in ascending and descending fibres (see section IIIA). However, simultaneous recordings were achieved in only 4 of the 8 experiments either through loss of the units and because much of the time was spent in developing the techniques and obtaining the results on the respiratory aspects as described earlier (section IIIA). In these experiments the respiratory pump rate was reduced and tidal volume increased so as to emphasize the reflex activity.

The results from one experiment are displayed in Fig. 34. Channel 1 shows the olivary activity, which is in phase with central inspiration, as monitored by the external intercostal nerve filament recording (channel 2). Panel A illustrates the control recordings, in which the olivary recording consists of a low amplitude (100uv) single unit discharging at low frequency (7-11/s) superimposed on an envelope of mass activity (channel 1). The olivary discharge, together with that of the inspiratory alpha and gamma motoneurones discharge occurred at the respiratory rate of nearly 24/min. When the thermode was applied to the dorsolateral surface of the spinal cord at C3 (arrow in panel B), there was an immediate increase in activity of the olive and of the inspiratory alpha motoneurones. The latter causes the continuous elevation of the baseline. The increased activity in the olive was superimposed on an equally augmented underlying tonic discharge. Following application of the thermode the rate of phasic discharge in both recordings immediately increased to 34/min which was the set rate of the respiratory pump. The olivary activity is in phase with the deflation reflex with reference to the record obtained from the inspiratory filament (channel 2). The recordings in panel C were made 80s after application of the thermode now showed a marked attenuation of the inspiratory motoneurone activity, which is attributed to partial block of the descending inspiratory bulbospinal axons (see section IIIA). Similarly, the increased tonic olivary activity which developed immediately after the

Fig. 34, The effects of cold blocking of the spinal cord on phasic olivary activity. Channel 1 displays the original olivary recording, channel 2 shows the integrated inspiratory alpha and gamma motoneuronal activity as recorded from an external intercostal nerve filament. Panel A, control recordings, with the olivary record consisted of a single unit discharging at low frequency superimposed on an envelope of mass activity. Panel B, shows the effects of thermode application to the dorsolateral surface of the spinal cord at C3 (arrow), note the immediate increase in activity and rate of both the olive and the inspiratory motoneurones. The recordings in panel C were made 89s after thermode application and show marked attenuation of both activities, with the appearance of diphasic, single olivary unit discharging at low frequency (4-7/s). Panel D, taken four minutes later showing complete cessation of the inspiratory motoneurone activity with the persistence of the olivary activity including that of the single unit described in panel C. Note that the respiratory rate also increased from 24/min in panel A to 34/min in panel B and then fell 30/min in panel C and eventually to 22/min in panel D. Pump rate= 34/min throughout.

Fig. 34.

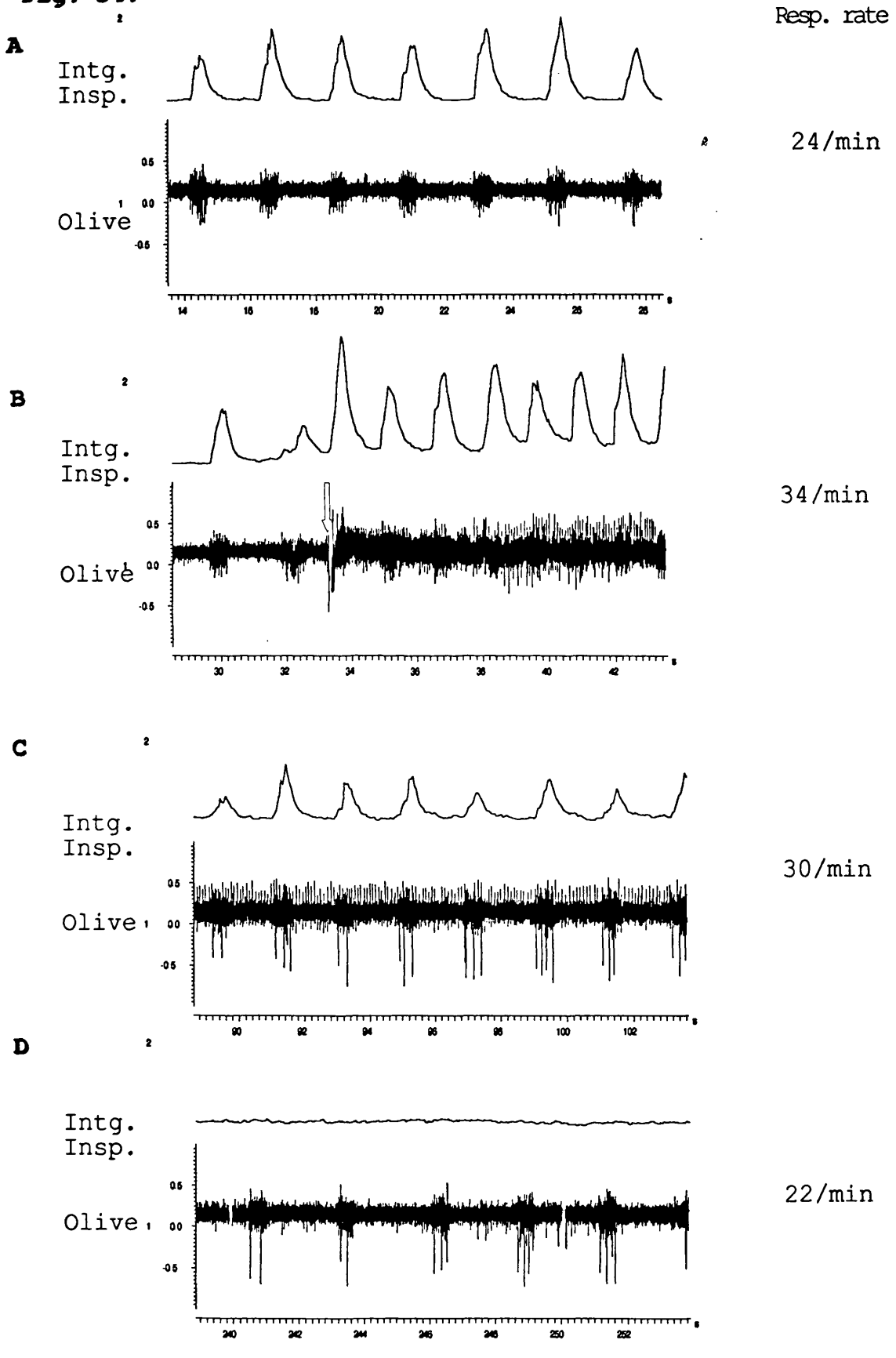
Resp. rate
A
Intg.
Insp.
Olive
24/min
B
Intg.
Insp.
Olive
34/min
C
Intg.
Insp.
Olive
30/min
D
Intg.
Insp.
Olive
22/min

thermode application itself declined, this being accompanied by the occurrence of a diphasic, moderate amplitude (250uv) single unit discharging throughout the inspiratory phase at low frequency (4-7/s). Four minutes later (panel D), whereas the inspiratory motoneurone activity had ceased completely due to total block of the inspiratory bulbospinal axons, the single olivary unit persisted on top of an envelope of mass activity whose period corresponds to a central respiratory rate of 30/min. These changes were also accompanied by disappearance of the tonic component developed after thermode application. The residual phasic activity in the olive, very strongly indicates the existence of converging inspiratory input to the olive from supraspinal sources. Interestingly, the respiratory rate also changed to 22/min, which is slower than the control rate.

5:2. Effects on olivary tonic activity

Another example of cold blocking was obtained from an olivary neurone located in the caudal part of the MAO. This is illustrated in Fig. 35. The lower trace in each panel shows the olivary activity while the upper trace displays the integrated neurograms of the inspiratory motoneurone activity recorded from an external intercostal nerve filament. Before cold blocking of the spinal cord, the olivary recording shows several individual units, one of which is a high amplitude (750uv), diphasic, 2.5ms duration spike discharging repetitively at 14Hz and shown at fast

Fig. 35. Effects of cold blocking of the spinal cord on tonic olivary activity as recorded from an olivary neurone located in the caudal part of the MAO. The bottom trace shows the olivary activity while the upper traces display the integrated neurograms of the inspiratory motoneurone activity recorded from an external intercostal nerve filament. A is the control, B, C and D during cold blocking.

Fig. 35.

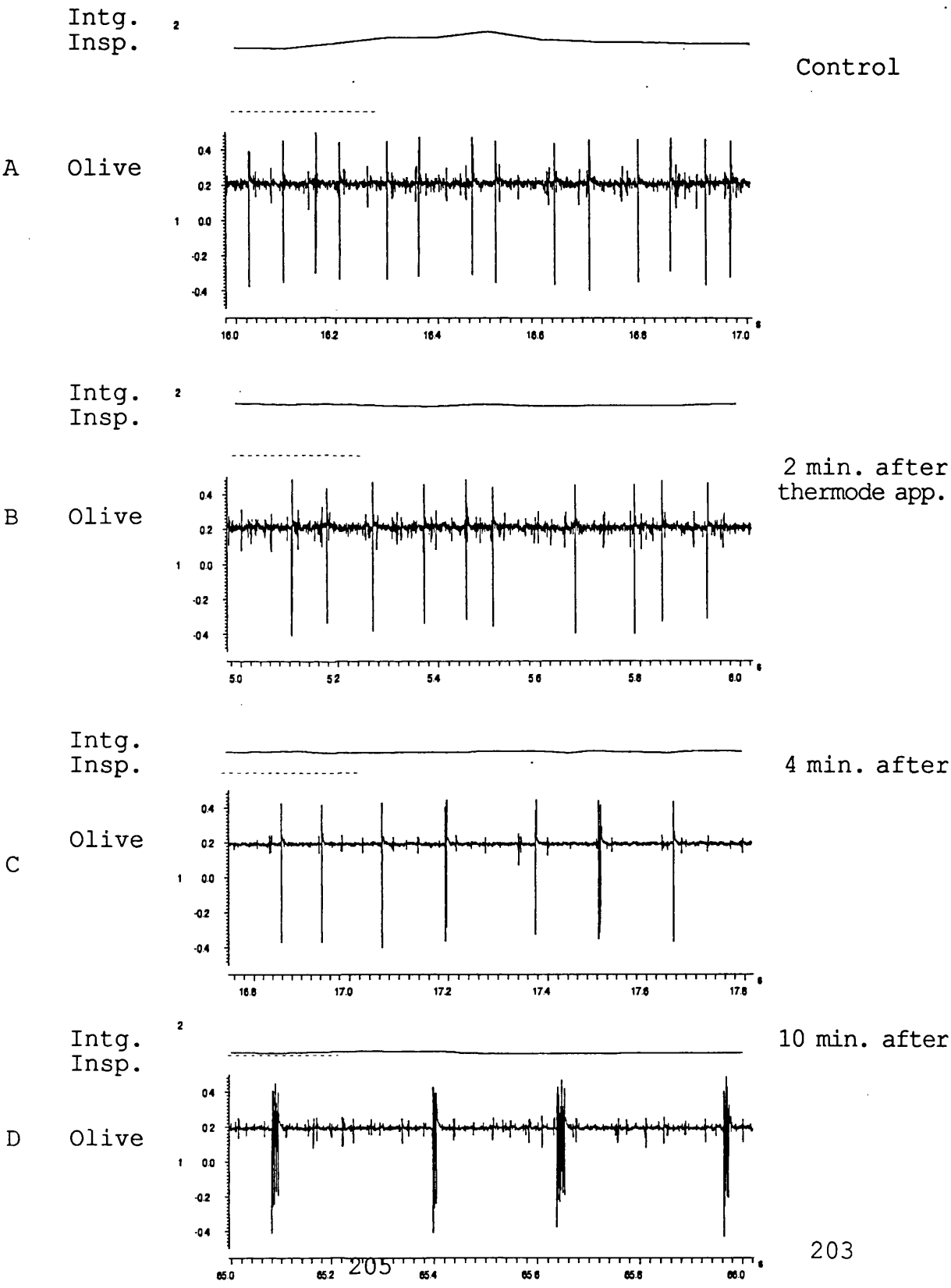
Intg.
Insp.
Control
A
Olive
Intg.
Insp.
2 min. after
thermode app.
B
Olive
Intg.
Insp.
4 min. after
Olive
C
Intg.
Insp.
10 min. after
D
Olive

sweep in the upper trace of Fig. 36. As, seen in Fig. 35 (panel A) this unit showed no relation to the respiratory cycle as monitored by the inspiratory record in the upper trace (note the zero level of the integral). When the thermode was applied to the dorsolateral surface of the spinal cord, the inspiratory motoneurone activity gradually declined after 2min (panel C) and became obvious after 4min (panel C) and virtually abolished after 10min (panel D, note the zero level). At which time the olivary unit discharge slowed (9Hz)and became slightly less regular in panel B; further slowing (7Hz) became obvious In panel C with occurrence of burst discharges. In panel D the unit discharged at lower overall frequency (4Hz), each discharge, now consisted of a burst of 2 - 7 brief duration impulses discharging at high frequency (400-500/sec) as shown on a fast time base in the lower trace of Fig. 36. This bursting pattern of discharge is similar to that of the units discharging during expiration or inspiration (Figs. 24 and 25), although the recording sites are different. As for that unit, it was also established that the number of wavelets in each discharge correlates with the interval between each burst discharge, such that the greater the number of wavelets in one discharge, the longer is the following interval, as illustrated in Fig. 37. This shows the relationship between the number of wavelets in each discharge and the duration of the subsequent interval obtained from a total of 105 complex spikes. It is apparent from this figure that the symbols

Fig. 36.

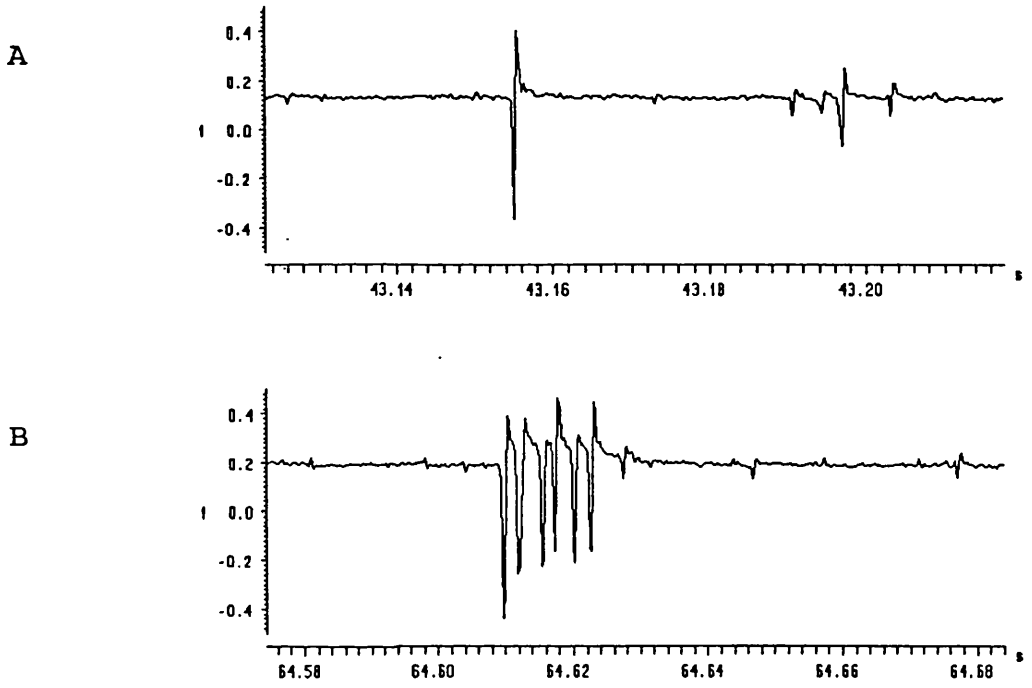

Fig. 36. Spike shape of the olivary unitary discharges shown in Fig. 35 displayed on a fast time base. The upper trace before cold block while the lower is obtained 3min after. Notice the development of the single spike into complex spike. Vertical calibration in mv.

Fig. 37.

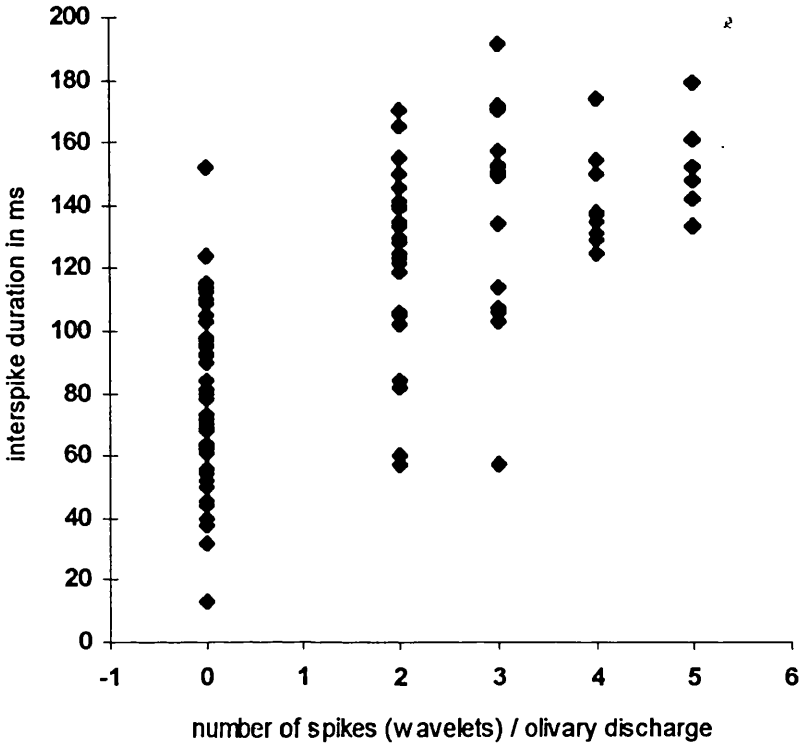

Fig. 37, shows the relationship between the number of wavelets in each olivary discharge and the duration of the subsequent interval obtained from a total of 105 consecutive discharges, recorded from the caudal part of the MAO before and after cold block of the spinal cord. Note that the symbols fall into two main clusters; the first (before cold block) lack wavelets and corresponds to spikes which plotted at zero, their corresponding interspike durations (30 - 120ms). The second cluster (after cold block) consisting of 2 - 5 wavelets/ discharge, have corresponding interspike durations ranging from 120-180ms.

fall into two main clusters; the first cluster represents olivary discharges before cold blocking of the spinal cord. They lack wavelets and hence are plotted at zero with their corresponding durations ranging between 30 - 120ms. The other cluster represents olivary discharges after cold block (arrow). Each burst consists of 2 - 5 wavelets and it is apparent that the majority of the subsequent periods are longer in duration than before cold block, now ranging from 120 - 180ms. This again strongly suggests that the number of spikes / olivary discharge determine the resulting period (see Figs. 26 and 27).

6. Other phasic activities in the olive

Another type of activity encountered within the caudal part of the dorsal accessory olive consisted of brief duration, positive-going monophasic spikes discharging at high frequencies in phase with expiration (Fig. 38). Channel 1 displays the original signal, with its mean rate and instantaneous frequency in channels 3 and 4, respectively. Channel 2 shows the integrated form of the inspiratory motoneurone activity recorded from an external intercostal nerve filament (T5). On close inspection this olivary activity appeared to be a single unit, as judged by its constant form and amplitude. When averaged (n = 150) it was found to be monophasic and of 1ms duration (Fig. 39A) Further support for this conclusion was obtained by autocorrelation of the spike train as events (Fig. 39B),

Fig. 38.

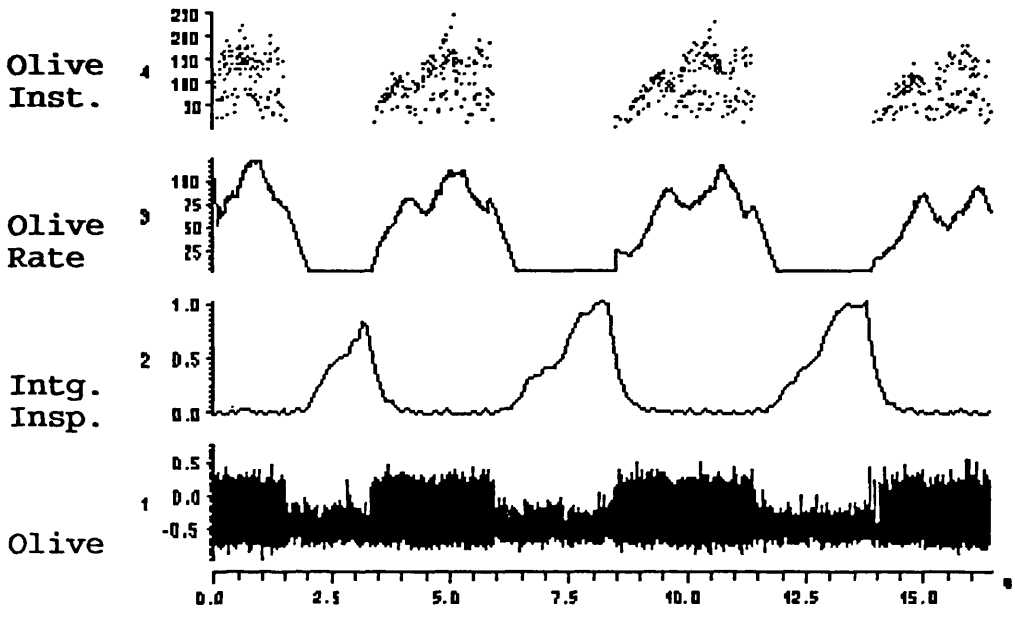

Fig. 38, shows an example of a single unit axonal activity in phase with expiration recorded from within the caudal part of the dorsal accessory olive (Channel 1). Its mean rate and instantaneous frequency are shown in channels 3 and 4, respectively. Channel 2 shows the integrated form of the inspiratory motoneurone activity. Note the pump modulation of this activity at a rate of 59/sec (channels 3 and 4).

Fig. 39, shows further analysis of the data displayed in Fig. 38. A, spike avarage; B, autocorrelation function note the shortest interval is 4ms corresponding to a peak instantaneous frequency of 250/s, also note that the side bands (also present in the averaged spike trace) correspond to a 120/s component C, on a fast time base shows that the same recording site contains low amplitude complex spikes discharging at low frequency (4-10/s) during the expiratory phase.

Fig. 39.

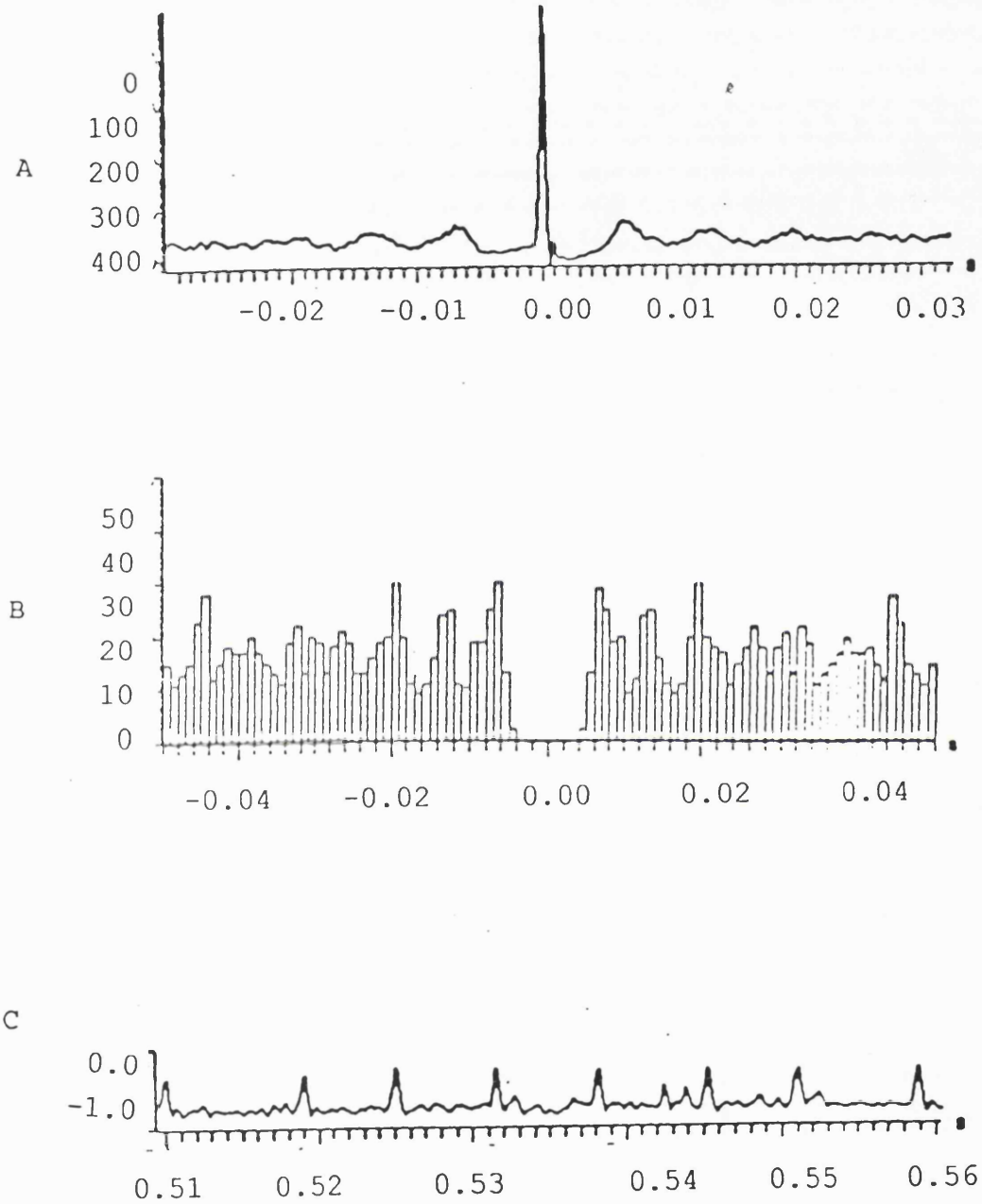
A
0
100
200
300
400
-0.02
-0.01
0.00
0.01
0.02
0.03
B
50
40
30
20
10
0
-0.04
-0.02
0.00
0.02
0.04
C
0.0
-1.0
0.51
0.52
0.53
0.54
0.55
0.56

when the shortest interval found was 4ms corresponding to a peak instantaneous frequency of 250/s with a strong 120/s component as shown by the second and third side bands, also present in the averaged spike trace. The peak firing rate of this unit in some half cycles was as high as 250/s to give the appearance of mass activity in phase with expiration. The characteristics of this unit classifies it as axonal or close to the axon hillock, with a discharge pattern resembling that of the expiratory bulbospinal axons originating in the ventral respiratory group (Merrill, 1970, 1974; Bainton and Kirkwood, 1979). Of particular interest, this activity was found to be modulated by the respiratory pump at a rate of 59/sec as shown in channels 3 and 4 as mean rate and instantaneous frequency, respectively. Airway pressure was not directly recorded in this experiment but the phasing of the respiratory pump can be inferred from the peak of the chest wall inflation reflex of the expiratory motoneurones during the expiratory half of the cycle. Thus by analogy with the expiratory motoneurones, this olivary activity contains both central (expiratory) and proprioceptive components. Also, the same recording site showed low amplitude complex spikes about 25uv in amplitude, discharging sporadically at low frequencies (4-10/s), during the expiratory phase (Fig. 39C). Each burst is composed of 3-4 or more brief duration small wavelets discharging at high frequency rates ranging from 400 - 500/s, similar to these high frequency burst discharges illustrated in Figs. 24 and 25, but of much

lower amplitude indicating the electrode position to be within or close to the olivary lamellae.

7. Location of respiratory related activities in the olive

Fig. 40 shows the spatial distribution of all the different respiratory related activities plotted in relation to the spatial outline of the DAO as determined from the histological materials of this study (see above). The total number of loci showing these activities is 203, of which 66 are high and 24 low frequency inspiratory; 27 high and 33 low frequency expiratory; and 26 proprioceptive. Additionally, 27 loci showed mixed activities with clear phasing (not plotted). Most of these points have disappeared in the figure due to the heavy overlapping and limitation of the analysing technique used in showing all of them. Furthermore, these points particularly with regard to the caudal part of the DAO, represent occasionally more than 5 positions, with the same or different activities, sharing the same mediolateral and rostrocaudal coordinates but having different depths, or with the same three coordinates but from different experiments. Hence, to allow for more detail and to provide a better understanding of the locations of these respiratory related activities in the DAO, each category is represented separately. Fig. 41 depicts the locations of the inspiratory (upper panel) and expiratory (lower panel) activities, Figs. 42 and 43 depict their high and low frequency activity locations in the

upper and lower panels, respectively. Fig. 44 shows the locations of the chest wall proprioceptive component. It is apparent from these figures that the loci with high frequency activities outnumber those discharging at low frequency, in particular those discharging during inspiration. All the points which represent the low frequency inspiratory and expiratory activities were found to be located within the DAO. Caudally some of the points representing the high frequency inspiratory or expiratory activities were found to occur just outside its territory, probably corresponding to the olivary hilae. Such a location could correspond with the spinal input to the olive described by Scheibel and Scheibel (1955) encountered at the caudal pole of the inferior olive. The overall distribution of these loci was found to form a central longitudinal narrow band extending almost from the rostral pole of the DAO to its caudal pole, with the greatest concentration of points in the caudal part (lower panel of Fig. 40).

Figs. 40-44. Diagrammatic display of the location of respiratory related activities in the DAO as obtained from 176 recording sites. The DAO is unfolded in the horizontal plane, produced from rostrocaudal reconstruction of horizontal transverse sections equally spaced by 0.250mm intervals. The location of symbols is determined by their rostrocaudl position from the obex, laterality from the midline and their depth from the dorsal surface of the medulla which ranged between 2.860 and 3.940mm.

Fig. 40, displays the locations of all the respiratory related activities in the DAO (upper panel), the lower panel is reproduced from the upper one with the dotted line representing the spino-olivary projections from the thoracic segments as studied anatomically by Matsushita et al. (1992).

Fig. 41. Shows the locations of inspiratory (upper) and expiratory (lower) activities in the DAO.

Fig. 42. Shows the locations of inspiratory high frequency (upper) and low frequency (lower) activities in the DAO.

Fig. 43. Shows the location of expiratory high frequency (upper) and low frequency (lower) activities in the DAO.

Fig. 44. Shows the location of proprioceptive activity in the DAO.

Fig. 40.

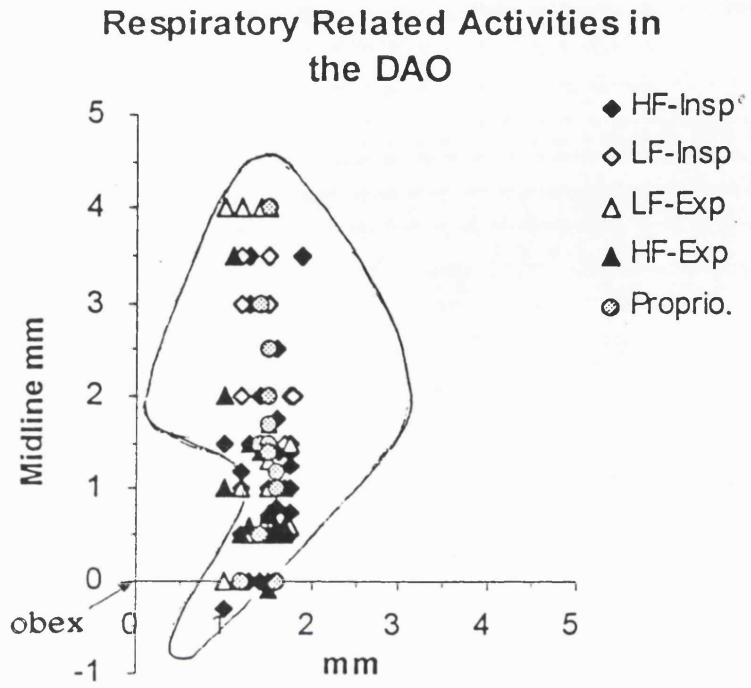
Respiratory Related Activities in the DAO
HF-Insp
LF-Insp
LF-Exp
HF-Exp
Proprio.
Midline mm
5
4
3
2
1
0
-1
obex
0
1
2
3
4
5
mm

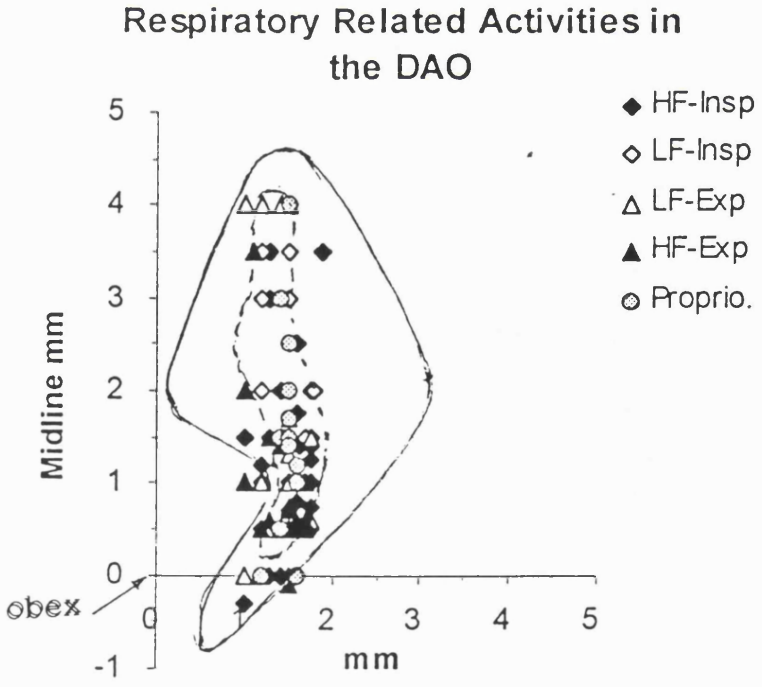
Respiratory Related Activities in the DAO
HF-Insp
LF-Insp
LF-Exp
HF-Exp
Proprio.
Midline mm
5
4
3
2
1
0
-1
obex
0
1
2
3
4
5
mm

Fig. 41.

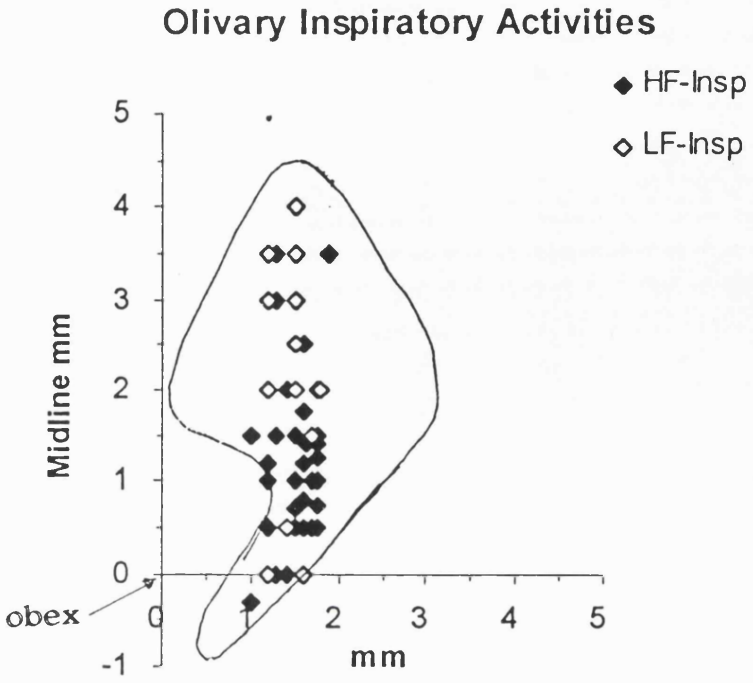
Olivary Inspiratory Activities
HF-Insp
LF-Insp
Midline mm
5
4
3
2
1
0
-1
obex
0
1
2
3
4
5
mm

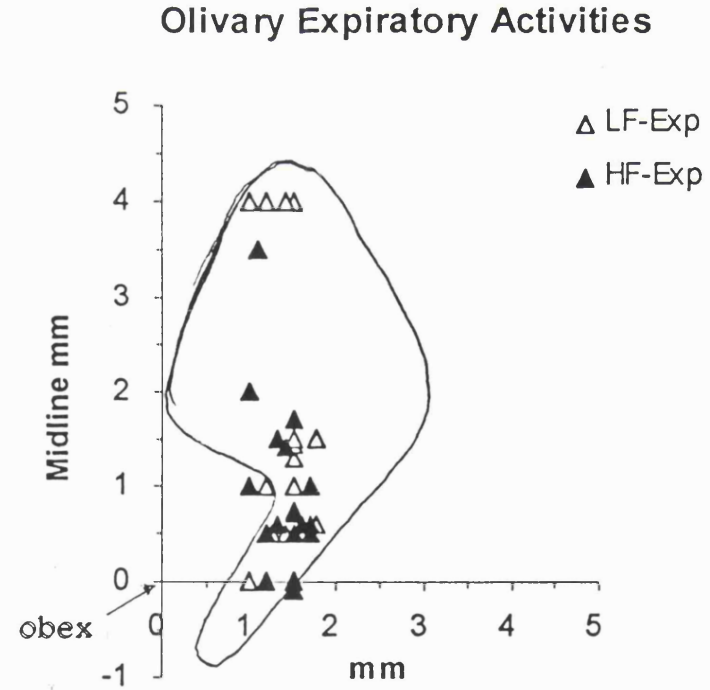
Olivary Expiratory Activities
LF-Exp
HF-Exp
Midline mm
5
4
3
2
1
0
-1
obex
0
1
2
3
4
5
mm

Fig. 42.

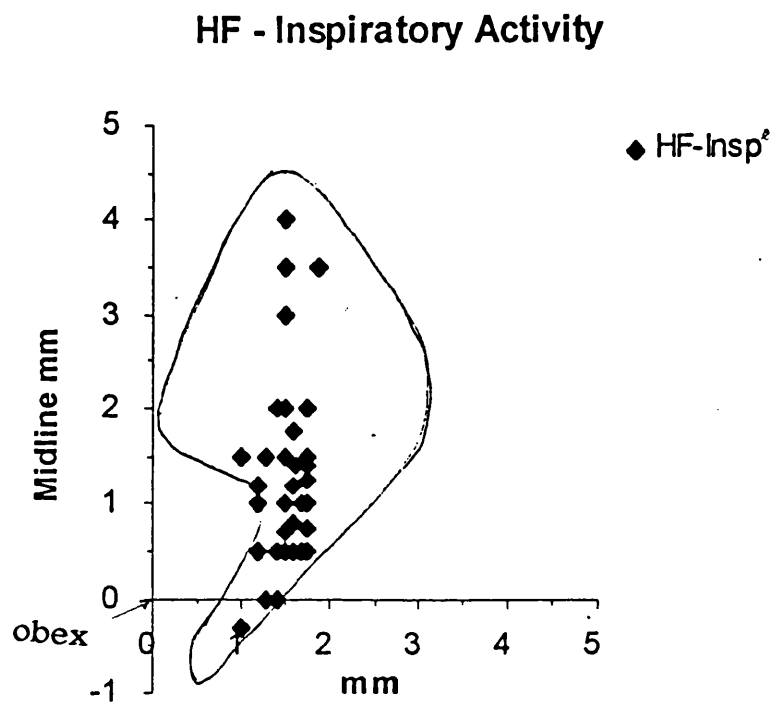
HF - Inspiratory Activity
HF-Insp
Midline mm
obex
mm
5
4
3
2
1
0
-1
0
1
2
3
4
5

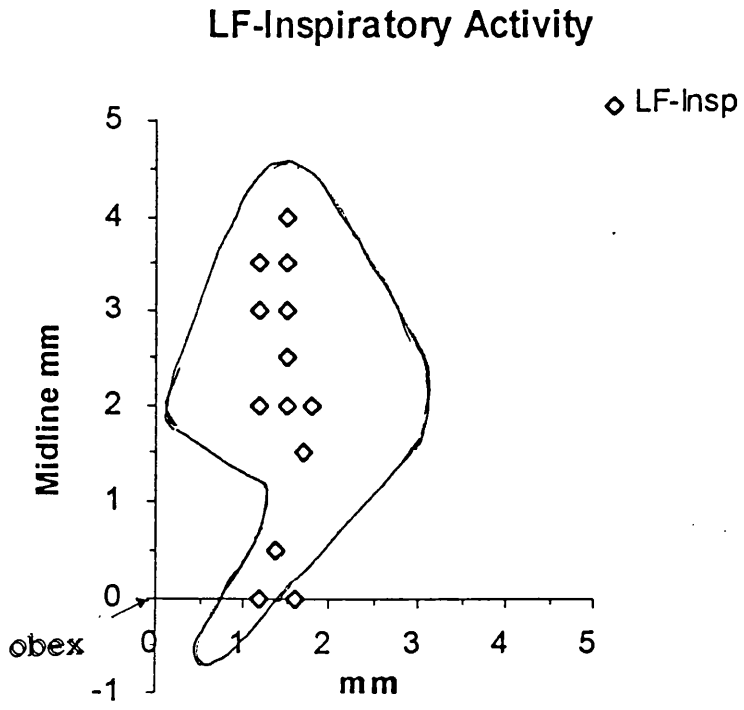
LF-Inspiratory Activity
LF-Insp
Midline mm
obex
mm
5
4
3
2
1
0
-1
0
1
2
3
4
5

Fig. 43.

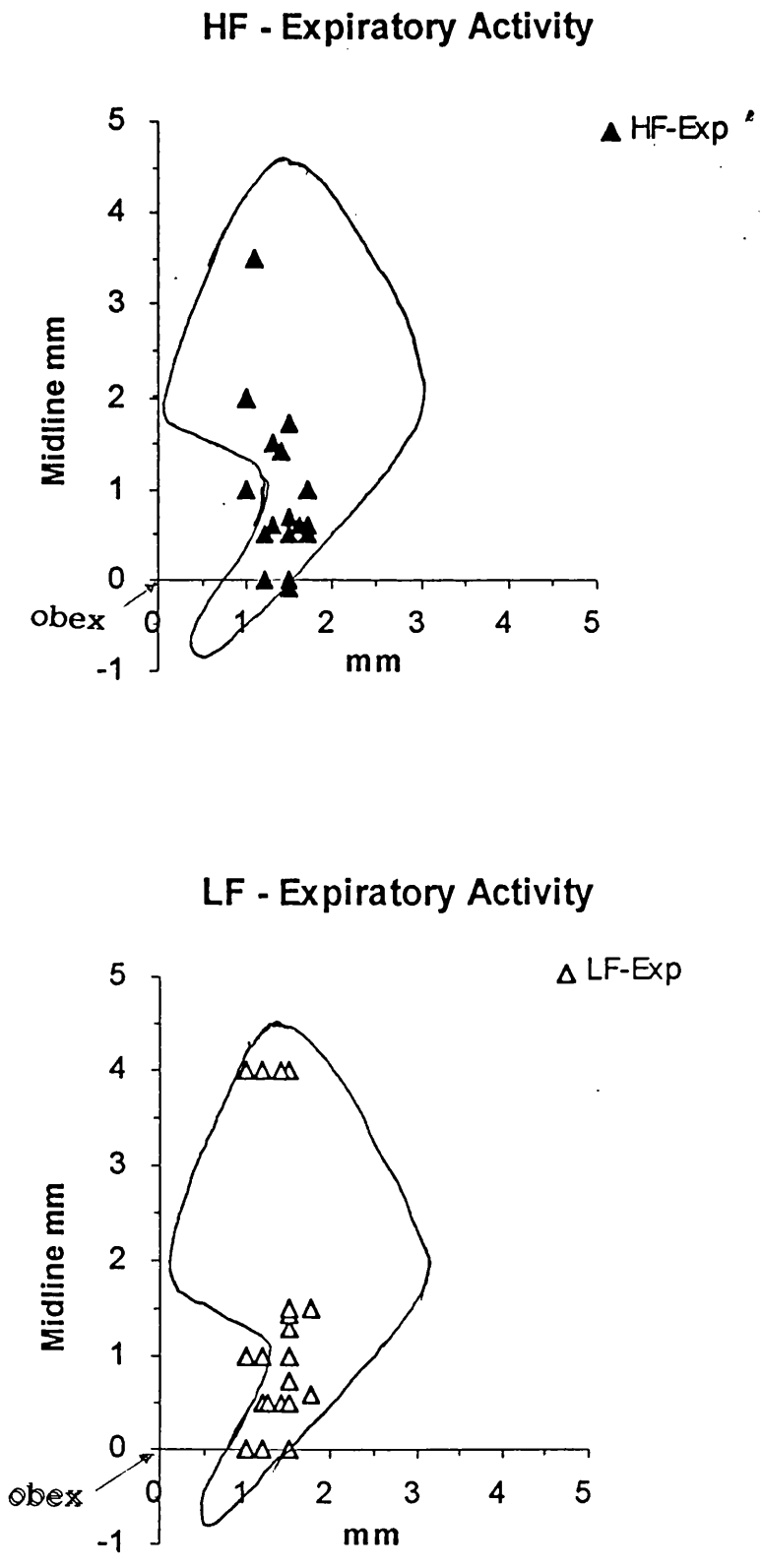
HF - Expiratory Activity
HF-Exp
Midline mm
mm
obex
LF - Expiratory Activity
LF-Exp
Midline mm
mm
obex

Fig. 44.

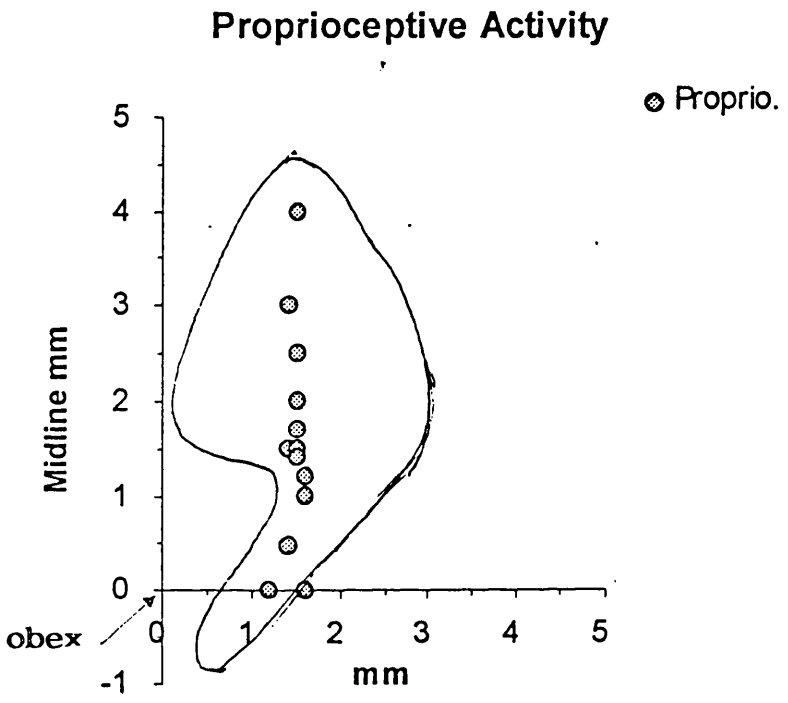
Proprioceptive Activity
Proprio.
Midline mm
5
4
3
2
1
0
-1
obex
0
1
2
3
4
5
mm

8. Discussion of olivary results

8:1. Respiratory phased low frequency activities

Previously the cerebellum has been shown to receive respiratory phased activities transmitted through mossy and climbing fibre systems (Baker, Seers and Sears, 1993; Baker, 1994, Tanaka and Hirai, 1994). The current study confirmed such findings at least for CFs, as inferred from the respiratory modulation of some olivary neurones. These neurones were classified as typical olivary neurones because of their low frequency firing rate (2-15Hz) and their high amplitude long duration spikes which were usually complex in form (Armstrong et al. 1968, Crill 1970). In decerebrate preparations, it was shown that during fictive breathing some Purkinje cells in the thoracic b microzone discharged spontaneous, low frequency complex spikes in phase with expiration and were inhibited during inspiration. One of these cells showed a peak discharge in the early expiratory phase (Baker, 1994). The origin of climbing fibres to the thoracic b microzone is from the caudal part of the DAO Groenewegan and Voogd, 1977) and, in accordance with this, the present study describes the occurrence of spontaneous, single unit olivary activity discharging at low frequency in phase with either expiration (Fig. 25) or inspiration (Figs. 23, 24 and 33). Such discharges were obtained throughout a narrow longitudinally organized centrally located band in the DAO (Fig. 40) and consisted of either single spike activity

(Figs. 23 and 33) or repetitive burst firing of the single units (Figs. 24 and 25).

Unlike inspiratory and expiratory motoneurones discharges which augment in frequency and number towards the end of each half cycle, the corresponding respiratory-phased low frequency discharges of olivary neurones (Figs. 23 and 25) were found to decrement in frequency thus forming a mirror image. This is obvious from comparison of the total spike counts in the first and second halves of 20 inspiratory (Table 1) and expiratory (Table 2) half cycles, where their mean ratio was found to be almost 2/1. Further evidence of this was the increase in interspike intervals towards the end of each expiratory half cycle (Fig. 27). Again, this pattern is in contrast to the augmenting discharge of expiratory motoneurones which is augmenting towards the end of the cycle (phase II expiration, see Richter, 1986). For simplicity schematic representation of the CRDP is shown superimposed on the olivary and expiratory integrals (Fig. 45). The lower trace in each panel displays the original in-phase olivary and expiratory motoneurone discharges, with their corresponding integrals in the upper traces. The olivary neuronal activity can be seen to form a mirror image of the expiratory motoneurone activity as judged by their integrals. This could be of importance supporting the idea that the command for breathing movements is fed into the olive as a mirror image (cf. Bell, 1984; Gellman et al., 1985). As in the case of its effects on the

Fig. 45.

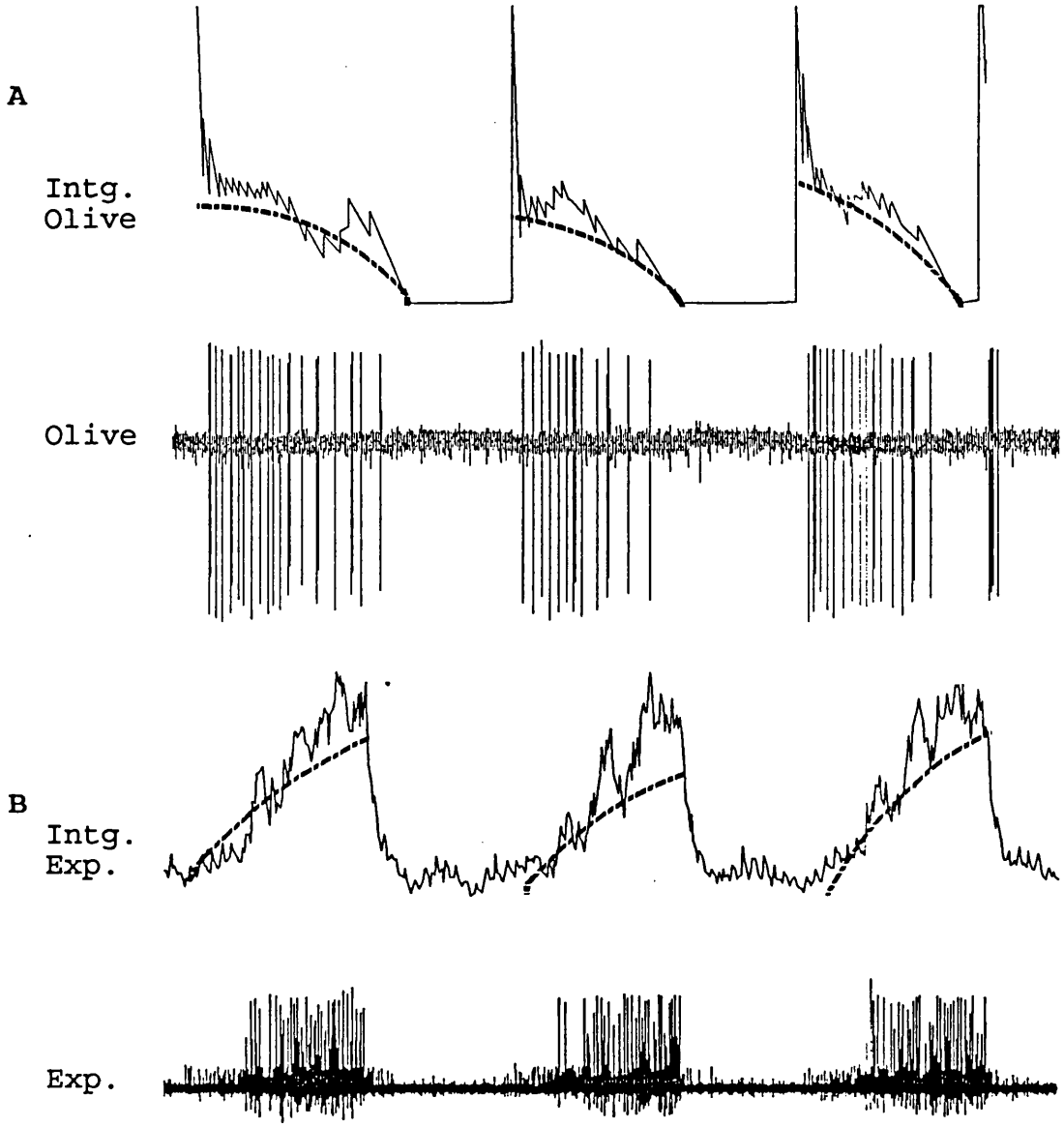

Fig. 45. Mirror image relationship of central respiratory rhythm in the olive (panel A) and expiratory motoneurone (panel B). Lower trace in each panel displays the in-phase olivary and expiratory original recordings, their corresponding integrals in the upper traces. The thick lines represents the CRDP like wave. See text for more details.

intercostal respiratory motoneurones, CO_2 was found to affect these low frequency respiratory discharging olivary neurones. This is evident in Fig. 33, so that when CO_2 was reduced, the olivary inspiratory phased activity gradually diminished and eventually ceased all together, to recover again after elevating CO_2 to its control level. These changes occurred in the olive before any major effect was observed in the discharge of the inspiratory motoneurones. Similarly expiratory-phased mass activity in the DAO became tonic during hypocapnia, reflecting the behaviour of expiratory motoneurones, but unfortunately this was not studied at the single unit level. This implies that the olivary neurones continuously signal to the cerebellum information closely related to the intensity of the current level of the chemical drive to breathe, and mechanical conditions obtaining within the rib cage could clearly contribute to homeostasis. According to this information, as in the case of limb movements, it can be proposed that any unexpected perturbations of the 'commanded' movements would be signalled to the cerebellum.

8:2. Respiratory phased high frequency activities

Respiratory phased high frequency activities can occur in phase with either inspiration (Fig. 21) or expiration (Fig. 22). They are within the representation of the thoracic segments throughout the DAO as defined by Matsushita et al. (1994), and some locations which fall outside its borders

(Figs. 40, 41-lower panel and 43-upper panel), would correspond to the cervical and lumbar segments. However, there is preponderance of inspiratory loci over expiratory loci, with a particular concentration in the caudal part of the DAO. The firing rate of these neurones (25 - 50/s) does not classify them as typical olivary neurones that give rise to climbing fibres which characteristically discharge at low frequencies with long duration spikes. Nor do these frequencies correspond to those of the inspiratory and expiratory bulbospinal axons which decussate rostral and caudal to the obex (Merrill, 1970; Bianchi, 1971; Bainton and Kirkwood, 1979; Kirkwood, 1995). This lead one to conclude the existence of interneurons either within the olivary lamellae themselves or immediately adjacent e.g. in the hilum (cf. Scheibel and Scheibel, 1955), or interestingly the only interneurons described thus for are the GABAergic interneurons with abundant GABAergic terminals within the inferior olive, as reported by Nelson and Mugnani (1989). It has been suggested that these interneurons may mediate the local inhibitory effects of rubrospinal inputs on olivary neurones (Weiss, Houk and Gibson, 1990). Hence such interneurones could convey the central respiratory drive to the olive and in this case the central inspiratory-phased discharge of the interneurones would provide reciprocal inhibition of the neurones to which they project, thus forming a 'mirror image of the command for movement (cf.).

8:3. Cold block of the spinal cord

8:3:1. Effects on 'central' respiratory olivary activity

The cold blocking experiments on the spinal cord, carried out in this study were made at the C3 segment i.e., above the level of the phrenic nucleus, to ensure the best likelihood of blocking conduction in both respiratory bulbospinal axons and ascending systems carrying respiratory or non-modulated afferent inputs to the olive. Fig. 34 showed clearly the persistence of mass inspiratory activity in the DAO, at which time the central inspiratory activity of the external intercostal motoneurones (panel D) was abolished. This strongly indicates that the DAO receives a phasic inspiratory input of supraspinal origin notwithstanding the possibility as discussed below, that afferents from the spinal cord convey a similar input. Although the olivary recording showed some attenuation of the mass inspiratory activity during cold block, there were also some high amplitude units discharging at low frequency throughout the cycle and in two experiments such units actually appeared during the cold block. Evidently cold blocking has led to the withdrawal of a spinal component, one of several inputs converging on the olive. Oscarsson (1973) postulated that such convergence in the olive might permit command signals from higher motor centres to be correlated with the activity these signals evoke at lower motor levels which are also affected by activity from the periphery. Thus the olive might be used as a 'comparator' in the cerebellar integration of higher motor and reflex

activity. Andersson and Eriksson (1981) investigated the possibility of such convergence but at the cerebellar level. They showed a remarkable matched convergence of evoked CF responses in the cerebellar B zone, elicited from stimulation both of peripheral nerves from different parts of the body including thoracic segments and their areas of representation in the cerebral cortex. The cortical projection to the B zone was found to correspond closely to the spinal projection via the VF-SOCP with respect to somatotopy and bilaterality, as well as in the amplitude and latency differences between the ipsilateral and contralateral projections.

In the case of automatic respiratory movements, it appears therefore that the command for these movements is fed from supraspinal sources (see later) to the longitudinal band within the DAO (Fig. 40) corresponding to the representation of thoracic inputs via the VF-SOCP (Matsushita et al., 1994). This convergence would allow the state of interneuronal and motor activity at the thoracic level to be correlated with supraspinal inputs, either inhibitory or excitatory in the DAO, before being forwarded to the cerebellar B zone for further integration.

8:3:2. Effects on respiratory rate

It is apparent from panel B of Fig. 34 that following application of the cold thermode to the dorsolateral surface of the spinal cord, there is an immediate transient

increase in respiratory rate from 24 - 34/min as seen both in the DAO and in the inspiratory motoneurone discharges. At the other extreme, when the cold block was established the central respiratory rate slowed from 24 to 22/min as observed in the olive mass activity (panel D of Fig. 34). At which time the inspiratory motoneurone activity was rendered silent. Furthermore a similar slowing in the respiratory rate was observed in the first appearance of the central activation of the intercostal motoneurones as activity recovered following removal of the thermode. The simplest interpretation of these results is that the afferent input from the spinal cord facilitates activity of the central respiratory rhythm generator (CRRG) and the withdrawal of this input depresses it, both in terms of respiratory rate and the net output. Hence this again strongly indicates that the inferior olive receive phasic inspiratory inputs reflecting the current status of the supraspinal rhythm generator which activity is available also for integration with inputs over spino-olivary pathways. The other possibility that pulmonary stretch afferents might cause these effects on respiratory rate is considered unlikely because the artificial ventilation was held constant throughout the procedure.

8:4. Olivary burst activity

In previous studies high frequency burst discharges of olivary neurones were obtained in response to electrical

stimulation of peripheral nerves (Armstrong et al. 1968, Crill 1970). The burst discharge of wavelets after the initial spike is generally assumed to be due to a strong depolarization of the olivary neurone produced by the highly synchronous afferent volley in the nerves. However, in the current study such bursting also occurred as a sustained discharge for an entire half cycle (inspiratory or expiratory) during rhythm generation, in response to the natural physiological stimuli relating to central respiratory rhythm generation and also during hypocapnic apnoea, to natural patterns of proprioceptive activity (chest wall inflation and deflation reflexes). These bursting activities were not dependent on high levels of the chemical drive, per se, as they were obtained at eupnoeic levels of CO_2 in paralysed and partially cerebellectomized preparations (e.g., Fig. 24) and also in non-paralysed intact preparations (e.g., Fig. 25).

Similar patterns of low frequency bursting discharges were also obtained from an olivary unit located in the MAO, but in this case when presumably the net afferent input to the olive was reduced due to cold block of the spinal cord. Initially the olivary neurone was discharging single spikes tonically at near 15 Hz (Fig. 35, panel A). As the spinal input was progressively reduced during cold blocking, this resulted first in a slowing of the discharge rate and when this fell to 8 spikes/s the neurone commenced burst firing (Fig. 35, panel C) which slowed still further to be

maintained at an overall 4-6 spikes per second, each spike being associated with burst firing of up to 6-7 wavelets. during total cold block (Fig. 35, panel D). Analysis of these results showed that the number of spikes (wavelets) in each burst correlates with the duration of the following interval before the occurrence of the next principal spike and its burst discharge, so that, there is a strong tendency for an increase in interspike duration when there is an increase in the number of wavelets within the preceding discharge (Figs. 26 and 37).

This pattern of discharge is best understood by reference to the work of Llinas & Yarom (1981a, b) on the inferior olive in vitro slices of cat medulla oblongata. They showed that the after-depolarization, whose time course generally corresponds to the duration of the burst discharge, is followed by an after-hyperpolarization whose amplitude is directly related to the amplitude of the preceding afterdepolarization. This afterdepolarization coincides with the period which has been attributed to 'low threshold' Ca^{++} spikes, the inactivation of which at resting potential, has been removed by prior hyperpolarization. Hence, it is assumed that the number of wavelets/olivary discharge would determine net Ca^{++} entry thus activating the Ca^{++} dependent K^{+} conductance which in turn would determine the resulting after-hyperpolarization and with this the period of the low frequency olivary discharge (Llinas et al, 1973; Benardo and Foster, 1986; also see below).

Neurones displaying similar characteristics to olivary neurones have been identified in the nucleus basalis (NB) (Khatib, Fort, Serafin, Jones and Muhlethair, i995), the nucleus reticularis thalami (NRT) of guinea-pig and in the perigeniculate nucleus (PGN) of cat (McCormic and Wang, 1991). In in vitro studies showed that the cholinergic neurones of the nucleus basalis, have the capacity to discharge spontaneously in rhythmic bursts (1.7-5Hz) for a few cycles, then switching to a single spike firing mode at nearly 15Hz which it could maintain indefinitely (Khatib et al., 1995). However, when the membrane was held at a hyperpolarized level, in the presence of NMDA (glutamate agonist) this bursting activity (0.5-6Hz) was sustained for as long as the application of NMDA was continued. This rhythmic burst activity appeared to be determined by an underlying low threshold Ca^{++} spike in these neurones, because in their voltage dependence and frequency they resembled the low threshold spike bursts elicited in control conditions by depolarizing current pulses. Thus, the pattern of discharge of the NB neurones before, and after, application of NMDA, appears to be similar to the pattern of discharge of the olivary neurones before and after cold block as described in this study (Fig. 35). Although these two types of neurones are different and have different locations in the CNS, their underlying mechanisms of discharge appear to be similar (see below).

Under the effect of 5-hydroxytryptamine (serotonin, 5-HT)

and noradrenaline (NA), the PGN and NRT neurones exhibited two discharge patterns, either rhythmic burst firing at 4-7Hz or at nearly 100Hz continuous single-spike activity. It was suggested that the switch between the two patterns is mediated by a depolarization induced by the increased release of 5-HT and NA, which block a specific K^+ channel which is normally open at resting potential (Khatib et al., 1995). Conversely a decrease in the release of these neurotransmitters, or their withdrawal in the in vitro situation promotes the occurrence of rhythmic burst firing. As for the NRT neurons, in in vitro studies showed that 5HT and NA were found to have an analogous role on transmission in the inferior olive, thus, modulating the excitability of its neurones. Application of 5-HT or dopamine depolarises these cells and also increases their input resistance and thus increases their dendritic excitability (Llinas and Yarom, i986). Recently, through multiple recording of complex spikes from rat cerebellar vermis (lobule VIb and crus IIa), Sugihara, Lang and Llinas (1995) found that microinjection of 5-HT into the olive increases the average firing rate of olivary neurones, while slowing their oscillation frequency and increasing the coherence of their oscillation (synchronization). Noradrenaline subsequently abolished established oscillations and promote single spike firing, possibly by a direct action on Ca^{++} channels. In the presence of harmaline, these agents induced a low frequency oscillation (0.5-2Hz) of membrane potential in previously silent cells (Llinas and Yarom, 1986). The serotonergic

projection to the inferior olive arises from the nucleus paragigantocellularis in the medullary reticular formation (Bishop and Ho, 1986) and the nucleus raphe (Compoint and Buisseret-Delmas, 1988). In in vivo experiments 5HT was reported to induce regular firing of the olivary neurones at nearly 3Hz when the animal is awake but not moving. However, during treadmill walking this firing frequency directly correlates to the speed of locomotion (Jacob and Formal, 1993).

The ability of NB, PGN, NRT and olivary neurones to exhibit these two modes of action potential generation in vitro studies, was revealed to be based on the intrinsic properties of these neurones on the one hand and an underlying ionic mechanism on the other. (Khatib et al., i995; McCormik and Wang, 1991; Llinas & Yarom 1981a,b; Bernardo and Foster, 1985). Such that application of NMDA, and 5HT and NA cause depolarization of the NB and PGN, NRT and olivary neurons, respectively, when their membrane potential was held at a hyperpolarized level.

The functional significance of these two different modes of discharges exhibited by the olivary and other systems of neurones, was assumed to influence motor output by enabling or disabling central rhythm generators. Hence, it was proposed that, the rhythmic oscillation in the basalis neurones would provide a rhythmic modulation to target neurones within the cerebral cortex and thereby potentially

promote slow oscillations within a delta or theta frequency range in cortical activity across sleep-waking cycle (Khatib et al., i995). In the NRT, the single-spike firing was prevalent during high levels of both applied 5-HT and noradrenaline and thought to occur during periods of attentiveness and vigilance. Bursts firing, however, was prevalent at low levels of 5-HT as would occur during periods of inattentiveness, drowsiness and slow wave sleep (Steriade and Llinas 1988). Similarly, it was suggested that during movement the activation of the serotonergic afferents to the inferior olive would result in an enhancement of the average firing rate, rhythmicity and synchronicity of its neurones (Sugihara, Lang and Llinas, 1995). Thus it was proposed that the primary function of these 5-HT olivary neurones would be to facilitate motor output by enabling central rhythm generators (CRGs) which in turn would excite alpha motoneurones (Jacob and Formal, 1993).

The present work showed clearly that olivary neurones can exhibit two distinct patterns of action potential generation in vivo, which depends strongly upon the state of the preparation. Single-spike activity at higher frequencies (15Hz) in the presence of the spinal input and rhythmic burst firing at lower frequencies (4-6Hz) in its absence. From the above it is postulated that, such changes in activity indicate that the inferior olive signals to the cerebellum two different behavioural states, single spikes

during alertness when the spinal input was on, presumably due to an increased level of 5-HT, and bursting discharges during inactivity due to the loss of spinal input or due to a decreased level of 5-HT.

The other possibility of discussing these results is in terms of the dynamic coupling of olivary neurones. It was shown that the roof nuclei project to the inferior olive via two separate pathways (Ruigrok and Voogd 1995), namely, an excitatory disynaptic nucleo-mesodiencephalo-olivary (CN-MDJ-IO) pathway, and a direct inhibitory, GABAergic cerebellar nucleo-olivary (CN-IO) pathway. Stimulation (short burst of 3 pulses) of the superior cerebellar peduncle (SCP) and the mesodiencephalic junction (MDJ) resulted -via these pathways- in short latency evoked action potential (SLAP) at 4-16ms in the rostral half of the MAO and PO. This SLAP was followed by a long latency evoked action potential (LLAP) at 180ms in half of the activated neurones. However, the same paradigm of stimulation after electrolytic lesioning of the CN-IO pathway, resulted in a five-fold increase of triggering a LLAP with a 50% decrease of triggering a SLAP in the same sites of the olive. As the GABAergic pathway provides olivary neurones with an inhibitory feedback circuit (Andersson et. al., 1988) that can decrease their electrical coupling (Llinas and Sasaki, 1989), the excitatory pathway was thought to mediate activation of these uncoupled neurones resulting in the SLAP (Ruigork and

Voogd, 1995). By contrast, lesioning of the CN-IO pathway was thought to increase the level of electrical coupling between olivary neurones, as attested by the initiation of a powerful oscillation in the membrane potential of the neighbouring neurones within aggregates of the olivary neurones which ultimately resulted in an increased probability of triggering a LLAP. Hence, those authors concluded that 'cerebellar output may not merely inhibit olivary neurones, but also, in conjunction with an excitatory nucleo-mesodiencephalo-olivary circuit modulate olivary excitability in rather a complex manner'.

Thus, in the present work it would be expected that, in the absence of the CN-IO pathway (Fig. 24) olivary neurones firing in phase with central inspiration would do so at low frequency and with an interspike period of more than 200ms. Also, the presence of the low amplitude burst discharges in the background could represent synchronized (within the respiratory cycle) neighbouring neurones in the same olivary ensemble. This conclusion is possible because subthreshold oscillations were found to be very frequent in coupled olivary neurones as demonstrated in the in vitro brainstem slice (Benardo and Foster, 1986; Llinas and Yarom, 1986). The long intervals (more than 180ms) encountered after cold block of the spinal cord (Fig. 35), may also, be interpreted by reference to the findings of Ruigork and Voogd (1995). They showed that Pentobarbitone anaesthesia suppresses the spontaneous discharges of the

CN-IO fibres. Since the same type of anaesthetic was used combined with cold block of the spinal cord, the massive loss of the afferent inflow to the olive over spino-olivary pathways and via the SCT inputs to the cerebellar cortex would also be expected to mediate activity of the inhibitory GABAergic CN-IO pathway leading to these long interspike periods.

8:5. Origin of the respiratory related activities in the DAO

8:5:1. Supraspinal origin

Supraspinal respiratory phasic inputs to the olive could come directly from the ventral or dorsal respiratory groups although no such direct anatomical projection appears to have been described. However, the presence of one can be inferred from the high frequency expiratory afferent activity resembling the discharge of bulbospinal neurones encountered within the immediate vicinity of the caudal DAO (Fig. 38). This activity was found in association with a background expiratory phased activity of complex spikes discharging at low frequency, indicating the electrode position to be within or close to the olivary lamellae. Also, this olivary activity was found to contain both central (expiratory) and proprioceptive components which typically simulate the discharge of the expiratory bulbospinal neurons (Merrill, 1970, 1974). Although neither Merrill (1974) nor Shannon (1982) described pump modulation of the expiratory bulbospinal neuronal discharges, some

expiratory bulbospinal neurones in the ventral respiratory group were recently shown to be pump modulated (Kirkwood, submitted for publication). Another possible source of these phasic olivary activities is via the cerebellar nuclei, through the nucleo-olivary pathways; but such inputs would be likely to be inhibitory (Gruart and Delgardo-Garcia, 1992), which would further require them to inhibit olivary neurones in receipt of tonic excitatory inputs to produce the final phasic discharge that has been observed.

8:5:2. Spinal origin

8:5:2:1. Phasic central respiratory activities

Recently Tanaka and Hirai (1994) have demonstrated in paralysed artificially ventilated animals the presence of respiratory related discharges, recorded from some thoracic spinocerebellar tract (SCT) neurones with crossed axons ascending in the ventral funiculus. These activities were in phase with either inspiration or expiration as monitored by the discharge in the phrenic nerve. The authors suggested that the ultimate source of these rhythmic inputs is the medullary respiratory rhythm generator. Interestingly these crossed SCT axons, which correspond to those of lumbar VSCT neurones, were found to originate in neurones lying ventral to Clarke's column in laminae VII and VIII. This is the same area which contains neurons that gives rise to the VF-SOCP, as identified by the retrograde transport of HRP from the olivary nuclei (Armstrong &

Schild 1980). Lamina VII forms the intermediate group of cells of origin of the bVF-SOCP, which is a continuous column of neurones extending from the cervical to lumbosacral segments. Lamina VIII contains the ventromedial group of cells which according to Armstrong & Schild (1980) is entirely confined to lumbosacral segments and is the source of fibres within the aVF-SOCP. It is proposed therefore, that being the site of convergence of the thoracic wall proprioceptive inputs and either inspiratory or expiratory phased components of the central respiratory drive (Tanaka and Hirai, 1994; also, see below), the crossed SCT neurones could also be the spinal site of origin of olivary phasic respiratory activities.

8:5:2:2. proprioceptive activities

The results shown in Figs 30, 31 and 32, strongly indicate that the pump locked activities recorded in the DAO are related to the chest wall inflation and deflation reflexes evoked by the alternating lengthening and shortening of the internal and external intercostal muscles, respectively. This is readily seen in Figs. 30 and 31, which show that when the respiratory pump was switched off both the inflation reflex of the alpha motoneurones and the pump locked activities in the olive disappeared, to be restored when the pump was switched on. Such proprioceptive activities would require a relay in spino-olivary neurones or elsewhere for transmission to the olive over one or more of the 'functional' spino-olivary pathways. As discussed in

the previous section Tanaka and Hirai (1994) described respiratory related rhythmic activity of the thoracic DSCT neurones, activated by the afferent inflow from the thoracic wall proprioceptors as its major source. These neurones project ipsilaterally to the cerebellum. They were divided into 'inflation' and 'deflation' neurones according to the phasing of artificial or spontaneous respiratory movements and hence, excitation of the internal and external intercostal muscle spindles, respectively. Furthermore, they found that SCT neurones projecting contralaterally to the cerebellum (mentioned above), in particular those discharging during expiration, were also excited from the periphery during inflation of the chest wall (induced by the respiratory pump) and suppressed when the passive expansion of the chest coincided with active (central) inspiration. When the pump was stopped, this activity immediately disappeared and returned with the pump on. It was concluded that the source of these pump locked activities is the thoracic wall proprioceptors. Hence, the crossed SCT neurones are the most likely candidate for the origin of the pump-locked olivary activity, as their crossed axons ascend in the ventral funiculus, which itself is known to contain axons with termination sites in the DAO (Armstrong & Schild, 1980; Matsushita et al., 1992).

8:6. Location of the respiratory related activities in the DAO

Figs. (40 - 44) show the spatial distribution of all the

different respiratory related activities plotted in relation to the spatial outline of the DAO. The overall distribution of these loci was found to form a central longitudinal narrow band extending almost from the rostral to the caudal end of the DAO, with the concentration of points in its caudal part(Fig. 40, lower panel; also see Sears, Magzoub and Seers, 1993). These loci were found to correspond closely with the central longitudinal narrow band in the DAO representing in a mediolateral orientation the rostro-caudal segmental projection of the spino-olivary neurones located in the thoracic spinal cord as recently identified by anatomical methods (Matsushita et al. 1992). This is shown by the dotted line in the lower panel of Fig. 40. This representation -as identified here- however, is different from that shown by Gellman et al., (1983) in their cutaneous map of the entire body in the DAO, with the trunk occupying its rostral pole. This is perhaps due to their use of cutaneous stimuli or 'deep pressure' occupying large receptive fields in the truncal area.

The coextensive distribution of central and proprioceptive signals suggests that the thoracic microzones of the DAO display a spatial mapping of the current distribution of the central command for respiratory movements across the chest wall for comparison with the current status of interneuronal circuits locally subserving the central respiratory drive and also the chest wall proprioceptive reflexes.

IV: GENERAL DISCUSSION

The inferior olive, through various anatomical features and the physiological properties of its neurones, is distinguished from other precerebellar relay nuclei. The special morphology of the olivary neurones, with their complex dendritic tree that carries many long and branching spiny appendages (Scheibel and Scheibel, 1955; King et al, 1976), already indicates a highly specialized input-output relationship (Sotelo et al., 1974; Ruigrok et al., 1990a). Also as the sole source of climbing fibres to the cerebellum, the inferior olive is believed to be of central importance for the proper functioning of the cerebellum as a co-ordinating centre for movements (Armstrong, 1974) with an important role in the timing process for motor control (Llinas and Sasaki, 1989). In the present work, the representation of the respiratory motor act in the inferior olive has been studied. Three principal types of respiratory related activities were encountered; 1), respiratory phased, mass activity; respiratory phased, low frequency activity; 3), respiratory pump locked activity. The overall distribution of these activities was found to form a central longitudinal narrow band corresponding closely with the segmental projection of the spino-olivary neurones located in the thoracic spinal cord (Matsushita et al., 1992).

The persistence of rhythmic inspiratory activity in the

DAO, when the central drive to the external intercostal motoneurones was abolished due to cold block of the spinal cord, strongly indicates that the DAO receives a phasic inspiratory input of supraspinal origin. This mass inspiratory activity showed some attenuation during cold block with the appearance of some high amplitude units discharging at low frequency throughout the phase. It is suggested that this change was induced by the withdrawal of the spinal component which would thus represent an example of the convergent inputs studied by Andersson and Eriksson (1981). It is assumed that the source of supraspinal inputs could come either directly from the ventral or dorsal respiratory groups and/or via the cerebellar nuclei based on electrophysiological studies in awake cats (Gruart and Delgardo-Garcia, 1992) or anatomical studies using labelling (Nunez-Abades, Pasaro and Sears, submitted for publication). With regard to the spinal origin, it has been shown that some neurones in laminae VII and VIII of the thoracic spinal cord belonging to the VSCT system receive converging inputs of both inspiratory and expiratory phased components of the central respiratory drive and the thoracic wall proprioceptive inputs (Tanaka and Hirai, 1994). This spinal origin corresponds to that containing the neurons giving rise to VF-SOCP (Armstrong & Schild 1980), hence they are assumed provisionally to be the site of origin of the olivary respiratory activities.

These spino-olivary neurones were suggested to monitor

interactions between command signals and reflex arcs in 'spinal motor centres', such that, these neurones forward to the olive via spino-olivary pathways, information about activity in these 'centres' rather than about peripheral events (Oscarsson, 1969, 1973; Miller and Oscarsson, 1970). The authors also postulated, that a further correlation occurs at the olivary level, but now, between the original command signals from 'higher motor centres' and the activity these signals evoked at spinal centres, so the results of such a comparison might be used in cerebellar integration of higher motor activity.

The present results strongly support the Oscarsson hypothesis both with regard to the converging elements needed for comparison, and interactions that take place at the spinal and olivary levels. This is because at segmental level the reciprocal pattern of inspiratory and expiratory motoneurone discharge, indeed reflects interaction between the central respiratory drive 'the command for respiratory movements' and reflex inputs (Sears, 1964c,d; 1979). Hence, it would be expected that spino-olivary neurones would feed back the outcome of this interaction or the actual movement performed to the DAO via the VF-SOCP and possibly the other SOCPs. The outcome would be compared with the original command signals (from supraspinal sources) in the DAO.

Thus in this study, the manipulation of the 'endogenous' command for breathing movements by lowering the CO_2 level

(which directly affect central respiratory drive) while holding the mechanical conditions in the thorax constant, resulted in changes in the olive. This change in olivary discharge would indicate that olivary neurons have detected the misalignment (error signal) between the demand for movement and the actual movement evolved at the spinal level. Indeed this observation could be said to constitute the first demonstration of the presence of a command to move being fed to olivary neurones and hence contributing to the role of the olivary neurones as a 'comparator'. Such an error signal would be expected to feed back to the cerebellum any hindrance to breathing movements which might compromise pulmonary ventilation and consequently homeostasis so that appropriate action could be summoned forth. Also, the change in olivary activity following withdrawal of the feedback information due to cold block of the spinal cord, could be thought of as indicating that the olive was signalling to the cerebellum an error in the respiratory motor system performance.

As the intercostal muscles also participate in postural changes and in particularly give structural stability to forelimbs movements, rotation or flexion of the trunk will result in the stretch of the intercostal muscles which would result in olivary discharge (cf. Gellman et al., 1985). Such stimuli were also adequate to activate the thoracic DSCT neurones (Tanaka and Hirai, 1994). Therefore the DAO over its CFs and the thoracic DSCT neurones over

mossy fibres forward respiratory and posture-related information to the cerebellum providing the basis for the integration of respiratory movement with the regulation of the body posture as a whole.

CONCLUSION

From this work, it would be possible to conclude that the DAO receives convergent respiratory related inputs from at least three sources; central respiratory pattern generator, cerebellar nuclei and spinal cord. However further study by intracellular recording and antidromic identification would be necessary to confirm such convergence while recording central respiratory activities in the DAO. A better understanding of these sources would provide insights concerning the mechanisms by which these inputs interact to modulate the activity of olivary neurones and eventually the cerebellar output, either directly or through neuromodulation.

Be this as it may, the respiratory system with its naturally occurring movements which remain subject to normal control and persist during spontaneous breathing or artificial ventilation during anaesthesia, with or without paralysis, would be one of the best models to elucidate the function of the olivocerebellar system. Furthermore by manipulation of the chemical drive, this system allows control over the "endogenous" command for movement. Thus the respiratory system provides an ideal opportunity for studying the interactions between the 'command' for movements as well as the 'outcome' so that the findings should serve as a model for other motor systems.

REFERENCES

AMINOFF, M.J., SEARS, T.A., (1971). Spinal integration of segmental, cortical and breathing inputs to thoracic respiratory motoneurones. Journal of Physiology 215: 557-575.

ANDERSSON, G., ARMSTRONG, D.M. (1987). Complex spikes in Purkinje cells in the lateral vermis (b zone) of the cat cerebellum during locomotion. Journal of Physiology 385: 107-134.

ANDERSSON, P., ECCLES J.C., SEARS, T.A. (1964). Cortically evoked depolarization of primary afferent fibres in the spinal cord. Journal of Neurophysiology 27: 63-77.

ANDERSSON, G., ERIKSSON, (1981). Spinal, trigeminal and cortical climbing fibre paths to the lateral vermis of the cerebellar anterior lobe in the cat. Experimental Brain Research 44: 71-81.

ANDERSSON, O., FORSSBERG, H., GRILLNER S., LINDQUIST, M. (1978). Phasic gain control of the transmission in cutaneous reflex pathways to motoneurones during "fictive" locomotion. Brain Research 149: 503-507.

ANDERSSON, G., GARWICZ, M., HESSLOW, G., (1988). Evidence for a GABA-mediated cerebellar inhibition of the inferior olive in the cat. Experimental Brain Research Series 72: 450-456.

ANDERSSON, G., OSCARSSON, O. (1978a). Projection to the lateral vestibular nucleus from the cerebellar climbing fibre zones. Experimental Brain Research 32: 549-564.

ANDERSSON, G., OSCARSSON, O. (1978b). Climbing fibre microzones in cerebellar vermis and their projection to different groups of cells in the lateral vestibular nucleus. Experimental Brain Research 32: 565-579.

ANDERSSON, P., SEARS, T.A. (1970).Medullary activation of intercostal fusimotor and alpha motoneurones. Journal of

Physiology 209: 739-755.

ANGAUT,P., CICRATA, F., SERAPIDE,F. (1985b). Topographic organization of the cerebellothalamic projections in the rat. An autoradiographic study. Neuroscience 15. 389-401.

APPS, R. (1990). Columnar organization of the inferior olive projection to the posterior lobe of the rat cerebellum. Journal of Comparative Neurology 302: 236-254.

APPS, R., LIDIERTH, M., ARMSTRONG, D.M. (1990). Locomotion related variation in the excitability of spino-olivocerebellar paths to the cerebellar cortical C2 zone in the cat. Journal of Physiology 424: 487-512.

ARMSTRONG, D.M. (1974). Functional significance of connections of the inferior olive. Physiological Reviews Volume. 54: 358-417.

ARMSTRONG, D.M. (1990). Topographical localization in the projections from the inferior olive to the paravermal cortex of the anterior lobe and paramedian lobule in the cerebellum of the cat. A brief review. Archives Italiennes de Biologie 128: 183-207.

ARMSTRONG, D.M., CAMPBELL, N.C., EDGLEY, S.A., SCHILD, R.F., TROTT, J.R. (1982). Investigations of the olivocerebellar and the spino-olivary pathways. In: The cerebellum New Vistas; Experimental Brain Research Series 6: eds. Palay, S.L., Chan-Palay, V., Springer-Valberg, Berlin, Heidleberg, New York. p. 195-232.

ARMSTRONG, D.M., ECCLES, J.C., HARVEY, R.J. MATTHEWS, P.B.C., (1968). Responses of the dorsal accessory olive of the cat to stimulation of hindlimb afferents. Journal of Physiology 194: 125-145.

ARMSTRONG, D.M., HARVEY, R.J. (1968). Responses of spino-olivocerebellar pathway in the cat. Journal of Physiology 194: 147-168.

ARMSTRONG, D.M., HARVEY, R.J., SCHILD, R.F. (1971). Climbing fibre pathways from the forelimbs to the

paramedian lobule of the cerebellum. Brain Research 25: 199-202.

ARMSTRONG, D.M., HARVEY, R.J., SCHILD, R.F. (1973). Branching of inferior olivary axons to terminate in different folia lobules or lobes of the cerebellum. Brain Research 54: 365-371.

ARMSTRONG, D.M., HARVEY, R.J., SCHILD, R.F. (1973). Spino-olivocerebellar pathways to the posterior lobe of the cat cerebellum. Experimental Brain Research 18: 1-18.

ARMSTRONG, D.M., HARVEY, R.J., SCHILD, R.F. (1974). Topographical localization in the olivocerebellar projection. An electrophysiological study in the cat. Journal of Comparative Neurology

ARMSTRONG, D.M., SCHILD, R.F. (1979). Spino olivary neurones in the lumbosacral cord of the cat demonstrated by retrograde transport of horseradish peroxidase. Brain Research 168: 176-179.

ARMSTRONG, D.M., SCHILD, R.F. (1980). Location in the spinal cord of neurones projecting directly to the inferior olive in the cat. In: COURVILLE, J., DE MONTIGNNY, C., LAMMARE, Y., eds. The Inferior Olive: Anatomy and Physiology. Raven Press, New York. p. 125-144.

ASANUMA,H., HUNSPERGER, R. W., (I975). Functional significance of projection from the cerebellar nuclei to the motor cortex in the cat. Brain Research 98: 73-92.

AZIZI, S.A., (1989). Principles of organization within the olivocerebellar system in the rat. Experimental Brain Research Series 17. Springer-Valberg, Berlin, Heidleberg. p. 46-51.

AZIZI, S.A., WOODWARD, D.J., (1987)Inferior olivary nuclear complex of the rat: morphology and comments on the principles of organization within the olivocerebellar system. Journal of Comparative Neurology 263: 467-484.

BAINTON, C.R., KIRKWOOD, P.A. (1979). The effects of carbon dioxide on the tonic and rhythmic discharges of expiratory bulbospinal neurones. Journal of Physiology 296: 291-314.

BAINTON, C.R., KIRKWOOD, P.A., SEARS, T.A. (1979). On the transmission of the stimulating effects of carbon dioxide to the muscles of respiration. Journal of Physiology 280: 249-272.

BAKER, S.C., (1994). Thesis: The control of transmission in spino-olivo-cerebellar pathways. University of London.

BAKER, S., SEERS, C., SEARS, T.A. (1990). Respiratory modulation of afferent transmission to the cerebellum. In: Respiratory Control, Central and Peripheral Mechanism. Edited by Speck, D.F., Dekin, M.S., Revelette, W.R. and Frazier, D.T. The University Press, Kentucky pp 95-99

BARMACK, N.H., HESS,D.T., (1980a). Multiple unit activity evoked in dorsal cap of inferior olive of the rabbit by visual stimulation. Journal of Neurophysiology 43: 151-164.

BARMACK, N.H., HESS,D.T., (1980b). Eye movements evoked by microstimulation of dorsal cap of inferior olive in the rabbit. Journal of Neurophysiology 43: 165-181.

BARMACK, N.H., SIMPSON, J.I., (1980). Effects of microlesions of dorsal cap of inferior olive of rabbits on optokinetic and vestibular reflexes. Journal of Neurophysiology 43: 182-206.

BELL, C.C., (1984). Effects of motor commands on sensory inflow, with examples from electric fish. In: Comparative Physiology of Sensory Systems, edited by L. Bolis, D. Keymes and S.H.P. Maddrell. Cambridge: Cambridge University Press. pp 637-646.

BENARDO, L.S., FOSTER, R.E. (1986). Oscillatory behaviour in inferior olive neurones: Mechanism, modulation and cell aggregates. Brain Research Bulletin, volume 17: 773-784.

BERKLEY, K.J., WORDEN, I.G., (1978). Projection to inferior

olive of the cat. I. Comparison of inputs from the dorsal column nuclei, the spino-olivary pathways, the lateral cervical nucleus, the cerebral cortex and the cerebellum. Journal of Comparative Neurology 180: 237-252.

BILLARD, J.M., BATINI, C., BUISSERET-DELMAS, C., DANIEL, H. (1989). The inferior olive innervation from the cerebellar and lateral vestibular nuclei: Evidence for a longitudinal zonal segregation of the cortico-nucleo-olivary connection in the rat. Experimental Brain Research Series 17. Springer-Valberg, Berlin, Heidleberg. p. 117-120.

BISHOB, G.A., HO, R.H., (1986). Cell origin of serotonin-immunoreactive afferent to the inferior olivary complex of the rat. Brain Research 399: 369-373.

BRODAL, A., (1980). Olivocerbellocortical projection in the cat as determined with the method of retrograde axonal transport of horseradish peroxidase. 2. Topographical pattern in relation to the longitudinal subdivisions of the cerebellum. In: COURVILLE, J., DE MONTIGNNY, C., LAMMARE, Y., eds. The Inferior Olive: Anatomy and Physiology. Raven Press, New York. p. 187-205.

BRODAL, A., KAWAMURA, K., (1980). Olivocerebellar projection: A review. In: BRODAL, A., HILO, W., VAN LIMBORGH, J., ORTMANN, R., SCHIEBLER, T.H.,YONDURY, G., WOLFF, F., eds. Advances in Anatomy, Embryology and Cell Biology. Berlin, Heidleberg, New York, Springer-Valberg. Volume 64: p.1-140.

BRODAL, A., WALBERG, F., BLACKSTAD (1950). Termination of spinal afferents to inferior olive in cats. Journal of Neurophysiology 13: 431-454.

BRODAL, A., WALBERG, F., (1977a). The olivocerebellar projection in the cat studied with the method of retrograde axonal transport of horseradish peroxidase. IV. The projection to the anterior lobe. Journal of Comparative Neurology 172: 85-108.

BRODAL, A., WALBERG, F., (1977b). The olivocerebellar projection in the cat studied with the method of retrograde

axonal transport of horseradish peroxidase. VI. The projection to onto longitudinal zones of the paramedian lobule. Journal of Comparative Neurology 176: 281-294.

BROOKS, V.B. (1983). Study of brain function by local, reversible cooling. Review of Physiology, Biochemistry and Pharmacology 95: 15-42.

BUDZINSKA, K., von EULER, C., KAO, F.F., PANTALEO, T., YAMAMOTO, Y., 1985c. Release of respiratory muscle activity by graded focal cold block in the medulla. Acta Physiologica Scandinavica 124: 341-351.

BUISSERET-DELMAS, C., ANGAUT, P., (1992). The cerebellar olivocorticonuclear connections in the rat. Progress in Neurobiology 40: 63-87.

BUSH, (1961). Thesis: An anatomical analysis of the white matter in the brainstem of the cat. aan de Rijksuniversiteit te Leiden.

CAMPBELL, E.J.M., AGOSTONI, E., NEWSOM DAVIS, J., (1970). The respiratory muscles. Lloyd Luke, London.

CAMPBELL, N.C., ARMSTRONG, D.M., (1985). Origin the medial accessory olive of climbing fibres to the X and lateral C1 zones of the cat cerebellum: a combined electrophysiological /WGA-HRP investigation. Experimental Brain Research 58: 520-531.

CAMPBELL, N.C, HESSLOW, G. (1986a). The secondary spikes of climbing fibre responses recorded from Purkinje cell axons in cat cerebellum. Journal of Physiology 377: 207-224.

CAMPBELL, N.C., HESSLOW, G. (1986b). The secondary spikes of climbing fibre responses recorded from Purkinje cell axons in cat cerebellum. Journal of Physiology 377: 225-235.

CHERNIACK, N.S., Von EULER, C., HOMMA, I. (1979). Graded changes in central chemoreceptor input by local temperature changes on the ventral surface of the medulla. Journal of Physiology 287: 191-211.

CICRATA, F., ANGAUT,P., CIONI,M., SERAPIDE, M.F., PAPALE, A., (1986). Functional organization of the thalamic projection to the motor cortex. An anatomical and electrophysiological study in the rat. Neuroscience 19: 81-99.

CICRATA, F., ANGAUT,P., SERAPIDE, M.F., PANTO, M.R., NICOTRA, G., (1992). Multiple representation in the nucleus lateralis of the cerebellum. An electrophysiological study in the rat. Experimental Brain Research :

COFFEY,G.L., GODWIN-AUSTIN, R.B., MacGILLIVRAY,B.B., SEARS, T.A., (1971) The form and distribution of the surface evoked responses in cerebellar cortex from intercostal nerves in the cat. Journal of Physiology 212: 129-145.

COHEN, M.I., (1970). Discharge pattern of brain-stem respiratory neurones in relation to carbon dioxide tension. Journal of Neurophysiology 31: 142-165.

COMPOINT, C., BUISSERET-DELMAS, C. (1988). Origin, distribution and organization of the serotonergic inactivation in the inferior olivary complex of the rat. Archive of Ital. Biologica 126: 99-110.

CORDA, M., Von EULER, C., LENNERSTRAND, G. (1966). Reflex and cerebellar influences on alpha and on 'rhythmic' and 'tonic' gamma activity in the intercostal muscle. Journal of Physiology 184: 898-923.

COURVILLE,J., (1975). Distribution of olivocerebellar fibres demonstrated by a radioautographic tracing method. Brain Research 95: 253-263.

CRILL, W.E., (1970).Unitary multiple spikes responses in cat inferior olive nucleus. Journal of Neurophysiology 33: 199-209.

CRITCHLOW, V., Von EULER, C. (1962). Rhytmic control of intercostal muscle spindles. Experimentia 18: 426-427.

CRITCHLOW, V., Von EULER, C. (1963). Intercostal muscle spindle activity and its gamma motor control. Journal of

Neurophysiology 168: 820-847.

DAVIS, McF., KIRKWOOD, P.A., SEARS T.A. (1985). The distribution of monosynaptic connexions from inspiratory bulbospinal neurones to inspiratory motoneurones in the cat. Journal of Physiology 386: 63-87.

DaSILVA, K.M.C., SAYERS, B.McA., SEARS, T.A., STAGG, D.T. (1977). The changes of configuration of the rib cage and abdomen during breathing in the anaesthetized cat. Journal of Physiology 266: 499-521.

DECIMA, E.E., Von EULER, C. (1969). Intercostal and cerebellar influences in efferent phrenic activity in the decerebrate cat. Acta Physiologica Scandinaphia 67: 148-158.

DEMER, J.L., ROBINSON, D.A., (1982). Effects of reversible lesions and stimulation of olivocerebellar system on vestibulo-ocular reflex plasticity. Journal of Neurophysiology 47: 1084-1107.

DIETRICHS, E., WALBERG, F. (1989). Direct bidirectional connections between the inferior olive and the cerebellar nuclei. Experimental Brain Research 17: Springer Verlag Berlin-Heidelberg.

DOWNMAN, C.B.B., (1955). Skeletal muscle reflexes of splanchnic and intercostal nerve origin in acute spinal and decerebrate cats. Journal of Neurophysiology 18: 217-235.

DURON, B. (1973). Postural and ventilatory functions of intercostal muscles. Acta Neurobiolgica Experimentia 33: 355-380.

DURON, B., MARLOT, D., (1987). Respiratory activity of intercostal nerves in the cat. In SIEK, G.C., GANDEVIA, S.C., CAMERON, W.E. Respiratory muscles and their neuromotor control: 185-194.

ECCLES J.C. (1964). The release of transmitter by presynaptic impulses. In: The Physiology of Synapses.

Berlin, Gottingeu, Heidleberg, Springer-Valberg. p. 75-100.

ECCLES J.C. (1964). The generation of impulses by the excitatory postsynaptic potential and the endplate potential. In: The Physiology of Synapses. Berlin, Gottingeu, Heidleberg, Springer-Valberg. p. 101-121.

ECCLES, R.M., SEARS, T.A., SHEALY C.N. (1962). Intracellular recording from respiratory motoneurones of the thoracic spinal cord of the cat. Nature 193: 844-846.

EKEROT, C.F., LARSSON, B. (1979a). The dorsal spino olivocerebellar system in the cat. I. Functional organization and termination in the anterior lobe. Experimental Brain Research 36: 201-217.

EKEROT, C.F., LARSSON, B. (1979b). The dorsal spino-olivocerebellar system in the cat. II. Somatotopical organization. Experimental Brain Research 36: 219-232.

EKEROT, C.F., GARWICZ, M., SCHOUENBORG, J., (1991). Topography and nociceptive receptive fields of climbing fibres projecting to the cerebellum anterior lobe in the cat. Journal of Physiology. 441: 257-274.

EKEROT, C.F., GARWICZ, M., SCHOUENBORG, J., (1991). The postsynaptic dorsal column pathway mediates cutaneous nociceptive information to cerebellar climbing fibres in the cat. Journal of Physiology. 441: 275-284.

EKEROT, C.F., LARSSON, B. (1979b). The dorsal spino olivocerebellar system in the cat. II. Somatotopical organization. Experimental Brain Research 36: 219-232.

EKEROT, C.F., LARSSON, B. (1982). Branching of olivary axons to innervate pairs of sagittal zones in the cerebellar anterior lobe of the cat. Experimental Brain Research 48: 185-198.

EKLUND, G., Von EULER, C., RUTKOWSKI, S. (1963). Intercostal gamma motor activity. Acta Physiologica Scandinavica 57: 481-482,

EKLUND, G., Von EULER, C., RUTKOWSKI, S. (1964). Spontaneous and reflex activity of intercostal gamma motoneurones. Journal of Physiology. 171: 139-163.

ELDRIDGE, F.L., MILLHORN, D.E., (1981). Central regulation of respiration by endogenous and neurotransmitters and neuromodulators. Annual Review of Physiology 43: 121-135.

Von EULER, C. (1980). Central pattern generation during breathing. TINS 3: 275-277.

Von EULER, C. (1983). On the central pattern generator for the basic breathing rhythmicity. Journal of Applied Physiology and Respiration Environmental Exercise Physiology 55: 1647-1659.

Von EULER, C. (1986). Brain stem mechanisms for generation and control of breathing pattern. In: Cherniak, N. Widdicombe J.G. eds. Hand book of Physiology volume 2 Control of breathing: Bethesda: American Society 463-524.

Von EULER, C., TRIPPENBACH, T., (1976). Excitability change of the inspiratory "off-switch" mechanism tested by electrical stimulation in nucleus parabrachialis in the cat. Acta Physiologica Scandinafia 97: 175-188.

FELDMAN, J.L. (1986). Neurophysiology of respiration in mammals. In: Bloom F.E. (ed) Hand book of Physiology volume 4. The Nervous System. Bethesda: American Physiological Society 4: 463-524.

FELDMAN, J.L., COHEN, M.I., (1978). Relation between expiratory duration and rostral medullary expiratory neuronal discharge. Brain Research 141: 171-178.

FENN, W.O., (1960). Introductory remarks. Ann. NY Acad. Sci. 109: 415-417.

FOSTER, R.E., PETERSON, B.E. (1986). The inferior olivary complex of guinea pig: Cytoarchitecture and cellular morphology. Brain Research Bulletin 17: 785-800.

FREDETTE, B.J., ADAMS, J.C., MUGNAINI, E. (1992). GABAergic

neurones in the mammalian inferior olive and ventral medulla detected by glutamate decarboxylase immunocytochemistry. Journal of Comparative Neurology 321: 501-514.

GARWICZ, M., EKEROT, C.F., (1994) Topographical organization of the cerebellar cortical projection to the nucleus interpositus anterior in the cat. Journal of Physiology. 474: 245-260.

GAYTAN, S.P.,PASARO, R., SEARS, T.A. (submitted for publication). Cerebellar projection to the ventral respiratory group in the rat.

GELLMAN, R., GIBSON, A.R., HOUK, J.C. (1985). Inferior olivary neurones in the awake cat: Detection of contact and passive body displacement. Journal of Neurophysiology 54: 40-60.

GELLMAN, R., HOUK, J.C., GIBSON, A.R. (1983). Somatosensory properties of the inferior olive in the cat. Journal of Comparative Neurology 215: 228-243.

GIBSON, A.R., ROBINSON, F.R., ALAM, J., HOUK, J.C. (1987). Somatotopic alignment between climbing fibre input and nuclear output of the cat intermediate cerebellum. Journal of Comparative Neurology 260: 362-377.

GROENEWEGEN, H.J., VOOGD, H. (1977). The parasagittal zonation within the olivocerebellar projection. I. Climbing fibre distribution in the vermis of cat cerebellum. Journal of Comparative Neurology 174: 417-488.

GROENEWEGEN, H.J., VOOGD, J., FREEDMAN, S.L. (1979). The parasagittal zonation within the olivocerebellar projection. II. Climbing fibre distribution in the intermediate and hemispheric parts of the cat cerebellum. Journal of Comparative Neurology 153: 551-602.

GWYN, D.G., NICHOLSON, G.P. FLUMERFELT, B.A., (1976). The Inferior Olivary nucleus of the rat: A light and electron microscopic study. Journal of Comparative Neurology 174: 489-520.

GRUART, A., DELGARDO-GRACIA, J.M, (1992). Respiration-related neurones recorded in the deep cerebellar nuclei of the alert cat. Neuroreport 3: 365-368.

GWYN, D.G., RUTHERFORD, H.G., NICHOLSON, G.P. (1983). An electron microscopic study of the direct spino-olivary projection to the Inferior Olivary nucleus of the rat. Neuroscience Letters 42: 243-248.

HADDAD, G.M., DEMER, J.I., ROBINSON, D.A., (1980). The effects of lesions of the dorsal cap of the inferior olive and the vestibulo-ocular and optokinetic systems of the cat. Brain Research 185: 265-275.

HRYCYSHYN, A.W., GHAZI, H., FLUMERFELT, B.A., (1989). Axonal branching of olivocerebellar projection in the rat. A double labelling study. Journal of Comparative Neurology 284: 48-59.

HUBBARD, J.I., LLINAS, R., QUASTEL, D.M. (1969). Extracellular field potentials in the central nervous system. In: Electrophysiological Analysis of Synaptic Function. Monographs of The Physiological Society. London, Edward Arnold Ltd. p. 265-293.

ITO, M. (1984). Spino-olivary system. In: The cerebellum and neural control; Raven Press, New York p. 256-277.

ITO, M. (1989). Long -term depression. Annual Review Neuroscience. 12: 85- 102.

ITO, M., ORLOV, I., SHIMOYAMA, I. (1978). Reduction of cerebellar stimulus effect on rat Deiters Neurones after chemical destruction of the Inferior olive. Experimental Brain Research 33: 143-145.

ITO, M., MIYASHITA, Y., (1972). The effects of chronic destruction of the inferior olive upon visual modification of the horizontal vestibulo-ocular reflex of rabbit. Proceedings of Japanese Academy 51: 716-723.

ITO, M., SAKURAI, M., TONGROACH, P., (1982). Climbing fibre induced depression of both mossy fibre responsiveness and

glutamate sensitivity of cerebellar Purkinje cells. Journal of Physiology 324: 113-134.

JACOBS, B.L., FORMAL, C.A., (1993). 5-HT and motor control: a hypothesis. Trendes in Science 16(9): i993.

JANSEN, J., BRODAL, A., (1940). Experimental studies on the intrinsic fibres of the cerebellum. II. The corticonuclear projection. Journal of Comparative Neurology 73: 267-321.

KONNO, K., MEAD, J., (1967). Measurements of separate volume changes of rib cage and abdomen during breathing. Journal of Applied Physiology 22:407-422.

KHATIEB, A., FORT, P., SERAFIN, M., JONES, B.E., MUHLETHALE, M., (1995). Rhythmical bursts induced by NMDA in guinea-pig cholinergic nucleus basalis neurones in vitro. Journal of Physiology. 487: 623-638.

KING, J.S. (1976). The synaptic cluster (glomerulus) in the inferior olivary nucleus. Journal of Comparative Neurology 165: 387-400.

KING, J.S., ANDREZIK, J.A., FALLS, W.M., MARTIN G.F. (1976). The synaptic organization of the cerebello-olivary circuit. Experimental Brain Research 26: 159-170.

KIRKWOOD, P.A., (1995). Synaptic excitation in the thoracic spinal cord from expiratory bulbospinal neurones in the cat. Journal of Physiology 484: 201-225.

KIRKWOOD, P.A., SEARS T.A. (1974) Monosynaptic excitation of motoneurones from secondary endings of muscle spindles. Nature. vol. 252: 5480; 243-244.

KIRKWOOD, P.A., SEARS T.A. (1974) Monosynaptic excitation of motoneurones from muscle spindles secondary endings of intercostal and triceps surae muscle in the cat. Proceedings of the Physiological Society, Journal of Physiology 245: 64-66.

KIRKWOOD, P.A., SEARS T.A. (1982) Excitatory post-synaptic potentials from single muscle spindle afferents in external

intercostal motoneurones of the cat. Journal of Physiology 332: 287-314.

KIRKWOOD, P.A., SEARS T.A., WESTGAARD, R.H. (1984). Restoration of function in external intercostal motoneurones of the cat following partial central deafferentation. Journal of Physiology. 350: 225-251.

LANGHOF, H., HOPPENER, U., RUBIA, F.J., (1973). Climbing fibre responses to splanchnic nerve stimulation. Brain Research 53: 232-236.

LARSON, B., MILLER, S., OSCARSSON, O. (1969a). Termination and functional organization of the dorsolateral spino olivocerebellar path. Journal of Physiology. 203: 611-640.

LARSON, B., MILLER, S., OSCARSSON, O. (1969b). A spinocerebellar climbing fibre path activated by the flexor reflex afferents from all four limbs. Journal of Physiology 203: 641-669.

LIDIERTH, M., APPS, R. (1990). Gating in the spino-olivary cerebellar pathways to the C1 zone of the cerebellar cortex during locomotion in the cat. Journal of Physiology 430: 453-469.

LLINAS, R. (1989). Electrophysiological properties of the olivocerebellar system. Experimental Brain Research 17: Springer Verlag Berlin-Heidelberg. p.201-207.

LLINAS, R., BAKER, R., SOTELO, C. (1974). Electronic coupling between neurones in cat inferior olive. Journal of Neurophysiology 37: 560-571.

LLINAS, R., SASAKI, K. (1989). The functional organization of the olivocerebellar system as examined by multiple Purkinje cell recording. European Journal of Neuroscience 1: 587-603.

LLINAS, R., VOLKIND, R.A. (1973). The olivocerebellar system: Functional properties as revealed by harmline-induced tremor. Experimental Brain Research 18: 69-87.

LLINAS, R., YAROM, Y. (1981). Electrophysiology of mammalian inferior olivary neurones in vitro. Different types of voltage-dependent ionic conductances. Journal of Physiology 315: 569-584.

LLINAS, R., YAROM, Y. (1986). Oscillatory properties of guina-pig inferior olivary neurones and their pharmacological modulation: An in vitro study. Journal of Physiology 376: 163-182.

MACGILLIVRAY, B.B., SEARS, T.A., GODWIN-AUSTIN, R.B., COFFEY, G.L. (1970). Thoracic segmental input to the cerebellum. International Journal of Neurology 7: 288-293.

MATSUSHITA, M., YAGINUMA, H., TANAMI, T. (1992). Somatotopic termination of the spino olivary fibres in the cat studied with the wheat germ agglutinin-horseradish peroxidase technique. Experimental Brain Research 89: 397-407.

MATTHEWS, P.B.C. (1972). Mammalian muscle receptors and their control action. From Monographs of the Physiological Society. London: Arnoid.

McCORMICK, D.A., WANG, Z. (1991). Serotonin and noradrenaline excite GABAergic neurones of the guina-pig and cat nucleus reticularis thalami. Journal of Physiology 442: 235-255.

MERRILL, E.G. (1970). The lateral respiratory neurones of the medulla: their association with nucleus ambiguous, nucleus retroambigualis, the spinal accessory nucleus and the spinal cord. Brain Research 24: 11-28.

MERRILL, E.G. (1972). Thoracic motor drives from medullary expiratory neurones in cats. Journal of Physiology 222: 154-155.

MERRILL, E.G. (1974). Finding a respiratory function for the medullary respiratory neurones. In: Bellairs R. and Gray E.G. Essays on the nervous system. A festschrift for Professor J.Z. Young Clarendon Press, Oxford 451-486.

MILLER, S.F., OSCARSSON, O. (1970). Termination and functional organization of spino-olivocerebellar path. In: The cerebellum in health and disease. eds. by W.S. Fields and W.D. Willis. pp. 172-200. Warren H. Green, St. Louis.

MIZUNO, N., (1966). An experimental study of the spino-olivary fibres in the rabbit and cat. Journal of Comparative Neurology 127: 267-292.

MOLINARI, H.H. (1988). Ultrastructural heterogeneity of spinal termination in the cat inferior olive. Neuroscience 27:425-435.

NELSON, B,J., MUGNAINI, E., (1989). Origins of GABAergic inputs to the inferior olive. Experimental Brain Research Series 17. Springer-Valberg, Berlin, Heidleberg. pp 86-107.

NEWOSOM-DAVIS,J., PLUM, F., (1972). Separation of descending spinal pathways to respiratory motoneurones. Experimental Neurology 34: 78-94.
60\last, 145\6 --1981-> 1982

OSCARSSON, O. (1968). Termination and functional organization of the ventral spino olivocerebellar path. Journal of Physiology 200

OSCARSSON, O. (1969a). Termination and functional organization of the dorsal spino olivocerebellar path. Journal of Physiology 196: 453-478.

OSCARSSON, O. (1969b). The sagittal organization of the cerebellar anterior lobe as revealed by the projection patterns of the climbing fibre system. In: Neurobiology of cerebellar evolution and development. eds. by R. Llinas. Chicago. American Medical Association. p.525-532.

OSCARSSON, O. (1973). Functional organization of spinocerebellar paths. In: Iggo, A. (ed.) HandBook of Sensory Physiology. Volume II. Somatosensory System, Berlin, Heidleberg, New York, Springer-Valberg. p.339-380.

OSCARSSON, O. (1980). Functional organization of olivary

projection to the cerebellar anterior lobe. In: COURVILLE, J., DE MONTIGNNY, C., LAMMARE, Y., eds. The Inferior Olive: Anatomy and Physiology. Raven Press, New York. p. 279-289.

OSCARSSON, O., SJOLUND, B. (1977a). The ventral spino olivocerebellar system. I. Identification of five paths and their termination in the cerebellar anterior lobe. Experimental Brain Research 28: 469-486.

OSCARSSON, O., SJOLUND, B. (1977b). The ventral spino-olivocerebellar system in the cat. II. Termination of zones in the cerebellar posterior lobe. Experimental Brain Research 28: 487-503.

OSCARSSON, O., SJOLUND, B. (1977c). The ventral spino olivocerebellar system in the cat. III. Functional characteristics of the five paths. Experimental Brain Research 28: 505-520.

PETERSON, B.W., COULTER, J.S., (1977). A new long spinal projection from the vestibular nuclei in the cat. Brain Research 122: 351-356.

PITTS, R.F. (1946). Organization of the respiratory centre. Physiological Review 26: 609-630.

PITTS, R.F., MAGOUN, H.W., RANSON, S.W., (1939a). Localization of the medullary respiratory centres in the cat. American Journal of Physiology 126: 673-688.

PITTS, R.F., MAGOUN, H.W., RANSON, S.W., (1939b). Interaction of the respiratory centres in the cat. American Journal of Physiology 126: 689-707.

RAMOS, J.G. (1959). On the integration of respiratory movements. Acta Physiologica Latinoamericana 9: 4: 246-256.

RAMOS, J.G., MENDOSA, E.L. (1959). On the integration of respiratory movements II. the integration at spinal level. Acta Physiologica Latinoamericana 9: 4: 257-266.

REMMERS, J.E., TSIARAS, W.G. (1973). Effect of lateral cervical cord lesions on the respiratory rhythm of

anaesthetized, decerebrate cats after vagotomy. Journal of Physiology 126:63-74.

RICHTER, D.W. (1982). Generation and maintenance of the respiratory rhythm. Journal of Experimental Biology 100: 93-107.

RICHTER, D.W., BALLANTYNE, D., REMMER, J.E. (1986). How is the respiratory rhythm generated? A model NIPS 1: 109-112.

ROSINA, A. PROVINI, L.(1987) Somatotopy of climbing fibre branching to the cerebellar cortex in cat. Brain Research 289: 45-63.

RUIGROK, T.J.H., VOOGD,J,. (1995). Cerebellar influence on olivary excitability in the cat. European Journal of Neuroscience 7: 679-693.

SALMORAGHI, G.C., BURNS, B.D., (1960).Notes on mechanism of rhythmic respiration. Journal of Neurophysiology 23: 14-26.

SEARS, T.A. (1958). Electrical activity in expiratory muscles of the cat during inflation of the chest. Journal of Physiology 142: 35.

SEARS, T.A. (1963). Activity of fusimotor fibres innervating muscle spindles in the intercostal muscles of the cat. Nature 197: 1013-1014.

SEARS, T.A. (1964a). The fibre calibre spectra of sensory and motor fibres in the intercostal nerves of the cat. Journal of Physiology 172: 150-160.

SEARS, T.A. (1964b). Some properties and reflex connections of respiratory motoneurones of the cat thoracic spinal cord. Journal of Physiology 175: 386-403.

SEARS, T.A. (1964c). The slow potentials of thoracic respiratory motoneurones and their relation to breathing. Journal of Physiology 175: 404-424.

SEARS, T.A. (1964d). Investigations on respiratory

motoneurones of the thoracic spinal cord. In Symposium on the structure and function of the spinal cord. Amsterdam: Elsevier.

SEARS, T.A. (1965). The role of segmental reflex mechanisms in the regulation of breathing. In: Studies in Physiology. Springer Valberg, Berlin, Heidelberg, New York.

SEARS, T.A. (1966). The respiratory motoneuron: integration at spinal segmental level. In: Breathlessness. eds. HOWELL, J.B.L., CAMPBELL, E.J.M., Blackwell, Oxford, UK. p.33-47.

SEARS, T.A. (1975). Servo control of the intercostal muscles. In: Electromyography 60: New Developments in Electromyography and Clinical Neurophysiology, ed by J.E. Desmedt Volume 3. Karger-Basel.

SEARS, T.A. (1971). Breathing: A sensory-motor act. The Scientific Basis of Medicine. Annual Reviews.

SEARS, T.A. (1977). The respiratory motoneuron and apneusis. Federation Proceedings 36: 10: 2412-2420.

SEARS, T.A. (1984). Spinal integration and rhythm generation in breathing. Bulletin of European Physiology and Respiration 20: 399-401.

SEARS, T.A. (1990). Central spinal integration and spinal integration. Chest 97: 45-51.

SEARS, T.A., BERGER, A.J., PHILLIPSON, E.A. (1982). Reciprocal tonic activation of inspiratory and expiratory motoneurones by chemical drives. Nature 299: 728-730.

SEARS, T.A., KIRKWOOD, P.A., BAINTON, C.R. (1975). Medullary spinal neuronal connectivity and breathing. Bulletin Physiopathology Respiration 11: 82-83.

SEARS, T.A., MAGZOUB, S., SEERS, C., (1993). Respiratory-phased activation of neurones in the inferior olive of the anaesthetized paralyzed cat. European Journal of

Neuroscience Supplement 6: 488A.

SHANNON, R., (1986). Reflexes from respiratory muscles and costovertebral joints. In: Bloom F.E. (ed) Handbook of Physiology volume II. The Respiratory System. Bethesda: American Physiological Society :

SCHEIBEL, M.E., SCHEIBEL, A.B.(1955). The inferior olive; a Golgi study. Journal of Comparative Neurology 102: 77-132.

SOTELO, C., LLINAS, R., BAKER, R., (1974). Structural study of the inferior olivary nucleus: Morphological correlates of electrotonic coupling. Journal of Neurophysiology 37: 541-559.

SUGIHARA, I., LANG, E.J., LLINAS,R., (1995). Serotonin modulation of inferior olivary oscillations and synchronicity: A multiple-electrode study in the rat cerebellum. European Journal of Neuroscience 7: 521-534.

SZENTAGOTHAI, J., (1970). Glomerular synapses, complex synaptic arrangements and their operation significance. In: The Neurosciences Second Study Program. F. O. Schmitt, eds. Rockfler Press, New York, p.427-443

TANAKA, Y., HIRAI, N. (1994). Physiological studies of thoracic spinocerebellar tract neurones in relation to respiratory movement. Neuroscience Research 19: 317-326.

TROTT, J.R., ARMSTRONG, D.M. (1987a). The cerebellar corticonuclear projection from lobule Vb/c of the cat anterior lobe: a combined electrophysiological and autoradiographic study. I. Projection from the intermediate region. Experimental Brain Research 66: 318-338.

TROTT, J.R., APPS, R., ARMSTRONG D.M. (1990). Topographical organization within cerebellar nucleocortical projection to the paravermal cortex of lobule Vb/c in the cat. Experimental Brain Research 80: 415-428.

TROTT, J.R., ARMSTRONG D.M. (1987b). The cerebellar

corticonuclear projection of lobule Vb/c of the cat anterior lobe: a combined electrophysiological and autoradiographic study. II. Projection from the vermis. Experimental Brain Research 66: 339-354.

VOOGD, J. (1969). The importance of fibre connections in the comparative anatomy of the mammalian cerebellum. In: The neurobiology of cerebellar evolution and development. Eds. by R. Llinas. Chicago, American Medical Association. p.493-514.

VOOGD, J. (1982). The olivocerebellar projection in the cat. In: The cerebellum New Vistas; Experimental Brain Research Series 6: eds. Palay, S.L., Chan-Palay, V., Springer-Valberg, Berlin, Heidleberg, New York. p. 209-219.

VOOGD, J. (1989). Parasagittal zones and compartments of the anterior vermis of the cat cerebellum. Experimental Brain Research Series 17. Springer-Valberg, Berlin, Heidleberg. p.

VOOGD, J., BIGARE, F., (1980). Topographical distribution of olivary and cortico-nuclear fibres in the cerebellum. A review. In: COURVILLE, J., DE MONTIGNNY, C., LAMMARE, Y., eds. The Inferior Olive: Anatomy and Physiology. Raven Press, New York. p. 207-234.

WALBERG, F., POMPEIANO, O., BRODAL, A., JANSEN, J., (1962). The fastigiovestibular projection in the cat. An experimental study with silver impregnation methods. Journal of Comparative Neurology 118: 49-76.

WALBERG, F., POMPEIANO, O., WESTRUM, L.E., HAUGLIE-HANSSEN, E., (1962). Fastigioreticular fibres in cat. An experimental study with silver impregnation methods. Journal of Comparative Neurology 119: 187-199.

WILSON, V.J., YOSHIDA, M., (1969b). Comparison of effects of stimulation of Dieter's nucleus and medial longitudinal fasciculus on neck, forelimb and hindlimb motoneurones. Journal of Neurophysiology. 32: 743-758.

WILSON, V.J., YOSHIDA, M., SCHOR,R.H., (1970). Supraspinal monosynaptic excitation and inhibition of the thoracic back motoneurones. Experimental Brain Research 11: 282-295.

WEISS, C.,HOUK, J.C., GIBSSON, A.R., (1990). Inhibition of sensory responses of cat inferior olive neurons produced by stimulation of red nucleus. Journal of Neurophysiology. 64: 1170-1185.

deZEEUW, C.I., HOLSTEGE, J.C.,RUIGROK, T.J.H., VOOGD, J. (1990). Mesodiencephalic and cerebellar terminals terminate upon the same dendritic spines in the glomeruli of the cat and rat inferior olive: An ultrastructural study using a combination of [3H]leucine and Wheat Germ Agglutinin coupled Horseradish Peroxidase anterograde tracing. Neuroscience 34: 645-655.

YAROM, Y., (1989). Oscillatory behaviour of olivary neurones. Experimental Brain Research Series 17: eds. Springer-Valberg, Berlin, Heidleberg, New York. p. 134-161.